PRODUCTION AND CHARACTERIZATION OF NANOCOMPOSITE MATERIALS FROM RECYCLED THERMOPLASTICS

A THESIS SUBMITTED TO
THE GRADUATE SCHOOL OF NATURAL AND APPLIED SCIENCES
OF
THE MIDDLE EAST TECHNICAL UNIVERSITY

BY

METİN KARABULUT

IN PARTIAL FULFILLMENT OF THE REQUIREMENTS FOR THE DEGREE
OF
MASTER OF SCIENCE
IN THE DEPARTMENT OF POLYMER SCIENCE AND TECHNOLOGY

JULY 2003

Approval of Graduate School of Natural and Applied Sciences

Prof. Dr. Canan Özgen
Director

I certify that this thesis satisfies all the requirements as a thesis for degree of Master of Science.

Prof. Dr. Ali Usanmaz
Head of the Department

This is to certify that we have read this thesis and that in our opinion it is fully adequate, in scope and quality, as a thesis for the degree of Master of Science.

Prof. Dr. Ülkü Yılmazer
Supervisor

Examining Committee Members

Prof. Dr. Güngör Gündüz
Prof. Dr. Teoman Tinçer
Prof. Dr. Ali Usanmaz
Assist. Prof. Dr. Göknur Bayram
Prof. Dr.Ülkü Yılmazer

ABSTRACT

PRODUCTION AND CHARACTERIZATION OF NANOCOMPOSITE MATERIALS FROM RECYCLED THERMOPLASTICS

Karabulut, Metin

M.S., Department of Polymer Science and Technology

Supervisor : Prof. Dr. Ülkü Yılmazer

July 2003, 124 pages

Nanocomposites are a new class of mineral-field plastics that contain relatively small amounts (<10%) of nanometer-sized clay particles. The particles, due to their extremely high aspect ratios (about 100-15000), and high surface area (in excess of 750-800 m^2/g) promise to improve structural, mechanical, flame retardant, thermal and barrier properties without substantially increasing the density or reducing the light transmission properties of the base polymer. Production of thermoplastic based nanocomposites involves melt mixing the base polymer and layered silicate powders that have been modified with hydroxyl terminated quaternary ammonium salt. During mixing, polymer chains diffuse from the bulk polymer into the van der Waals galleries between the silicate layers.

In this study, new nanocomposite materials were produced from the components of recycled thermoplastic as the matrix and montmorillonite as the filler by using a co-rotating twin screw extruder. During the study, recycled poly(ethylene terepthalate), R-PET, was mixed with organically modified quaternary alkylammonium montmorillonite in the contents of 1, 2, and 5 weight %. Three types of clays were evaluated during the studies. For comparison, 2 weight % clay containing samples were prepared with three different clay types, Cloisite 15A, 25A, 30B. The nanocomposites were prepared at three different screw speeds, 150, 350, 500 rpm, in order to observe the property changes with the screw speed.

Mechanical tests, scanning electron microscopy and melt flow index measurements were used to characterize the nanocomposites. The clay type of 25A having long alkyl sidegroups gave the best results in general. Owing to its branched nature, in nanocomposites with 25A mixing characteristics were enhanced leading to better dispersion of clay platelets. This effect was observed in the SEM micrographs as higher degrees of clay exfoliation. Nearly all the mechanical properties were found to increase with the processing speed of 350 rpm. In the studies, it was seen that the highest processing speed of 500 rpm does not give the material performance enhancements due to higher shear intensity which causes defect points in the structure. Also the residence time is smaller at high screw speeds, thus there is not enough time for exfoliation. In general, the MFI values showed minimum, thus the viscosity showed a maximum at the intermediate speed of 350 rpm. At this processing speed, maximum exfoliation took place giving rise to maximum viscosity. Also, the clay type of 25A produced the lowest MFI value at this speed, indicating the highest degree of exfoliation, highest viscosity, and best mechanical properties.

Key Words: Nanocomposite, Thermoplastic Nanocomposites, Recycled PET, Montmorillonite

ÖZ

GERİ KAZANILMIŞ TERMOPLASTİKLERDEN NANOKOMPOZİT MALZEMELERİN ÜRETİLMESİ VE KARAKTERİZASYONU

Karabulut, Metin

Yüksek Lisans, Polimer Bilimi ve Teknolojisi Bölümü

Tez Yöneticisi : Prof. Dr. Ülkü Yılmazer

Temmuz 2003, 124 sayfa

Nanokompozit malzemeler oldukça az miktarda (%<10) nano boyutlarda kil parçacıkları içeren mineral dolgu maddeli plastiklerdir. Parçacıklar çok yüksek boyut oranlarına (yaklaşık 100-15000) ve yüksek yüzey alanına (750-800 m^2/g) sahip oldukları için baz polimerin yoğunluk ve ışık geçirme özelliklerini fazla etkilemeden mekanik, ateşe dayanıklılık, ısısal ve geçirmezlik özelliklerini iyi yönde etkilerler.Nanokompozit üretim işlemi polimeri ve hidroksil-sonlu kuarterner amonyum tuzu ile etkileştirilmiş silikat tabakalarını karıştırmakla yapılır. Karıştırma sırasında polimer zincirleri aralanmış silikat tabakaları arasına yerleşirler.

Bu çalışmada resin olarak geri kazanılmış termoplastik ve katkı maddesi olarak montmorillonit kullanılarak yeni nanokompozit malzemeler üretilmiştir. Çalışma sırasında, geri kazanılmış poli (etilen tereftalat), PET, organik olarak modifiye edilmiş kil ile %1, 2, ve 5’lik oranlarda karıştırılmış ve çalışmalar sırasında üç tip kil örneği incelenmiştir. Karşılaştırma için ağırlıkça % 2’lik üç farklı kil örneği, Cloisite 15A, 25A, ve 30B, içeren numuneler hazırlanmıştır. Özelliklerdeki değişimin gözlenebilmesi için nanokompozit malzemeler üç farklı vida hızında, 150, 350, 500 rpm, hazırlanmıştır. Mekanik testler, taramalı elektron mikroskopu, ve akış indeksi ölçümleri nanokompozit malzemelerin karakterizasyonu için kullanılmıştır. Uzun alkil yan gruplarına sahip 25A kil tipi genellikle en iyi sonuçları vermiştir. 25A kil tipi dallanmış yapısı nedeniyle, karıştırma özelliklerini arttırmakta ve kil tabakalarının daha iyi dağılabilmesine yol açmaktadır. Bu etki yüksek kil dağılımına sahip yapılar olarak taramalı electron mikroskobu fotoğraflarında gözlenmiştir. Neredeyse bütün mekanik özelliklerin 350 rpm vida hızında arttığı görülmüştür. Çalışmalarda, 500 rpm olan en yüksek işleme hızının yapıya verdiği zarardan dolayı malzemede bir performans arttışı sağlamadığı görülmüştür. Ayrıca, yüksek işleme hızlarında geçiş zamanının daha düşük olması, kil dağılımı için yeterli zamanın olmamasına yol açmaktadır. Genelde, 350 rpm hızında MFI değerleri minimum gösterirken, viskozite maximum göstermiştir. Bu vida hızında maximum dağılım sonucu yüksek viskozite görülmüştür. Ayrıca, bu işleme hızında 25A kil tipi en düşük MFI değerini vererek, en yüksek dağılımı, en yüksek viskoziteyi, ve en iyi mekanik özellikleri göstermiştir.

Anahtar Kelimeler: Nanokompozit, Termoplastik Nanokompozitler, Atık PET, Montmorillonit

Dedicated to my family and Prof. Dr. M. Tuncoku..

ACKNOWLEDGEMENTS

I want to express my sincere thanks to my thesis supervisor, Prof. Dr. Ülkü Yılmazer, for his guidance, gentle understanding, kind support, and both theoretical and practical experiences throughout the research program. I also thank Asst. Prof. Göknur Bayram for her encouragement during the studies.

I thank Prof. Dr. Teoman Tinçer from the Chemistry Department for providing the injection molding machine and the impact test machine, and Prof. Dr. Erdal Bayramlı for providing the injection molding machine in their laboratories, also Mihrican Açıkgöz from the Chemical Engineering Department for DSC studies, Cengiz Tan from Metallurgical and Materials Engineering Department for SEM Analysis.

I would like to express my special thanks to Salih Sarıkaya from the Chemistry Department for his support and experiences both in technical and daily life during the machine problems. Also special thanks to Nevzat Bekçi, Metin Yanık, Metin Kırmaç, Şerife Çitiloğlu and all technicians in Chemical Engineering Department. I am very happy while writing these words to Münevver Gün in the Graduate School of Natural and Applied Sciences, thanks her from the very beginning.

Special thanks to my friends in Polymer Group, Işıl Işık, Güralp Özkoç, Çiğdem Başara, Cansu Altan, Elif Alyamaç, Özcan Köysüren, Hande Durgun, Ali Keyfoğlu, Pelin Toprak, and Gülsüm Özden.

I thank to Mert Kılınç, Ebru Acar, and Belma Soydaş for their special friendships, supports and sharings during studies.

TABLE OF CONTENTS

CHAPTER

LIST OF TABLES

TABLE

LIST OF FIGURES

FIGURE

CHAPTER I

INTRODUCTION

Polymer layered silicate nanocomposites have become an important area studied more widely in academic, government and industrial laboratories. These type of materials were first reported as early as 1950, [1]. However, it was not widespread until the period of investigation on this type of structures by Toyota researchers, [2-5]. This early work of Toyota group was based on the formation of nanocomposites where montmorillonite was intercalated with ε-caprolactam in situ.

Polymeric materials can be filled with several inorganic and/or natural compounds in order to get the wide array of property enhencements, e.g, increased stiffness and strength, improved solvent and UV resistance, greater dimensional stability, decreased electrical conductivity, enhanced gas barrier properties. The property improvements of clay based nanocomposites are due to the nanoscale nature of the formed system resulting in very high surface areas.

From an industrial approach, owing to high costs of development, synthesis and commercialization of new polymers, most researchers look for new materials by reinforcing or blending existing polymers, so the tailor made properties of the materials can be achieved, [6].

Poly(ethylene terepthalate) (PET) is a low-cost, and high performance thermoplastic that finds use areas in a variety of applications, such as in fabrics and soft drink bottles, reinforcement of tires and rubbery goods, food and beverage packaging. PET has excellent surface characteristics, and high heat deflection temperature. PET regrinds from postconsumer soft drink bottles have slightly reduced molecular weight and structure related properties as compared to pure polymer.

In this study, the aim is to produce nanocomposite materials from recycled PET regrinds as the matrix with the addition of organically modified montmorillonite (mmt) clays as the filler, and observe the effects of clay content, clay type and processing speed on sample properties, e.g, mechanical, thermal, and morphological ones. In this study, the matrix polymer, recycled PET, was purchased from the SASA Co., Turkey, in the form of flakes.

Montmorillonite is one of the major silicate groups of phyllosilicates containing an octahedral metal oxide lamina (containing aluminum or magnesium cations) sandwiched between two tetrahedral sheets of silica laminae with metal atoms (containing silicon and sometimes aluminum, i.e. Al for mica). This type of phyllosilicate has a very high surface area of 750 m^2/g, if it is completely exfoliated, and has a high aspect ratio of 100 to 15000. Spacing between silicate layers can be increased and these silicate platelets can be separated due to the flexible edges of silicate platelets, increasing the possible interactions between the components in the system. The layered silicate is generally made orgonaphilic by exchanging the inorganic cation with an organic ammonium cation. Alkylammonium ions lower the surface energy of the clay particles, so that polymers with different polarities can get intercalated between the layers and cause further separation and dispersion of silicate layers. In the present study, the fillers, montmorillonite, types of Cloisite 15A, 25A, and 30B, were purchased from the Southern Clay Products. Proper choice of organoclay chemistry is critical.

At the present, there are four principle methods for producing exfoliated nanocomposites, namely in situ polymerization, emulsion polymerization, sol-gel templating, and melt compounding. A majority of nanocomposite researches has focused on polymerization-based techniques. Little information is available concerning the formation via melt compounding. Melt processing is environmentally sound since no solvents are required, and gives freedom to end use manufacturers, and minimizes capital costs due to its compatibility with existing processes.

Indeed, nanocomposites can be formed using variety of shear devices, e.g. extruders, mixers, ultrasonicators etc. Of these melt-processing techniques, twin-screw extruder is the most appropriate one for the exfoliation and dispersion of silicate layers. Optimum residence time and shear intensity during processing is required to obtain the exfoliated and dispersed layered silicates. In this study, intermeshing co-rotating twin-screw extruder purchased from ThermoPrism Co. in England was used.

To examine the effects of selected parameters on structures, and observe the level of clay dispersion and crack propagation paths upon impact test specimens Scanning Electron Microscopy (SEM) Analysis was performed.

Tensile, flexural, and impact tests were performed to characterize the mechanical behavior of the nanocomposites in terms of strength, modulus, strain at break, impact and energy to break values. Most plastic materials are used because of their desirable properties at an economical cost, for this reason, the mechanical properties are considered to be important.

Thermal properties were determined to see the effects of clay type and content, and processing speed.

Melt flow index (MFI) measurements were done to observe the viscosity of nanocomposite as affected by the degree of exfoliation of the clay particles.

CHAPTER II

BACKGROUND INFORMATION

2.1 COMPOSITE MATERIALS

It is evident that the material advances have been the key to significant breakthroughs throughout the history. The Stone Age, the Iron Age, the Industrial Revolution, the Nuclear Age, the Electronic Revolution, the aerospace of today; all have critically resulted from breakthroughs in material technology. [7]

2.1.1 WHAT ARE COMPOSITES ?

A composite material is a combined material created from two or more components, selected filler or reinforcing agent and a compatible matrix, binder (i.e. resin) in order to obtain specific characteristics or properties that were not there before. The matrix is the continuous phase, and the reinforcement constitutes the dispersed phase. It is the behavior and properties of the interface that generally control the properties of the composite. [8]

2.1.2 HISTORY OF COMPOSITES

The first man made composites based upon polymers appeared in about 5000 B.C. in the Middle East where pitch was used as a binder for reeds in boat-building. The three key steps leading to modern composites were,

1. The commercial availability of fiberglass filaments in 1935,

2. The development of strong aramid, glass, and carbon fibers in the late 1960’s and early 1970’s, which are parallel to the development of resins dating back to 1968 (phenolics) and 1937 (epoxies),
3. The promulgation of analytical methods for structures made from those fibers. [7]

2.1.3 THE REASON FOR CONSUMPTION OF COMPOSITES

The increases in consumption of composite materials were primarily due to the need for nonconductive electrical components, noncorroding and noncorrosive storage containers and transfer lines, and sporting goods.

Designers of structures have been quick to capitalize on the high strength-to-weight or modulus-to-weight ratios of composites. The advantages include,

- Weight reduction (high strength- or stiffness-to-weight ratio)
- Tailorable properties (strength or stiffness can be tailored to be in the load direction)
- Redundant load paths (fiber to fiber)
- Longer life (no corrosion)
- Lower manufacturing costs because of lower part count
- Inherent damping
- Increased (or decreased) thermal or electric conductivity
- The ease of formability

The disadvantages include,

- Cost of raw materials and fabrication
- Possible weakness of transverse properties
- Weak matrix and low toughness
- Environmental degradation of matrix
- Difficulty in attaching
- Difficulty with analysis

Composites provide the designer, fabricator, equipment manufacturer, and consumer with sufficient flexibility to meet the demands presented by different environments(e.g. heat or high humidity) as well as any other special requirements. Proper design and material selection can avoid many of the disadvantages. [7]

2.1.4 BASIC CONCEPTS OF COMPOSITES

The combination of dissimilar materials can have unique and very advantageous properties if the materials have appropriate characteristics, and result in a material that is better in certain key properties than either of the materials alone. The reinforcements and the matrix are usually very distinct types of materials with widely different properties. [9]

It is probably true to say that all polymers contain some form of additives ranging from small fractions of catalyst residue to large-scale incorporation of mineral filler. The most important additives are these introduced for some specific purpose and would therefore include fillers, plasticisers, colorants, reinforcing fibers, blowing agents, stabilizers, flame retardants, processing aids, and final group of miscellaneous additives. Because of low specific gravities, the strength-to-weight and the modulus-to-weight ratios, and also fatigue strength-to-weight ratios of these materials are superior to those of metallic materials. [7]

Most low-density material would be weak, but in the case of composites, the reinforcement provides the structural attributes. [9]

In general, the properties of a fiber-reinforced composite depend strongly on the direction of measurement, whereas the traditional structural materials have weaker dependence.

Heterogeneous nature of composites provides mechanisms for high-energy absorption on a microscopic scale comparable to the yield process, exhibiting gradual deterioration in properties, but they do not usually fail in catastrophic manner.

Coefficients of thermal expansion (CTE) for many fiber-reinforced composites are much lower than that of metals, exhibiting a better dimensional stability over a wide temperature range.

High internal damping leads to better vibrational energy absorption within the composite material, resulting in reduced transmission of noise and vibrations to neighboring structures. [7]

2.1.5 REINFORCEMENT-MATRIX INTERFACE

The load acting on the matrix has to be transferred to the reinforcement via the interface. Thus reinforcements must be strongly bonded to the matrix, if their high strength and stiffness are to be imparted to the composite. The fracture behavior is also dependent on the strength of the interface. A weak interface results in low stiffness and strength, but high resistance to fracture, whereas a strong interface produces high stiffness and strength but often a low resistance to fracture, i.e., brittle behavior. The exact role of interface may differ with the type of reinforcement. The interface can be viewed as a planar region of only a few atoms in thickness across in which there is a change in properties from those of the matrix to those of the reinforcement. Thus, the interface is usually a discontinuity in chemical nature, crystal and molecular structure, mechanical and other properties. [10]

2.1.5.1 WETTABILITY

Interfacial bonding is due to adhesion between the reinforcement and the matrix and mechanical keying. For adhesion to occur during the manufacture of a composite, the reinforcement and the matrix must be brought into intimate contact. Wettability defines the extent to which a liquid will spread over a solid surface. Covering every bump and dip of the rough surface of the reinforcement and displacing with air carries out good wettability. [10]

2.1.5.2 INTERFACIAL BONDING

Once the matrix has wet the reinforcement, therefore in intimate contact with it, bonding will occur. For a given system more than one bonding mechanism may be operative at the same time.

2.1.5.2.1 Mechanical bonding

A mechanical interlocking or keying of two surfaces can lead to a reasonable bond. The rougher the interface, the greater the interlocking, Figure 2.1 (a),

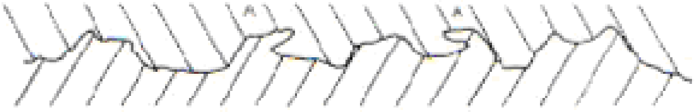

Figure 2.1 (a) Mechanical bonding

2.1.5.2.2 Electrostatic bonding

Bonding occurs between the matrix and the reinforcement when one surface is positively charged and the other negatively charged, Figure 2.1 (b), leading to an electrostatic attraction between the components of the composite depending on the difference in charge on their surfaces. Electrostatic interactions are short range and are only effective over small distances.

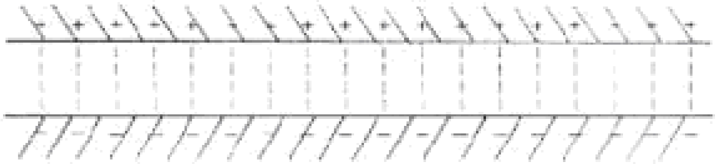

Figure 2.1 (b) Electrostatic bonding

2.1.5.2.3 Chemical bonding

Chemical bonding is the bond formed between chemical groups on the reinforcement surface, marked X in Figure 2.1 (c) and the compatible groups (R) in the matrix. Strength depends on the type of bond and the number of bonds.

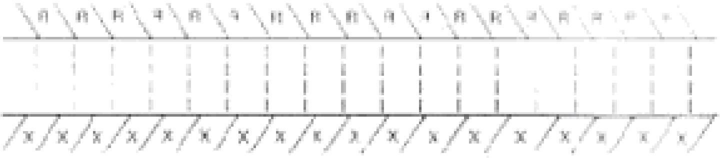

Figure 2.1 (c) Chemical bonding

2.1.5.2.4 Reaction or interdiffusion bonding

The atoms or molecules of two components of the composite may interdiffuse at the interface to give this type of bonding, Figure 2.1 (d), considered as due to the intertwining of molecules. The strength of this type of bonding depends on the distance over which the molecules have entwined, the extent of the entanglement of the molecules and the number of molecules per unit area of interface, [10]

Figure 2.1 (d) Interdiffusion bonding [10]

2.1.6 BASIC RESIN CONCEPTS

Resins are of the general class of materials called polymers. The length of the chain determines a basic polymer property known as the molecular weight. As the chains get larger, the mechanical properties (such as tensile strength and toughness) improve. The improvement in properties is thought to result from interchain forces, including entanglements of chains. Therefore, the entanglement of nearby polymer chains is a key characteristic in determining the nature of polymeric materials. Both polymer molecular weight and crystallinity affect mechanical and thermal properties like another key feature of polymers; this is stiffness of the polymer chain. As a chain stiffened, both mechanical and thermal properties increase. [9]

2.1.7 THERMOPLASTIC RESIN PROPERTIES

Chemical Structures

The matrix in a fiber-reinforced resin-matrix composite has several functions. It transfers the imposed loads to the fibers, so it must have a good bond with the reinforcing agents. It gives the shape to the part, so must be readily formable, and it must retain that shape and mechanical properties throughout the temperature range of use. In order to protect the reinforcing agents from environmental damage, the matrix should have toughness and impact resistance. [9]

Mechanical Properties

The discussion of mechanical properties of resins used for matrix materials in composites must consider the effect of reinforcement material. Domination of composite properties by the reinforcement is true for many properties such as tensile strength, flexural strength, and thermal expansion. [10]

Thermal Properties

As the temperature of the composite is increased, more and more energy is imparted to the polymer, converting into molecular motion. At lower temperatures, the motion is largely vibrational which is relatively unrestricted motion. When temperatures become higher, the molecules gain sufficient energy to flex and rotate and at even higher temperatures they begin to translate. In highly crystalline polymers the crystal lattice energies are strong resulting in tightly held molecules with very little rotation and almost no translation till the imposed energy is to overcome the lattice energies. This phenomenon is called the crystalline melting point for the polymer. In totally amorphous polymers there is no crystalline structure and therefore no crystal lattice energy. The transition from solid to melt is more gradual with only small indications of the increased mobility of the molecules. The temperature at which this transition occurs is called the glass transition temperature, T_g, for the polymer. The T_g, crystalline melting point,T_m, and the heat distortion temperature, HDT, the maximum use temperature for the polymer for continuous service, define general thermal characteritics of a given polymer to be used. [9]

Environmental Resistance

Mostly related with their structures, the high performance thermoplastics have an excellent solvent resistance (to water and organic solvents), that is better than the common thermoset matrix materials. The engineering thermoplastics are generally much more sensitive to solvent attack performing roughly the same resistance level as the common thermoset materials. Another environmental consideration namely the flame resistance of the polymers is important in composite uses. Highly aromatic polymers (including most of the high performance thermoplastics) are inherently flame retardant because of their tendency to form char. [9]

2.1.8 POLYMER MATRIX COMPOSITES

The major classes of structural composites exists today are being defined by the types of their matrices, namely polymer, metal, ceramic, carbon-carbon, intermetallic matrix composites. Polymer matrix composites are the most developed class of composite materials, fabricated into large, complex shapes, and have been accepted in a variety of aerospace and commercial applications. [7]

2.2 NANOTECHNOLOGY

Nanoscience is the study of atoms, molecules, and objects whose sizes are in nanometer scale (1-100 nanometers) and consists of applying the science of the small. It is multidisiplinary, and involves physicists, chemists and biologists in studying, researching and engineering ever smaller structure. Physics is different on the nanometer scale. Properties not seen on a macroscobic scale now become important, such as quantum mechanical and thermodynamic properties. Rather than working on bulk materials, one works on individual atoms and molecules. [11]

2.3 NANOCOMPOSITE MATERIALS

From the viewpoint of today’s industrial and economical activities, it can be easily assumed that the technology has opened window for us which determines the standards of our lives. These requirements result in continuous efforts for new, high peformance besides low cost materials to meet increasing demands. Polymers are commonly mixed with a variety of both synthetic and natural compounds to improve their performance capabilities.

Polymer layered silicate (PLS) nanocomposites are a new class of materials which consist of polymer matrices filled with low amounts (<10%) of layered silicates dispersed at nanoscale level, their properties can not be achieved by either macro- or microscopic dispersion of inorganic compounds. The essential raw material for a nanoclay (nano-sized layered silicate) is montmorillonite, a 2-to-1 layered smectite clay with a platelet structure. Benefits from this clay technology result in part from the way high-surface area of montmorillonite (750-800 m^2/g) and high-aspect ratio (about 100 to 15000). [12]

In the case of the interaction between a clay and a macromolecule, the work by Bower, [13], was the earliest one dates back to 1949. Polymer layered silicate (PLS) nanocomposites were first reported by Blumstein, [14], in the literature as early as in 1961, demonsrating the polymerization of vinyl monomers intercalated into montmorillonite clay.

2.3.1 REASONS FOR INTEREST FOR NANOCOMPOSITE TECHNOLOGY

A number of factors are of interest in nanocomposite technology using clay minerals,

- Low loading levels
- Transparency
- Incorporation flexibility
- Safety
- Synergies with other additives
- Low cost

- Nanocomposites typically contain 2-10% loadings on a weight basis, yet property improvements can equal an exceed traditional composites containing 20-35% mineral or glass. Machine wear is reduced and processability is increased,

- Nanoclay particles have a dimension below the visible light wavelength,
- The particles are tough. They can withstand solvents, polymerization temperatures and compounding shear. They can be processed without concern about degradation,
- Clays are generally innocuous materials and have been used safely in consumer products for decades,
- A wealth of experience demonstrates that they act synergistically with other minerals. [15]

2.3.2 NANOCOMPOSITE FORMATION AND STRUCTURE

Structure

Polymer layered silicate nanocomposites are hybrid between an organic phase (the polymer) and an inorganic phase (the silicate) and can be classified depending on the shape of the nanofiller, where particles are characterized by a 3D nanosize distribution; nanotubes or whiskers nanosize is limited to two-dimensions in space; and phyllosilicates (e.g. clay) single silicate layers are characterized by one-dimensional nanosize distribution. [16]

Materials at interfaces can constitute a seperate phase, often called the ‘interphase’ including interfacial interactions contributing to materials’ properties increase. In principle, because of the similarity between length scales nanocomposite materials, it is possible to make materials completely interphase rather than the bulk form. [17]

Mainly due to their very high interfacial area, and a very short distance between reinforcing particles surface, nanocomposite materials show specific features. For polymer based nanocomposites, the percolation of reinforcing particles depending on their shape factor plays an important role in determining the final type of the network, either stiffer or softer. [18]

Formation

In general, an interplay of entropic and enthalpic factors in the reaction media determines the structure of outcome by affecting the dispersion characteristics of an organically modified montmorillonite (o-mmt) in a polymer.

Dispersion of mmt in a polymer requires sufficiently favorable enthalpic contributions to overcome any entropic penalties. Confinement of the polymer inside the interlayers results in a decrease in conformational entropy of the polymer chains. However, this penalty can be compansated in part by the increased conformational freedom of the tethered surfactant chains locating in a less confined environment as the layers seperate. Favorable enthalpy of mixing for the polymer-o-mmt is achieved when the polymer/mmt interactions are more favorable compared to the surfactant/mmt interactions. [19]

For most polar or polarizable polymers, an alkyl-ammonium surfactant is adequate to offer sufficient excess enthalpy and promote nanocomposite formation. The structure of these nanocomposites does not change markedly with processing. If the organically modified montmorillonite dispersion is not thermodynamically favored, the layers will be in low d-spacing parallel stacks during the high temperature processing, forming conventionally-filled nanocomposite. Structures that do not have sufficient thermodynamics can be ‘trapped’ in exfoliated structures (through solvent casting or high shear/high temperature extrusion), but these are not desirable for further processing. [20]

Polymer/clay composites are divided into three general types, namely conventional, intercalated, and delaminated or exfoliated. Illustrated structures can be seen in Figure 2.2.

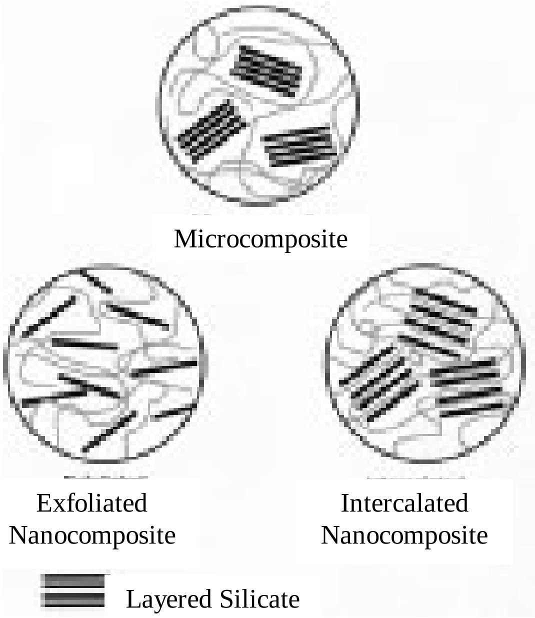

Figure 2.2 Schematic representation of composite structures obtained using layered silicate [16]

Conventional

This structure occurs when the miscibility between the polymer matrix and the filler does not support favorable interactions to overcome the thermodynamic considerations leading the silicate layers to collapse. In these structures, system is totally immiscible.

Intercalated

The single polymer chains are intercalated between unaltered silicate layers with their regular alternation of galleries. The space occupied by the polymer is typically in the order of a few nanometers. These systems display limited miscibility.

Delaminated (or Exfoliated)

The silicate layers are totally delaminated and dispersed in the polymer matrix. Its ordered structure is lost and the distance between the layers is in the order of the radius of gyration of the polymer. System is totally miscible. [16]

2.3.3 PREPARATION METHODS

Polymer layered silicate (PLS) nanocomposites are currently prepared in four ways, [16]

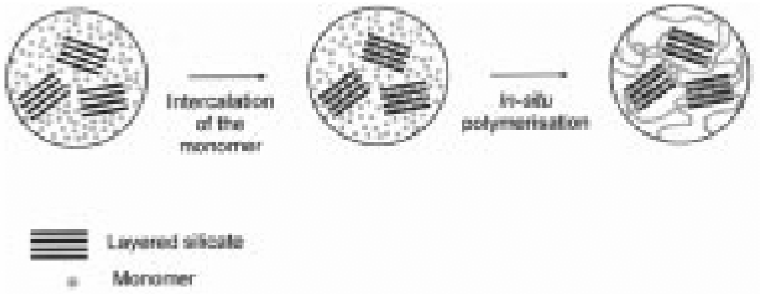

Figure 2.3 Schematic representation of PLS obtained by polymerization *in situ* [16]

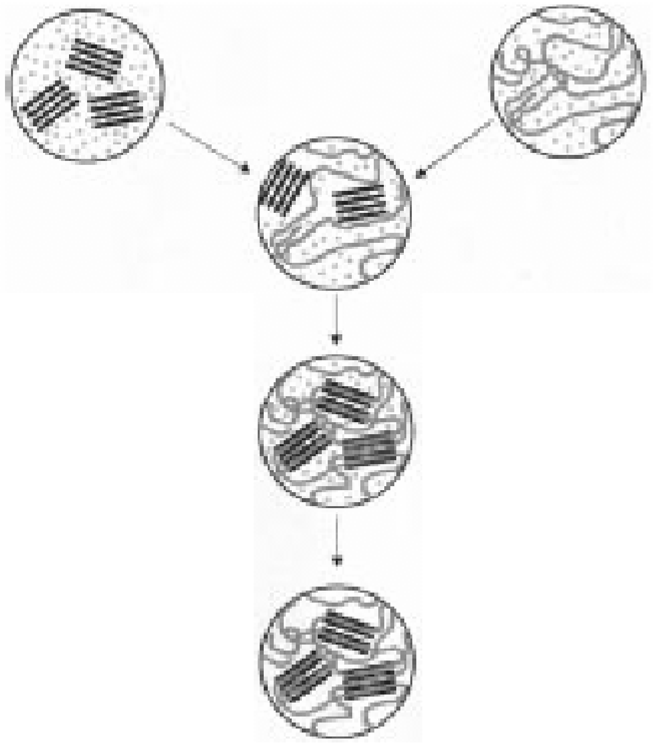

Figure 2.4 Schematic representation of PLS obtained by intercalation from solution [16]

In Situ Polymerization

First, all monomers and the filler are mixed and swollen. A molecule (the monomer) is absorbed into a host compound containing interplanar spaces (channels or cavities) and then polymerized. The polymer thus obtained is called ‘intercalated’ if confined between layers, or ‘occulated’ if confined between cavities. The process is illustrated schematically in Figure 2.3.

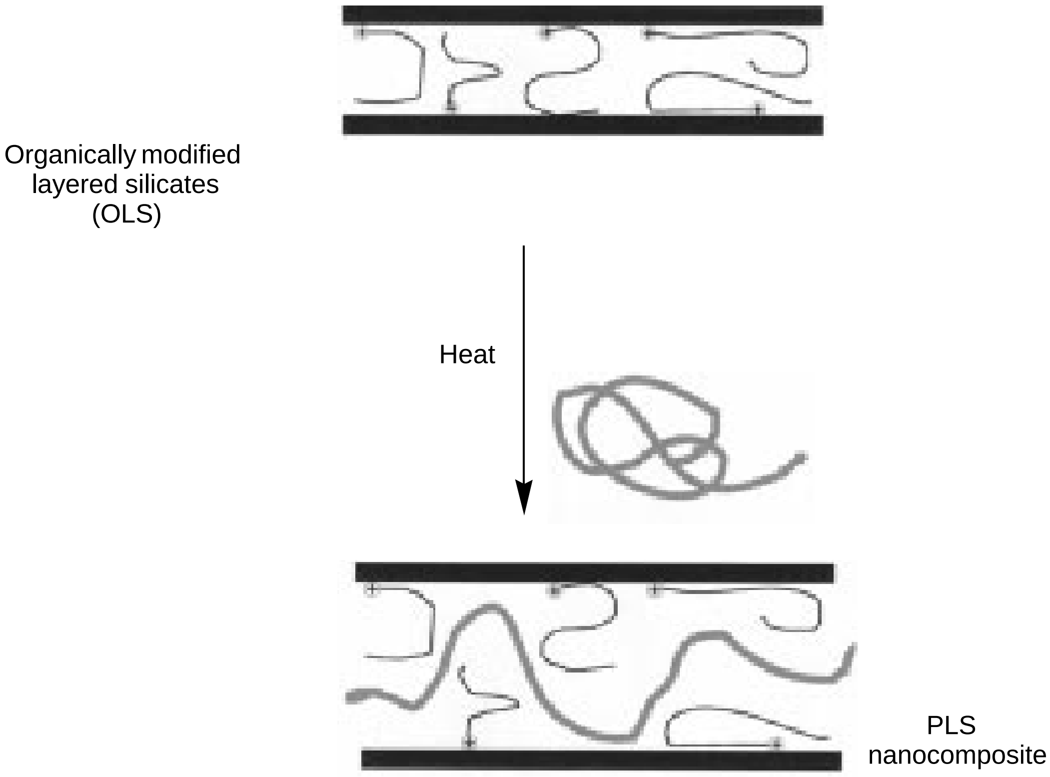

Figure 2.5 Schematic representation of PLS obtained by direct polymer melt intercalation [16]

Solution Process

Intercalation of the polymer from a solution is a two-stage process in which the polymer is exchanged with an appropriate solvent. There are two immiscible phases present, an aqueous (continuous) phase containing initiator and a nonaqueous (discontinuous) phase containing the monomer or prepolymer. Spontaneous exchange requires a negative variation in the Gibbs free energy. The diminished entropy due to confinement of the polymer is compansated by an increase due to desorption of intercalated solvent molecules. The process is illustrated schematically in Figure 2.4.

Melt Compounding

A polymer and layered silicate mixture is annealed above the T_g or T_m of the polymer in either static or flow conditions. The polymer chains spread from the molten mass into the silicate galleries to form hybrids according to the degree of penetration. The decreased entropy in this case is compansated due to the greater conformational energy of the aliphatic chains of the alkylammonium cations due to the increase in the size of the galleries caused by insertion of the polymer. Semi-quantitative calculations show that this gain is enough to offset the loss of entropy and make the process isoentropic. Maintenance of spontaneity requires enthalpy as the driving force. The process is illustrated schematically in Figure 2.5.

Sol-gel Technology

It consists of a direct crystallization of the silicate clays by hydrothermal treatment of a gel including polymer. Gels contain organics and organometallics, such as silica sol, magnesium hydroxide, lithium fluoride etc. It has the potential of promoting the high dispersion of the silicate layers in one-step process, without requiring an anium ion as a surfactant.

2.3.4 IMPORTANCE OF THE MELT COMPOUNDING PROCESS

Melt processing is environmentally sound since no solvents are required, making the production of industrially significant polymers practicable. It shifts the nanocomposite production downstream by giving end-use manufacturers many degrees of freedom with regard to final product specifications (e.g. selection of polymer grade, choice of organoclay, level of reinforcement, etc.). Application of this process also minimizes capital costs due to its compatibility with existing processes. [20]

2.4 FILLERS

The result of filler incorporation depends in most of cases on filler dispersion in matrix, affecting the system rheology. The addition may increase the viscosity of the composition, limiting the level of incorporation, thus fillers must be chosen based on their effect on viscosity. Fillers may be in the form of organic, inorganic or metallic structures, leading to enhancements in thermal, optical, mechanical, electrical or resistance properties of base resins. [21]

2.4.1 CLAY MINERALS

Clay is a natural earthy, fine-grained material comprised largely of a group of crystalline minerals known as the clay minerals. Clay minerals were initially defined on the basis of their crystal size. Their very diverse physical and chemical properties are dependent largely on their structure and composition comprising of hydrous phyllosilicates. The phyllosilicates are generally platy in shape and differ from one another with regard to the structural arrangement of the layers, the water content, and the associated cations. Main clay groups are kaolins, illites, chlorites, and palygorskite-sepiolite. [23]

2.4.1.1 PHYSICAL PROPERTIES OF CLAYS

The properties of clays are indeed dominated by their large surface areas compared to the volume of the particle. The minerals have the particularity of being sheet-shaped. This means that they have even more surface area than other minerals of the same grain size tending to be cubes or spheres in their fine-grained size. [22] The uses and properties of clay minerals are dependent on the clay and non-clay compositions, presence of organic material, the type and amount of exchangable ions and soluble salts, and texture. [24]

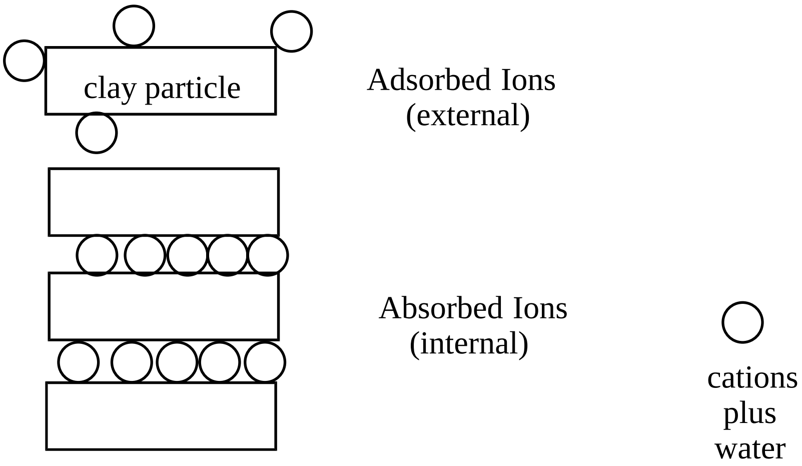

Figure 2.6 Absorbed and adsorbed ions on clay and the size of their fixation on clay particles [22]

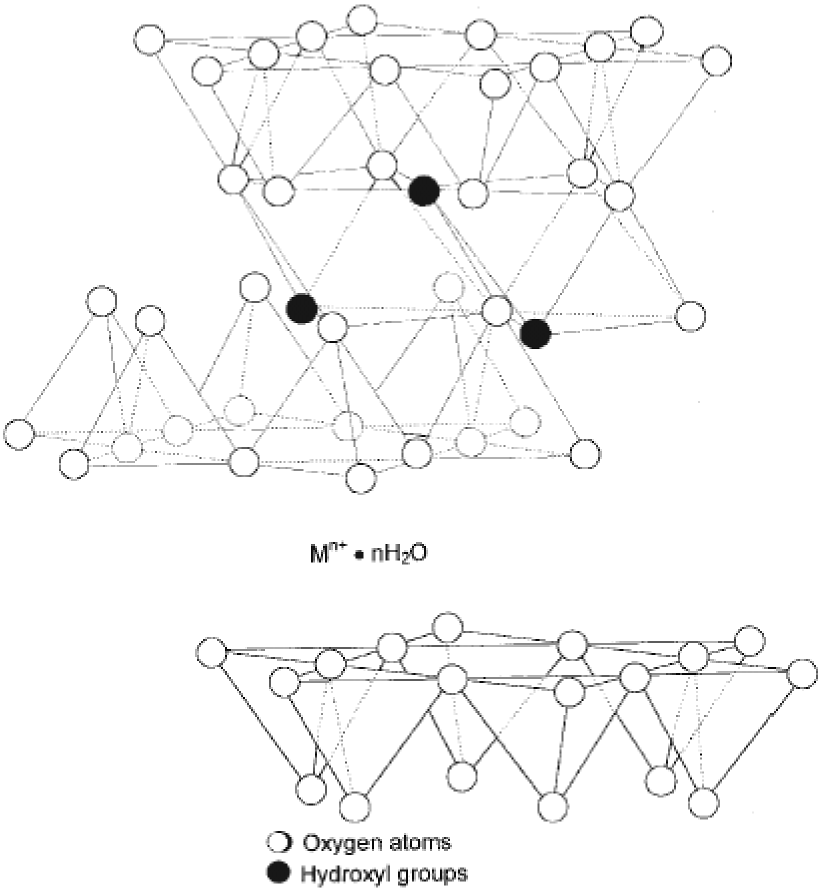

Figure 2.7 Idealized structure of 2:1 layered silicate showing two tetrahedral-site sheets fused to an octahedral-site sheet [16]

2.4.1.2 EXHANGE OF IONIC SPECIES (CEC)

A very important property of clay surfaces is their chemical activity, and their interaction with ions in aqueous solution including dissolved species (charged ions or molecular species adsorbed onto surface). The adsorbed ions are normally accompanied by water molecules expanding the clay galleries. Figure 2.6 shows schematically the states of adsorbed and absorbed ions.

The property of adsorbing and absorbing ionic species in solution is called cation exchange capacity (CEC) measured by the number of moles of ionic charge fixed on 100g of dry clay. The values are expressed in milli-equivalents of charges (moles)/100g. The selection between different species present in aqueous solution depends upon the species of clay and its chemical constitution, affinity of ions to remain in a free hydrated state and the concentration of ions in solution.

When an ion held on, it is displaced with another due to a change in its aqueous concentration, it is desorbed. If this ion is replaced by another ionic species introduced into the media, it is exchanged and this process is known as an ion exchange. The normal laws of mass action are active in the exchange process. [22]

2.4.1.3 STRUCTURES AND PROPERTIES OF PHYLLOSILICATES

The major silicate groups of phyllosilicates are mica, talc, montmorillonite, vermiculite, hectorite, saponite, etc. Their crystalline structure consists of one octahedral metal oxide lamina (containing aluminum or magnesium cations) sandwiched between two tetrahedral sheets of silica laminae with metal atoms (containing silicon and sometimes aluminum, i.e. Al for mica). Each layer is seperated from its neighbours ($10A^o$ unit layer) by a van der Waals gap called a gallery, usually occupied by cations counterbalancing the negative charge generated from the isomorphous substitution of the atoms forming the crystal (Mg^{2+} in the place of Al^{3+} in montmorillonite). These cations are hydrated alkaline and alkaline-earth metal cations, where the structure can be seen in Figure 2.7. The net negative charge of the clay may originate from substitutions within the mineral structure and from surface reactions, such as those with ‘broken’ bonds. [22]

The distance between the atoms in a gallery is 3.6A^o, whereas in Na-O bond, it is between 2.1 to 2.2A^o. Since, the colombic interaction is inversely proportional to the square of the distance between the charges, about 60% of the bonding strength between the cation and oxygen is not used. The partial positive charge thus formed for each cation within the gallery makes it highly hydrophilous. Montmorillnite neutralizes these partial charges by an ion-dipole interactions with holding water molecules. [16]

Organic molecules or polymers containing functional groups with partial negative charges can displace the water molecules forming an 'intercalation hybrid'. The ionic bonding in clays is highly covalent, roughly half of the ions present are oxygen, and among the cations, silicon and aluminum are the major constitutients. These ions form highly covalent units interlinked into what is called a network. [16]

2.4.2 COMPATIBILIZING AGENTS

The use of silicates as such, however, greatly limits the use area of the intercalable polymers because of their hydrophlic structure. This limitation is overcome by their alternation to form organically modified layered silicates.

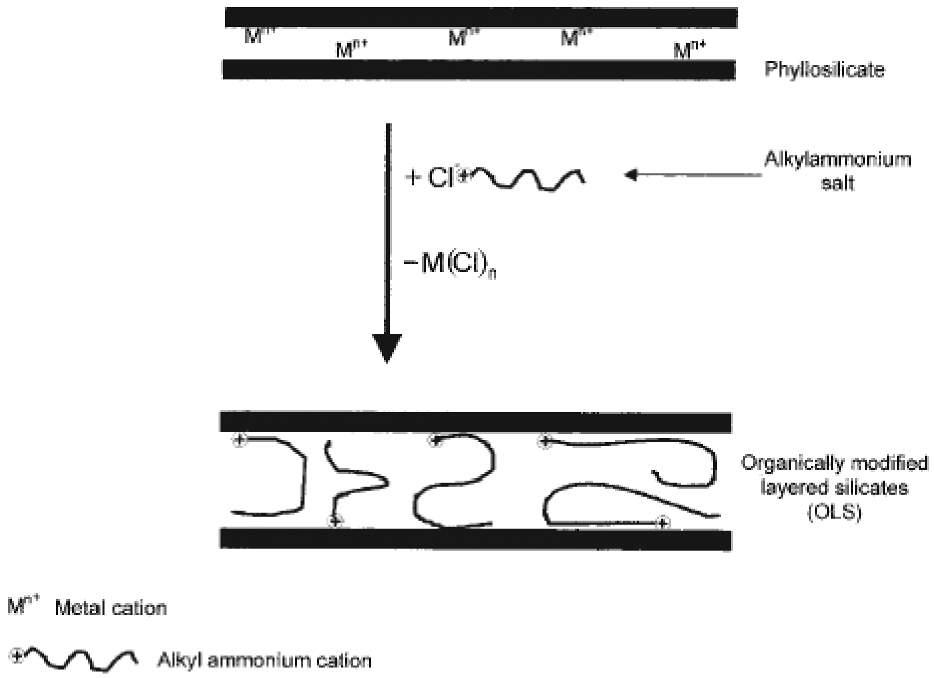

Figure 2.8 Schematic representation of a cation-exchange reaction between the silicate and an alkylammonium salt [16]

These are produced by replacing the cation originally present in the galleries with one organic cation. Alkylammonium ions are mostly used, showed in Figure 2.8, and the other ‘onium’ salts can be used, such as sulfonium and phosphonium. The cationic head of the alkylammonium salt preferentially resides towads the walls of the gallery via colombic interaction and its aliphatic tail radiates away from the wall making normally hydrophilic surface hydrophobic. [16] Water swelling of the silicate is needed to obtain the exchange process of onium ions with cations in the galleries. Two or higher valent cations prevent water swelling, thus, the hydrate formation of monovalent intergallery cations is the driving force for water swelling.

2.5 IMPORTANCE OF MATRIX MOLECULAR WEIGHT DURING PROCESSING

Generally, rheological properties at processing temperatures determine the conducivity of the polymer to applications in its related field. In such a process like reprocessing, there is an increase in deterioration of many of the most important properties of polymers due to the change of molecular weight in repeated production cycles.

The most important structural variable determining the flow characteristics of polymers is their molecular weight or chain length, Z (the number of atoms in the chain), Fox suggested an equation that log η was related with Z, for values of Z above a critical value Z_c, 25]

$\log \eta = 3.4Z_w + k$, where k is temperature dependent, and Z_w is weight-average chain length.

In a melted polymer, there is a change in viscosity behavior with decreasing molecular weight, changing the exponent of the viscosity equation from 3.4 to 1.0. This change is attributed to a critical minimum molecular weight below which the polymer chains are not long enough to be effectively entangled. Martinez et al., [26], observed this result in the experiment attaining to define the influence of reprocessing on properties of poly(ethylene terepthalate). They observed a sudden decrease in ductility after the third processing cycle in injection molding, that the viscosity molecular weight, M_v, is below the critical level needed to maintain the minimum entanglement network in the solid state. The material thus becomes brittle.

T.D. Fornes et al., [20], studied the effects of the matrix molecular weight on the properties of Nylon-6/clay nanocomposites based upon three different grades of Nylon-6, namely high, medium, and low. The higher molecular weight systems, due to higher melt viscosities, transfer more stress or energy to achieve seperation of platelets by decreasing the length of clay particles, whereas the low molecular weight ones impart low shear stresses on the agglomerates skewing the stack of platelets rather than seperating them, Figure 2.11.

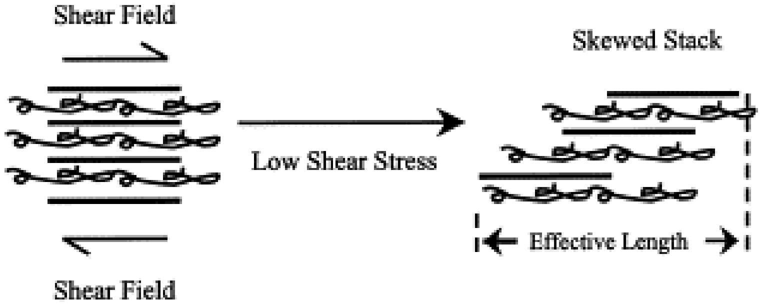

Figure 2.9 Schematic representation of lower shear impart on tactoids [20]

2.6 EXTRUSION PROCESS

2.6.1 DESCRIPTION OF MIXING

Polymer processing has elementary operations, namely, 1)handling of particulate, 2)melting, 3)pressurization and pumping, 4)mixing, 5)devolatilization. Among all, mixing is the main element of most polymer processing operations to obtain high-quality products. [27]

2.6.2 DISTRIBUTIVE AND DISPERSIVE MIXING

Dispersive mixing involves the reduction in size of a cohesive component and is also referred to as intensive mixing. Distributive mixing occurs in the absence of cohesive resistance and is also called as extensive or nondispersive mixing. [27]

2.6.3 THE MACHINE : EXTRUDER

In order to describe an extruder, we need to define some related terms. To extrude is to push out, simple. When a material is extruded, it is forced through an opening called the die. As the material flows through the die, it acquires the shape of the die flow channel. A machine used to extrude the material is called an extruder. [28]

Extrusion is basically the transformation of the raw material into a continuous, specified shape product by forcing it through a die. Many different materials can be formed through an extrusion process, such as metals, ceramics, clays, foodstuffs, and plastics either in the molten or solid state. [28]

Extruders in the polymer industry come in many different designs, where the main distinction is their mode of operation; either continuous having a rotating member or discontinuous having a reciprotating member. [28]

2.6.4 TWIN SCREW EXTRUDER

A twin screw extruder is a machine with two Archimedian screws which can be categorized by the degree of intermeshing, by the sense of rotation (co- or counter-rotating), by the functions of screws designed to perform, or by screw speed.

Two main areas of application for twin screw extruders are profile extrusion of thermally sensitive materials (e.g. PVC), and specifically polymer processing operations, such as compounding, chemical reactions etc. A classification is shown in Table 2.1., primarily based on the geometrical configuration of twin screw extruder. [28]

Table 2.1 Classification of Twin Screw Extruders

Intermeshing Extruders	Co-Rotating Extruders	-Low Speed Extruders (profile extrusion) -High Speed Extruders (compounding, devolatilization)
	Counter-Rotating Extruders	-Conical Extruders (profile extrusion) -Cylindrical Extruders (profile extrusion)
Nonintermeshing Extruders	Counter-Rotating Extruders	-Equal Screw Length -Unequal Screw Length
	Co-Rotating Extruders	-Not used in practice
	Coaxial Extruders	-Inner Melt Transport Forward -Inner Melt Transport Rearward -Inner Solids Transport Rearward -Inner Plasticating, Rearward Transport

(a) (b)

Figure 2.10 Cross Section Through the Intermeshing Region in (a) co-rotating, and (b) counter-rotating extruders [28]

Main difference between the intermeshing and the nonintermeshing extruders is the capability of them to form a shear region due to the openness between the screws allowing machine to determine the mixing type, dispersive or distributive according to process aim.

In the case of co- or counter rotating types, moving directions of the screws are different, where co- rotating ones move in opposite directions in the intermeshing region; counter rotating ones move in the same direction in this region affecting, as a result, the mixing capability. Figure 2.12, (a) and (b).

Screw speeds are defined according to fit capability of the flight profile into the channel profile. These profiles define the amount of pressure in the intermeshing region affecting the mixing characteristics. The flight profile fitting closely into the channel profile has a structure of good conveying characteristics causing high pressures in the intermeshing region, whereas the structures having narrower flights than the channels allow back flowing causing low pressure values. [27]

2.6.5 INSTRUMENTATION AND MOST IMPORTANT PARAMETERS

Instrumentation can be consdered as the ‘window to the process’ to measure important parameters and to be able to control the process.

The most important process parameters are melt temperature and pressure. Other parameters related to the extruder are,

- Screw Speed
- Motor Load
- Barrel Temperatures
- Die Temperatures
- Power Draw of Various Heaters
- Cooling Rate of Various Cooling Units
- Vacuum Level in Vented Extrusion

Parameters for the entire extrusion line are,

- Line Speed
- Dimensions of the Extruded Product
- Cooling Rate or Cooling Water Temperature
- Line Tension

Melt Pressure

Measurement of melt pressure is important for the reasons which are process monitoring and control, and safety. The diehead pressure determines the output from the extruder. When the diehead pressure changes with time, the extruder output correspondingly changes and so do the dimensions of the extrudate. Monitoring presssure changes with time gives us to see how stable the extrusion process is. [28]

Temperature Measurement

Temperature is usually measured by sensors, such as thermocouple(TC) using the temperature difference between two dissimilar metals to obtain a value; by resistance detectors (RTD) measuring the resistance of metals against the temperature changes; or by infrared (IR) detectors with principle based on emitting radiation by objects through changing temperature. IR probes are useful due to their noncontact temperature measurement, but have high cost. [27]

Melt Temperature Measurement

The temperature of the plastic melt is often measured with an immersion TC where the probe protrudes into the melt and reads the temperature. Since it causes the changes in flow velocities, actual temperature is changed. Another effect is that dead spots occur behind the immersion probe, which can be detrimental in plastics that are susceptible to degradation. Melt temperatures are always higher than the set (barrel) temperatures because of the conversion of mechanical energy into heat during processing. It is also known as the viscous dissipation. The amount of conversion is determined by the product of viscosity and shear rate squared,

$G_v = \tau : V_u$, where G_v, is the viscous heat generation; τ and V_u, show stress components and velocity gradients, respectively. [28]

Barrel Temperature Measurement

It is usually measured with TC or RTD sensors pressed on the barrel. The accuracy of the measurement is strongly dependent on the depth of the well, the type of sensor, and the air velocity in the environment. [28]

In the extrusion process, good temperature control is important to achieve good process stability. This is done by systems, namely on-off control where the power is either fully on or completely off; proportional control where the power is proportional to the temperature within a certain temperature region, the power decreases as the temperature increases in this proportional band; and fuzzy logic control (FLC) which is an artificial intelligence-based technology, designed to simulate human decision making. System uses many process variables and their membership functions, such as high, low, or medium, and fuzzy rules based on previous operating experience. [28]

2.6.6 OVERVIEW OF EXTRUDER TYPES

Most co-rotating twin screw extruders are high-speed extruders used primarily in compounding applications, approximately 75% of the twin screw market is in compounding.

Counter-rotating ones are primarily used in profile extrusion, having 95% of the twin screw market in this field. Most of them are manufactured as cylindrical. The nonintermeshing, counter-rotating twin screw extruders are well suited for compounding operations in which dispersive mixing has to be avoided, such as in applications where desired to reduce the fiber breakage resulting good reinforcing. They are also used in many reactive extrusion operations due to their good distributive mixing and devolatilization characteristics, and the high Length/Diameter (up to 120) ratios. [28]

2.6.7 PROCESS PARAMETERS IN PRODUCTION OF NANOCOMPOSITES

Polymer layered silicate nanocomposites have been studied in industrial, academic, and government laboratories for nearly 50 years, focused mostly on the chemistry used to modify the clay surface. The role of processing becomes more important in nanocomposite production affecting the resulting structure.

Hybrid formation requires an optimal interlayer structure and process conditions. There are many parameters affecting the resulting structure, such as silicate functionalization, annealing temperature, polymer molecular weight, feed rate, screw configuration, and screw speed. All of them direct or indirectly affect the shearing intensity and the residence time during processing, and consequently the structure of the obtained product.

In such a study, Vaia and Giannelis, [29], studied the effects of various characteristics of the silcate and polymer including silicate functionalization, annealing temperature, polymer molecular weight, and intermolecular interactions on the resulting material, using a variety of styrrene-derivative polymers in alkylammonium treated silicates.

Depending on the functionality, packing density, and length of the organic modifiers, the organically layered silicates may be engineered to optimize their compatibility with a given polymer. At constant annealing temperature, they observed the chains adopt a disordered monolayer arrangement at low interlayer packing densities of the organic modifier. Whereas, the chains adopt more extented conformations (leading larger initial gallery heights) as the packing density increases. Similarly, they observed in both cases where in increasing and decreasing, the host area per organic modifier chain results in immiscible, unintercalated systems. Also, the difference between primary and quaternary ammonium head groups does not affect predominantly the polystyrene intercalation, and, the different type of ammonium head does influence the final gallery height increase. The larger size of the quaternary ammonium head group and more localized cationic charge give additional gallery height. The state of polystyrene-organically layered silicate hybrid, whether intercalated or immiscible, does not depend on the distribution of the anionic charge on the silicate surface.

As the number of carbon atoms, n, of the aliphatic chain in the organosilicate increases, the arrangement of the aliphatic chain changes due to the layer height increase. For $n \leq 12$, the gallery height of the unintercalated systems is constant, and the aliphatic chains are arranged in a pseudo-bilayer with the highest segment density, $n=12$. For $n \geq 12$, chains adopt disordered pseudo-trilayer to liquid crystal like arrangements. Higher annealling temperatures favor the formation of hybrids in which the stacking of the silicate layers is disrupted. [29]

Annealing can be carried out either statically or under shear. In this study, effect of matrix molecular weight on the final hybrid structure was estimated zero. It only appears to affect the kinetics of polymer intercalation. If the process annealing were carried out under shear, the effect of matrix molecular weight had to be estimated as a determining factor due to effects on rheological properties, e.g. viscosity changes, in melt compounding. [29]

The structure of the pendant group on the polymer greatly affects the hybrid formation. Increasing the electron density and polarity of the pendant group, results in more disordered hybrid structures. In nonpolar polymers, only van der Waals interactions are present and an immiscible system is obtained. [29]

In the study of Dennis et al., [1], the effects of extruder types and screw design on the degree of dispersion of montmorillonite platelets in a polyamide matrix were studied.

Shear intensity is required to start the dispersion process, by shearing particles apart into tactoids or intercalants. Residence time is required to allow polymer to enter the clay galleries and peel the platelets apart. The shear intensity of mixing can be altered by changing the screw configuration. Screw configurations differ in the number of kneading disc blocks in the screw. These sections can be made up of different width paddles, the wider the paddle the more elongational shear and dispersive mixing, whereas narrow width discs favor distributive mixing and impose less shear intensity. In order to facilitate the movement of the resin forward, reverse or not at all, the discs in the kneading block can be fabricated at different staggering angles. Imparting a reverse or neutral kneading element to the kneading block section causes an element of polymer to spend more time in the kneading block leading to increase in the shear intensity of the screw configuration. The conveying elements vary from closed (higher shear) to open flighted (lower shear) design. The shearing elements not only increase the extentional flow, but also increase the residence time by creating an additional barrier for the polymer to more through. [1]

The extruder type and screw configuration affect both the mean residence time and residence time distribution related to backmixing in the extruder. All of the twin screw extruder types provide much more backmixing and broader residence time distribution than the single screw extruder. For a given extruder type, the mean residence time generally increases while the degree of backmixing decreases, as the screw is configured to more intense shearing. From the observations of Dennis et al. in this study, the best delamination and dispersion for each type of twin screw extruders was obtained using the medium shear intensity screw configuration. As the shear intensity was increased for a given extruder type, the degree of delamination and dispersion did not increase, but got worse. Thus, it appears that very high shear, dispersive mixing is not a key feature for delamination. [1]

Residence time during processing is an important variable affecting the degree of delamination, where there is a trend of improved delamination as the residence time increases. This trend can be concluded from the notion of diffusion of the polymer into the clay galleries. However, it is not a sufficient variable only itself, the delamination in single screw extruder is an evident of poor values in spite of relatively long residence times. There must be backmixing in the extruder in order to disperse the clay platelets into polymer matrix. Thus, the degree of delamination also be a function of the degree of backmixing since this is a measure of the distribution of residence times, and reflects the extent of mixing in the extruder. [1]

Davis et al., [30], worked with different processing conditions, including the screw speed and the residence time variables, to obtain poly(ethylene terepthalate)/montmorillonite clay nanocomposites. Longer residence times led to the degradation of organic modifier on the surface of the clay causing the brittle, tarlike nanocomposite structure. Higher screw speeds also resulted in lower quality nanocomposites in this study.

2.7 PLASTICS IN MUNICIPAL SOLID WASTE (MSW)

Management of solid waste is an important problem in today’s world where people pursue the higher quality of life as a result of economic growth and development.

For example, the United States generates more than 200 million tons of solid waste each year. Of that ≈16% is incinerated, ≈22% is recycled or recovered, and ≈62.6% is put into landfill. [31]

Plastics have become an integral part of our lifes. Its low density, strength, user-friendly design and fabrication capabilities, and low cost are the drivers to such growth. The amounts of plastics consumed annually have been growing steadily (Table 2.2). An integrated waste management approach comprises of source reduction, reuse, recycling, landfill and waste-to-energy conversion. [32]

Table 2.2 Growth of plastics in MSW

Year	Plastics in Solid Waste (%)
1960	0.5
1970	2.6
1980	5.0
1990	9.8
1992	10.6
1994	11.2
1995	11.5
1996	12.3

Polymer recycling would be any process which diverts the polymer waste to any place or use, other than landfill, but its options could be far from optimal as a result of economic (e.g. very expensive) and environmental (e.g. high energy consumption) reasons. Material recycling is a term used to describe processes in which the macromolecular structure is kept basically intact, and the material is reformed into a new product. Chemical recycling refers to the decomposition of the macromolecular structure to generate low molecular weight compounds. Incineration is a third category of polymer waste utilization where the product is heat used in the production of electricity. [31]

Table 2.3 shows the amounts of materials disposed in landfills, recycled or composed or disposed by combustion, the recycling rate increases steadily. Between 1990 and 1996, there has been a 17% decrease in waste being landfilled. [32]

Table 2.3 Management of MSW in the US

	1988	1990	1994	1996
Landfill (%)			60.9	55.5
Recycling: composting (%)	13	17	23.6	27.3
Combustion (%)			17.2	15.5

2.7.1 RECYCLING OF PLASTICS

The recycling of today is the continuation of much of the recycling started in the 1970s with more and better available technology and more concerns.

Recycling of plastics is an important industrial application due to its damage to the environment. The aim in recycling is to decrease the amount of waste by recirculation of raw materials and to improve the material utilization. [33]

There are four main types of methods used specifically for plastic recycling, namely primary, secondary, tertiary and quaternary. In the primary recycling, there is a conversion of scrap plastics by one or a combination of products having performance characteristics equivalent to the original products made of virgin plastics. In the secondary one, the conversion occurs with yielding products having less demanding performance requirements than the original material. Melt recycling is considered as a secondary recycling. There is a process involving chemical treatment in tertiary recycling producing chemicals and fuels from scrap or waste plastics. The quaternary recycling involves process technologies of recovering energy from scrap or waste plastics by incineration. [33]

Table 2.4 Plastics bottle recycling rates

Plastic bottle (million kg)	1996	1997	Change (%)
PET soft drink	240	246	2.7
PET custom	46	48	3
Total PET bottles	286	295	2.8
HDPE natural	183	188	2.7
HDPE pigmented	115	132	14.9
Total HDPE bottles	297	319	7.4
All plastic bottles	593	617	4.1

Recycling of rigid plastic containers has grown to about 1.4 billion pounds- 704 million pounds of waste HDPE and 649 million pounds of waste PET bottles, in 1997. The growth of plastics recycling can be seen in Table 2.4. [32]

However, the recycling rate has declined due to the factors currently limiting plastics recycling, such as collection and supply, including curbside collection, drop-off centers, buy-back centers, and container deposit legislation (i.e. bottle bills), and markets preferring the virgin resins priced very low. [34]

2.7.1.1 RECYCLING OF DURABLE MATERIALS

As opposed to most packaging and convenience goods which are discarded after a single use, durable materials tend to have a life of 3 or more years, including automobiles, computers, household applications etc. Their seperation, recovery and purification require several ateps and the volumes of such materials available for recovery are limited. Manufacturers of such products tend to use recycled materials as a part of their total material needs. [32]

2.7.1.2 DESIGN IN MATERIALS

It is the category that includes the components and the systems consisting of plastic, paper, metal, and natural products. Adhesives used in the assembly of the products often, prevent easy seperation of attached plastic parts. Designers are thus exploring new designs and material combinations to enhance the recyclability. [32]

2.7.2 THE RECYCLING OF POLY(ETHYLENE TEREPTHALATE) (PET)

PET, a polyester, has been known for many years since the first laboratory samples of this fiber were developed by a small English company in 1941. Then, this research was enlarged by the findings of Dupont on textiles in the 1950s, and the work of Goodyear introducing the first polyester tire fabric in1962s. In the late 1960s and early 1970s, polyesters were developed specifically in the area of packaging- film, sheet, coatings and bottles. [33]

The recycling of PET soft drink bottles began soon after their introduction in 1977. Over the past decades, the technology for recycling PET soft drink bottles has been advancing. Though the most commercial recycling systems, like water bath/hydrocyclone, solution/washing, and solvent/flotation processes depending on some flotation or hydrocyclone processes to seperate the PET from HDPE base cup-resin, have been developed. The commercial types of recycling systems were designed to process PET at the rate of 10-40 million pounds ($4\text{-}18\times10^3$ tons) per year. [33]

2.7.3 CHARACTERISTICS OF RECYCLED PET AND PET MARKETS

PET is a linear molecule existing either in an amorphous or a crystalline state. In crystalline state, the molecules are highly organized and form crystallites extending no more than a few hundred angstrom units. The crystallinity in the PET soft drink bottle is normally about 25%. Molecules of either amorphous or crystalline can be unaxially or biaxially oriented. In each case, orientation greatly increases the strength of PET, because strain induced orientation usually imparts some crystallinity.

The crystallization rate of PET is of great concern in processing. This feature greatly affects the product clarity and processability. Recycled PET has to be considered with its intrinsic viscosity value, its aluminum content and its color. Generally, contamination with paper fibers from the labels and HDPE, incompatible with PET producing a hazy material, from base cups is minimal. The most troublesome contaminants present in PET bottles are the adhesives used for the labels and the base cup. Often, these residues are trapped in the PET granules and remain there after washing. Since these adhesives darken when treated at PET extrusion temperatures, the recycled PET becomes discolored and hazy. [33]

2.7.4 EFFECTS OF CONTAMINANTS ON PET REPROCESSING

During processing, PET undergoes three different degradation phenomena, namely thermal, mechanical, and hydrolytic chain scission including chemical and oxidative degradation. The latter is the fastest and the most destructive process leading to a remarkable molecular weight reduction, besides the mechanical property deterioration, as a result of the presence of small amounts of water or other polymeric contaminants, such as PVC. [35]

Degradation causes the reduction in physical properties, surface defects, and process instability increasing the machine wear. Even if the most sophisticated techniques being used today cannot achieve a PVC content lower than 100ppm. Polyvinylchloride (PVC), easily degrades at normal processing temperatures, releasing hydrochloric acid (dechlorination) which occurs more rapidly in the presence of oxygen atmosphere. [36]

Hydrolysis catalysts are acids or bases promoting mechanism at elevated temperatures but below 205 ^{o}C. Once it occurs, the reaction, between ester bonds and the retained moisture, is autocatalytic. Degradation of the polymer chain leads to low molecular weight polymers with carboxylic acid end groups causing the further hydrolysis. [33]

The effect of moisture content (even of 0.005% or less) is a still important factor causing a modest reduction of molecular weight of the PET, shown in Figure 2.13.

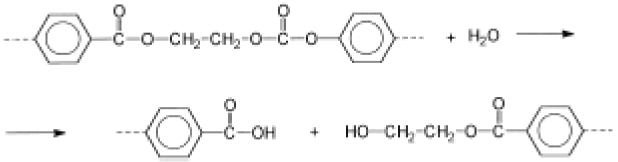

Figure 2.11 Chain cleveage due to the moisture content [36]

Other troublesome contaminants in PET bottles are the adhesives used for the labels and the base resin cup. Often, these residues are trapped in the PET granules and remain there after washing. These are typically hot melt adhesives normally contain rosin acids and esters, rosin, EVA (Ethylene vinyl acetate), acrylic derivatives, and some elastomers. During treating PET at extrusion temperatures, these adhesives are darken leading the recycled PET discolored and hazy. [33]

2.8 CHARACTERIZATION OF POLYMER/CLAY NANOCOMPOSITES

In order to obtain some points about the characteristic properties of the materials produced, we need some methods testing the specifications which allow us to describe the requirements.

Main purpose of a standard is to make a bridge between thoughts with using same language to communicate. [37]

The product specifications, such as mechanical properties (tensile, flexural, and impact) thermal properties (T_g, T_d, T_m etc.) and morphological properties (homogeneity etc.), can be expressed using standard test methods defined by authorized foundations, like the American Society for Testing and Materials (ASTM).

2.8.1 MECHANICAL TESTS

The mechanical properties are often the most important sources to make a decision about product specifications. The material selection for a variety of end-use applications is mostly dependent on these properties, such as tensile strength, modulus, elongation and impact strength. [37]

2.8.1.1 TENSILE TESTS (ASTM D 638-91a)

Tensile test is a measurement of the ability of a material to applied forces tending to pull it apart and observe the extent of material stretches before breaking. Different types of plastic materials are often compared based on tensile property data (i.e. strength, modulus, and elongation data). [37]

As a testing machine, the machine of a constant-rate-of-crosshead movement, containing a stationary member carrying one grip, and a movable member carrying the second grip, is used. The test specimens are mostly either injection or compression molded. Test specimen dimensions vary considerably depending on the requirements and are described in related section in the ASTM book of standards. The specimens are conditioned using standards of procedures. The recommended test conditions are 23±2 ^{o}C as a standard laboratory atmosphere and 50±5 percent relative humidity. [37]

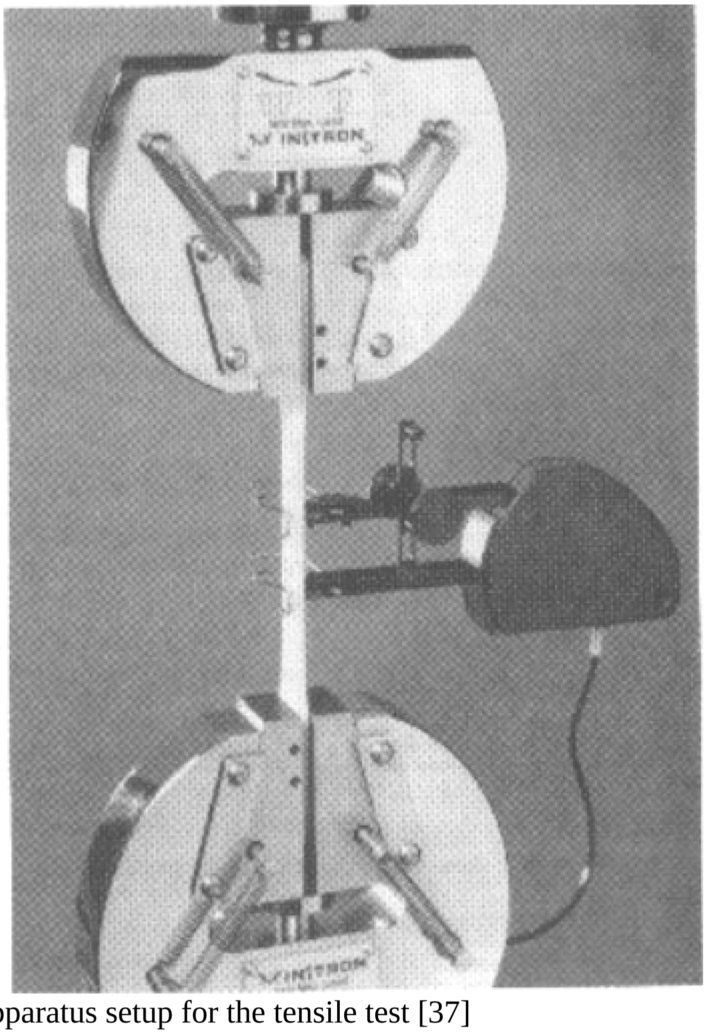

Figure 2.12 Apparatus setup for the tensile test [37]

There are basically five different testing speeds mentioned in the ASTM D638 Standard. As the specimen elongates, the resistance to the tension increases, and it is detected by a load cell. The tensile strength can be calculated by dividing te maximum load in newtons by the original minimum cross sectional area of the specimen in square millimetres, and the result can be explained in the term of megapascal (MPa). The tensile strength at yield and at break (ultimate value) are calculated. [37]

$$\text{Tensile Strength} = \frac{\text{Force (Load) (N)}}{\text{Cross Section Area (mm}^2\text{)}} \tag{2.1}$$

$$\text{Tensile Strength at Yield (MPa)} = \frac{\text{Max. Load recorded (N)}}{\text{Cross Section Area (mm}^2\text{)}} \tag{2.2}$$

$$\text{Tensile Strength at Break (MPa)} = \frac{\text{Load recorded at break (N)}}{\text{Cross Section Area (mm}^2\text{)}} \tag{2.3}$$

Tensile modulus and elongation values are derived from the stress-strain curve. If the specimen gives a yield load larger than the load at break, percent elongation at yield is calculated; if not, percent elongation at break is calculated. [38]

$$\text{Strain} = \frac{\text{Change in Length (elongation)}}{\text{Original Length (gauge length)}}$$

$$\varepsilon = \frac{\Delta L}{L} \tag{2.4}$$

$$\text{Elongation at yield} : \Delta L = \varepsilon \underset{\text{on the x-axis}}{\text{(the value at the yield point)}} * L \tag{2.5}$$

$$\text{Percent Elongation at yield} = \Delta L * 100 \tag{2.6}$$

Tensile modulus (the modulus of elasticity) can be determined by extending the initial linear portion of the load-extension curve and dividing the difference in stress obtained from any segment of section on this straight line by the corresponding difference in strain, expressing the result in the unit of megapascal (MPa). [38]

$$\text{Tensile Modulus} = \frac{\text{Difference in Stress}}{\text{Difference in corresponding Strain}} \qquad (2.7)$$

2.8.1.1.1 FACTORS AFFECTING THE TEST RESULTS

The employed process to prepare the specimens and the molecular orientation has a significant effect on tensile strength values. A load applied parallel to the direction of molecular orientation may yield higher values than the load applied perpendicular to the orientation. Injection molded specimens generally yield higher values than the samples molded in compression.

As the strain rate, the change in strain value per unit time, is increased the tensile strength and modulus values increase.

The tensile properties of some plastics change with small changes in temperature. Tensile strength and modulus decrease while elongation at break is increases by the temperature increase. [37]

2.8.1.2 FLEXURAL TESTS (ASTM D790M)

Flexural strength is the ability of the material to applied bending forces perpendicular to the longitudinal axis of the specimen. The stresses induced by flexural load are a combination of compressive and tensile stresses (Figure 2.15), and properties are calculated in terms of the maximum stress and strain occuring at the outside surface of the test bar. [37] These test methods are generally applicable to rigid or semirigid materials. [39]

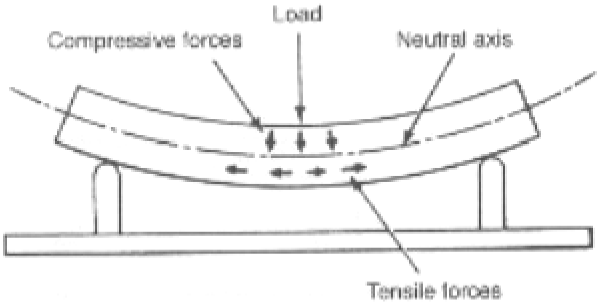

Figure 2.13 The stresses on the sample during flexural testing [37]

Two basic methods, including a three-point loading system utilizing center loading on a sample supported beam, and a four-point loading system utilizing two load points, are employed to determine the flexural properties. The former is designed particularly for materials undergoing small deflections, whereas the latter particularly for materials with large deflections during testing. [36] The test specimens used for flexural testing are obtained from sheets, plates or molded shapes by cutting as bars with rectangular cross section. [39]

Flexural strength is egual to the maximum stress in the outer fibers at the moment of break, and calculated using the following equation,

$$S = \frac{3PL}{2bd^2} \tag{2.8}$$

where; S is the stress in the outer fibers at midspan (MPa), P is the load at a given point on the load-deflection curve (N), L is the support span (mm), b and d are the width and the depth of beam tested,respectively (mm).

The max. strain in the outer fibers occurs at midspan is calculated as follows,

$$r = \frac{6Dd}{L^2} \tag{2.9}$$

where; r is the maximum strain in the outer fibers (mm/mm), D is the maximum deflection of the center of the beam (mm), L is the support span (mm), and d is the depth of the sample (mm).

The modulus of elasticity is the ratio, within the elastic limit of stress to corresponding strain, and can be represented by the slope of the initial straight-line portion of the stress-strain curve, calculating as follows. [39]

$$E_b = \frac{L^3 m}{4bd^3} \qquad (2.10)$$

where; E_b shows the modulus of elasticity in bending (MPa), L is the support span (mm), b and d are the width and the depth of beam tested,respectively (mm), and m is the slope of the tangent to the initial straight line portion of the load-deflection curve (N/mm).

2.8.1.2.1 FACTORS AFFECTING THE TEST RESULTS

The specimen with high degree of molecular orientation perpendicular to the applied load will show higher values than the one which is parallel to the applied load with the parallel ones. Another factor is the environmental temperature; there is an inverse proportion between it and the flexural strength and modulus. In addition, the strain rate (depend on testing speed), sample thickness and the distance between supports (span) can affect the results. [37]

2.8.1.3 IMPACT TESTS (ASTM D 256)

The impact properties of the polymeric materials depend mainly on the toughness of the material. Toughness can be described as the ability of the polymer to absorb applied energy. The molecular flexibility has a great significance in determining the relative brittleness of the material. Impact energy is a measure of toughness, and the impact resistance is the ability of a material to resist breaking (fracture) under a shock-loading. [37]

Two basically different test methods, namely Izod type and Charpy type, are used generally. In Izod type testing, the specimen is clamped vertically to a cantilever beam and broken by a single swing of the pendulum released from the fixed distance from the specimen clamp. (Figure 2.16) [40]

In the Charpy-type test method, the specimen is supported horizantally and broken by a single swing of the pendulum in the midlle. (Figure 2.17) [40]

The results are expressed in terms of kinetic energy consumed by the pendulum in order to break the specimen. The breaking energy is the sum of energies needed to deform it, to initiate cracking, to propagate the fracture across it and the energy expanded in tossing the broken ends of the specimen. [37]

The impact strength is calculated by dividing the impact values obtained from the scale by the thickness of the specimen. One point indicating the advantages of the Charpy test over an Izod test is that the specimen does not have to be clamped, therefore, it is free of variations in clamping pressures. [37]

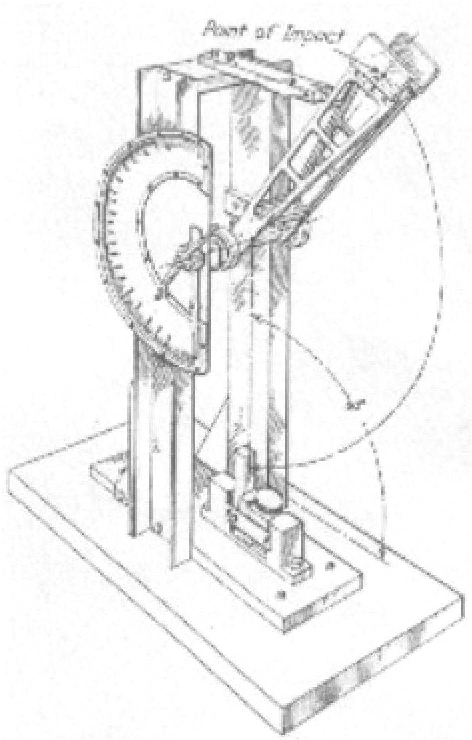

Figure 2.14 Cantilever Beam (Izod-Type) Impact Test Machine [40]

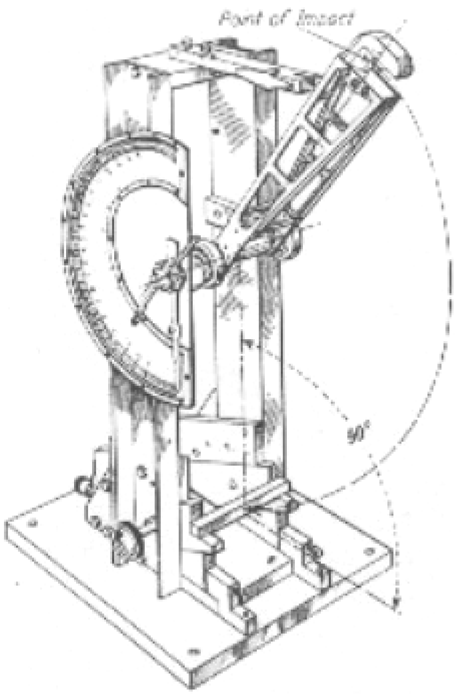

Figure 2.15 Simple Beam (Charpy-Type) Impact Test Machine [40]

2.8.1.3.1 FACTORS AFFECTING THE IMPACT STRENGTH

The rate of loading has a significant effect on the behaviour of the polymer during testing. At high rates of impact, even rubber-like materials may exhibit brittle failure. All plastics are notch-sensitive. A notch or a sharp corner in a fabricated part creates a localized stress concentration, therefore, both the notch depth and notch radius have an effect on the impact behavior. Larger radius will have a lower stress concentration, resulting in a higher impact energy of the base material. The temperature increase lowers the impact resistance drastically. The impact strength is usually higher in the direction of flow. In addition, processing conditions and types play an important role in determining the impact behavior as well as in the case of degree of crystallinity, molecular weight, and the method of loading. [37]

2.8.1.4 STANDARD DEVIATION

In order to indicate the deviation between the individual and an average values, a method, namely 'Standard Deviation', is used and can be calculated as follows, [39]

$$S = \sqrt{\frac{\Sigma X^2 - n(\overline{X})^2}{n - 1}} \qquad (2.12)$$

where; S is the estimated standard deviation, X is the value of single observation, n is the number of observations, and $\overline{X}$ is the arithmetic mean of the set of observations.

2.8.2 X-RAY DIFFRACTION (XRD) ANALYSIS

X-Rays are usually obtained by bombarding a metal target with a beam of high-voltage electrons inside a vacuum tube. Choice of the metal target and the applied voltage determines the output wavelength. X-Rays of a given wavelength are diffracted only for certain orientations of the sample. If the structures are arranged in an orderly array or lattice, the interference effects with structures are sharpened. The information obtained from scattering at wide angles describes the spatial arrangements of the atoms, while low angle X-Ray scattering is useful in detecting larger periodicities. X-Ray diffraction patterns of unoriented polymers are characterized by rings. As the specimen is oriented, these rings break into arcs, and this structure reaches the relatively sharp patterns at high degrees of orientation. [25]

Due to its easiness and availability, this technique is commonly used to research the nanocomposite structures. However, the XRD can only detect the periodically stacked montmorillonite layers; disordered (not parallel stacked) or exfoliated layers can not be detected, thus the only intercalated structures, where individual silicate layers are seperated by 2-3 nm, give rise in XRD while others remain silent. [19]

XRD measurements can characterize these structures if diffraction peaks are observed in the low-angle region, indicating the d-spacing of ordered-intercalated or delaminated nanocomposites. A schematic representation of the theory can be seen in Figure 2.18, where X-Ray beams of wavelength, λ, are incident on the planes of the layers at an angle, θ. These rays are scattered by atoms while constructive interference of them occur at the same angle, θ, to other planes. A whole number, n, of wavelengths are equal to the distance between SQ+QT. Angles of SQ and QT are also equal to the angle of diffraction. This method is characterized by Bragg's Law as follows, [41]

$$n\lambda = 2d\sin\theta \qquad (2.13)$$

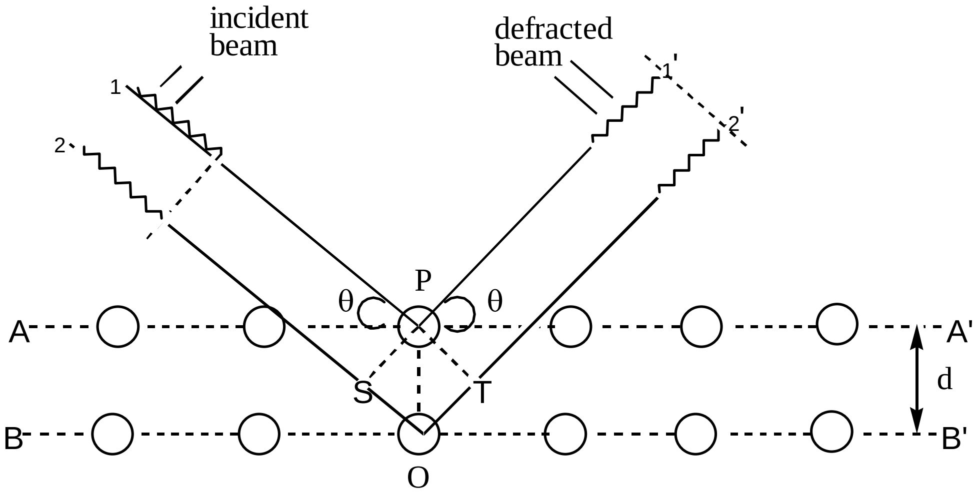

Figure 2.16 Diffraction of X-Rays by planes of atoms (A-A' and B-B') [41]

2.8.3 SCANNING ELECTRON MICROSCOPY (SEM)

Resolution of smaller objects can be provided from electron microscopy, allowing direct observation of thin specimens, like single polymer crystals, and the electron diffraction patterns. It is carried out in the conditions of temperature well below the room temperature and source of accelerated voltages (higher than the usual 50000 – 100000V) in order to prevent of damage to single polymer crystals. In scanning electron microscopy (SEM), a fine beam electrons is scanned across the surface of an opaque specimen. These photons are emitted when the beam hits to surface, then collected to provide a signal used to strengthen the intensity of the electron beam. [25]

In the case of nanocomposites, no peaks are observed in X-Ray analysis (XRD) in their disordered state due to lack in structural observation of the layers having large d-spacings. Thus, in such cases, scanning electron microscopy (SEM) yields more accurate results than XRD analysis in characterization. [42] Therefore, the use of

XRD and SEM methods yield the best result for morphological properties in testing such structures.

2.8.4 DIFFERENTIAL SCANNING CALORIMETER (DSC) ANALYSIS

Measurements of specific heat and enthalpies of transition can be carried out on quite small samples in a differential scanning calorimeter (DSC). In DSC, an average temperature circuit measures and controls the temperature of the sample and the reference holders to conform to predetermined time-temperature program. This temperature is plotted on one axis of an x-y recorder. During the experiment, the sample undergoes a thermal transition, the power supply to the two heaters is adjusted to maintain their temperatures, and a signal proportional to the power difference is plotted on the second axis of the recorder. The area under the resulting curve is a direct measure of the heat of transition. (Figure 2.19) [25]

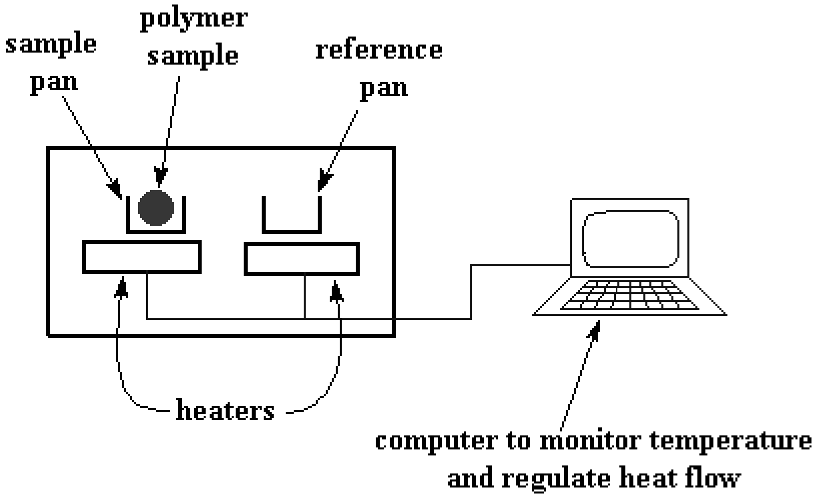

Figure 2.17 A schematic representation of DSC experimental setup

2.8.5 MELT FLOW INDEX (MFI) TEST

It is important to note that there is a critical treshold molecular weight to maintain the entanglement of the polymer chains. Melt viscosity is a measure of the tendency of melted materials to flow. Whereas the melt index is a measure of flow inversely related to melt viscosity and often described in particular terms such as the time for ten grams of material to pass through a standard orifice at a specified time and temperature. [43]

2.9 PREVIOUS STUDIES

2.9.1 STUDIES ON THERMOPLASTIC BASED COMPOSITE MATERIALS

Li et al., [44] prepared nanocomposites with a new approach. According to the method, common crystalline polymer blends were converted into stiff and strong nanofiber reinforced composites. A commercial high-density polyethylene (HDPE) and propylene (PP) were melt-mixed and extruded into thick tapes, which were drawn through a pair of steel rollers. The fibrillated profiles were processed at a high temperature between the melting points of the components. The fibrils of the polymer with higher melting point should survive and reinforce the polymer matrix formed due to the melting of the component with the lower melting point. With this way of processing, a pair of semicrystalline polymers with more widely spread melting points can provide a much wider processing window.

Gloaguen and Lefebvre, [45] examined the plastic deformation behaviour of thermoplastic/clay nanocomposites to gain some basic understanding on the deformation mechanisms. Two systems were considered in this study: the first one consisted of Nylon-6/clay hybrids prepared by in-situ polymerization and the second one was polypropylene/clay nanocomposite formed by melt processing. Dynamic viscoelastic measurements, plasticity results and morphological properties were obtained.

Sun et al., [46] reported the preparation of polypropylene composite with a new type of filler: rice husk(RH). The major inorganic component of the rice husk is silica (~20%) known to be highly pure. In this work, RH was directly used as filler in PP. The tensile strength increased while the impact strength decreased with the increasing filler loading. Torques and melt index (MI) of composites with various filler loading were investigated.

Zhu and Sternstein, [47] studied a series of composites of poly(vinyl acetate) (PVAc) filled with various types of fumed silica with different specific surface areas and surface treatments at and above the glass transition temperature. They showed that an increase in filler content or change in surface treatment has no effect on the relative relaxation time spectrum at the T_g. The dynamic shear data were examined showing interesting results in terms of modulus and loss factor.

2.9.2 STUDIES ON PET BASED MATERIALS

Ke et al., [48] studied the crystallization process and crystal morphology of poly(ethylene terepthalate) (PET) – clay nanoscale composites prepared by intercalation, followed by in-situ polymerization. Properties were investigated by scanning electron microscopy (SEM), transmission electron microscopy (TEM), dynamic scanning calorimetry (DSC) and X-Ray techniques, together with mechanical methods. In PET-clay nanoscale composites, the nanoscale ranged from 30 to 100nm. The exfoliated clay particles played a nucleating role and had strong interactions with PET molecular chains. Results of nonisothermal crystallization dynamics showed that the nano-PET have three times greater crystallization rate that of pure PET. The thermal properties showed heat distortion temperature (HDT) to be 20-50 ^{o}C higher than the pure PET.

Tornes et al., [49] compared the thermal properties (glass transition, melting point and crystallinity) and mechanical properties (Young’s modulus, elongation at break and impact strength) of post-consumer PET bottles, one arising from homogeneous and the other of heterogeneous deposites soiled by PVC, with those of the virgin resins before and after injection molding.The study focused on the mechanical recycling of post-consumer PET bottles. The presence of contaminants generated problems, such as cleavage of chains, an increase in carboxylic end groups, a reduction in molecular weight, a decrease in intrinsic viscosity leading to a decrease in mechanical properties.

Guozhen et al., [6] synthesized PET-clay hybrids with improved tensile strength with a new method. In this work, the hybridization of PET with montmorillonite(Mont) was investigated by using hydroxypenthyltrimethyl ammonium iodide (HPTA) as an ionic anchor monomer adsorbed onto clay surfaces by ion exchange instead of the simple mixing of the organo-clay with PET. The HPTA / Mont hybrid films were copolymerized with bis(hydroxyethyl terepthalate) (BHET) to form a tensile strength-improved PET-clay hybrid as well as to get optically transparent materials.

Abu-Isa et al. , [50], studied the development of impact strength characteristics of PET resin by adding aromatic phosphites, such as triphenyl phosphite (TPP), for blends of PET and elastomeric polyesters, such as block co-polymer of n-butyl terepthalate hard segment and ethylene oxide/propylene oxide soft segment or butyl acrylate-methyl methacrylate core shell polymer. Two grades of PET soft drink bottle regrinds, namely green and clear, and the pure one were employed for comparison, and similar results were obtained, such as impact strength improvement up to 60-fold increase, tensile strength and solvent resistance improvement.

Incarnato et al., [51], studied the structure and rheological behavior of recycled PET modified by reactive extrusion. The aim of this study was to increase the melt viscosity and the melt strength of PET scraps with a low intrinsic viscosity to obtain a grade suitable for film blowing or blow molding. PMDA was used as a chain extender to increase the molecular weight of the PET scraps, since it has a melting point (about 283 ^{o}C) near to that of PET, leading to branching. Extruder screw rotation speed determined the residence time of the polymer and the reactive blending effectiveness of the system.

2.9.3 STUDIES ON MELT PROCESSING OF NANOCOMPOSITES

Vaia et al., [52] examined the microstructure of various (ordered and disordered) polymer-organically modified layered silicate hybrids, synthesized via static polymer melt intercalation with X-Ray diffraction and transmission electron microscopy. The polymers utilized were polystyrene(PS) and poly(3-bromostyrene) (PS3Br). XRD results allowed for precise measurements of silicate layer spacing (1-4nm) and TEM and high-resolution transmission microscopy (HRTEM) provided information in real space on morphology, spatial distribution and defect structures influencing the transport of polymer into the silicate interlayer, movement of the layers into the polymer bulk and the potential number of favorable polymer-silicate interaction sites.

Results enhanced the understanding of various thermodynamic and kinetic issues surrounding hybrid formation.

Vaia and Giannelis, [29] studied the effect of silicate functionalization, anneal temperature, polymer molecular weight, and constituent interactions on polymer melt intercalation of a variety of styrene-derivative polymers in alkylammonium-functionalized silicates. The polymers utilized were polystyrene, poly(3-bromostyrene) (PS3Br), poly(vinylcyclohexane) (PVCH) and poly(2-vinylpyridine) (PVP). In this work, general guidelines of hybrid formation were established from the observations of an optimal interlayer structure for the organically-modified layered silicate (OLS), with respect to the number per host area and size of the alkylammonium chains, as well as the presence of polar interactions between the OLS and polymer. Entropic and energetic factors determined the outcome of polymer melt intercalation. Experimental results indicated that the outcome of polymer intercalation depends critically on silicate functionalization and constituent interactions.

Kawasumi et al., [53] studied the preparation and mechanical properties of polypropylene (PP)-clay hybrids (PPCH) by simple melt mixing of three components, i.e. PP, maleic anhydride modified polypropylene oligomers (PP-MA), and clays intercalated with stearylammonium. Since PP does not include any polar groups in its backbone, they reported a novel approach to prepare a PP-clay hybrid by using a functional oligomer with polar telechelic OH groups (PO-OH) as a compatibilizer to achieve the exfoliated and homogeneous dispersion of the silicate layers in the PP matrix. In the study, it was found that there are two important factors to achieve the exfoliation and homogeneous dispersion of the layers in the hybrids: (1) the intercalation capability of the oligomers in the layers, they should include a certain amount of polar groups, and (2) the miscibility of the oligomers with PP, the content of the functional groups in the oligomers affect the miscibility of it with PP.

Liu et al., [54] studied the preparation of Nylon-6/clay nanocomposites by a melt intercalation process. The properties of the Nylon-6/clay nanocomposites were superior to the Nylon-6 matrix in terms of the HDT, strength, and modulus without sacrificing its impact strength. Crystallization behaviour of the nanocomposites was studied by dynamic scanning calorimetry. The nanostructure features were revealed by X-Ray diffraction analysis, transmission elctron microscopy (TEM) and Molau testing, showing the dispersion state of samples in formic acid solutions.

Huang et al., [55] prepared Polyimide-MMT(montmorillonite) nanocomposites by melt blending an organo-modified MMT with a thermoplastic poly(etherimide) (PEI) in an internal mixer in an attempt to improve the solvent resistance and thermal property of the PEI. An exfoliated morphology was verified using X-Ray diffraction and transmission electron microscopy. Owing to the molecular dispersion of the MMT layers and the strong interaction between PEI and MMT, the nanocomposites exhibited a substantial increase in glass transition (T_g) and thermal decomposition temperature, and a dramatic decrease in solvent uptake compared to virgin PEI.

Cho and Paul, [56] prepared Nylon-6/organoclay nanocomposites via direct melt compounding using a typical co-rotating twin screw extruder and compared the mechanical properties and morphology of these nanocomposites to similar materials made by in-situ polymerization process (composites containing glass fibers and untreated clay). They also investigated optimization of processing parameters such as processing temperature, residence time, and amount of shear. The mechanical properties of organoclay nanocomposites were significantly increased with marginal decrease of ductility (increase in the ductile-to-brittle transition temperature) and showed much greater values than glass fiber composites.

Dennis et al., [1] studied the effect of melt processing conditions on the extent of exfoliation in organoclay-based nanocomposites. This work demonstrated the importance of both the chemistry of the clay surface and how the clay was melt processed into the thermoplastic. Two different clay treatments (Cloisite 15A and 30B) were added to polyamide-6 using four different types of extruders (single screw, twin screw extruder [co- and counter-rotating intermeshing], and counter-rotating nonintermeshing). Characterization was done with X-Ray diffraction, TEM and mechanical property tests. The degree of dispersion was interpreted in terms of the residence time distribution in the extruder and intensity of shear. It was recognized that the extruder process conditions were important variables which must be optimized to affect a high degree of delamination and dispersion.

Fornes et al., [20] prepared organoclay nanocomposites based on three different molecular weight grades (low, medium and high) of Nylon-6 by melt processing using a co-rotating twin screw extruder. The purpose of this work was to examine the effect of Nylon-6 molecular weight on the properties of nanocomposites. These materials were characterized by TEM, X-Ray diffraction, and rheological measurements (dynamic and steady shear capillary experiments). This study also explored organoclay structure-property relationships, thermo-mechanical behaviour, and orientation effects in injection molded specimens.

Liu and Wu, [44] prepared the polypropylene (PP)/clay nanocomposites (PPCN) via grafting-melt compounding by using a new kind of co-intercalation organophilic-clay (epoxypropyyl metacrylate MMT) which had a larger interlayer spacing and reaction heat than the ordinarily organophilic-clay only modified by alkylammonium. One of the co-intercalation monomers was unsaturated so it could tether on the PP backbone by virtue of the grafting reaction. Co-intercalation process improves the dispersion effect of silicate layers in PP matrix confirmed by XRD and TEM. The addition of clay did not change the crystal structure of PP, they acted as nucleating agents for the crystallization of PP.

Lepoittevin et al., [57] studied the mechanical, thermal and rheological properties of poly(ε-caprolactone) nanocomposites (PCLN) prepared by melt blending the polymer with natural Na^+ MMT and MMT modified by hydrogenated tallow alkyl (HTA)-based quaternary ammonium cations: dimethyl 2-ethylhexyl(HTA) ammonium and methyl bis(2-hydroxyethyl) HTA ammonium. An intercalated/exfoliated structure was observed by both XRD and TEM analyses. Stiffness and thermal stability improved with the filler loading until a content of 5 wt%. Further loading resulted in the levelling off. A significant improvement in thermal stability of PCL was noted at very low clay content (1 wt%).

Shen et al., [58] compared the polymer-clay nanocomposites of poly(ethylene oxide)/Na-montmorillonite (PEO/MMT) and PEO/organo-modified bentonite (B34) systems prepared via solution intercalation and melt intercalation by XRD and Fourier transform infrared (FT-IR) analysis. FT-IR analysis showed no difference in spectrum of samples prepared by solution intercalation compared to melt intercalation. The PEO conformation in the PEO/clay intercalated hybrids was concluded to be a distorted helical structure.

Gilman et al., [59], developed a fundamental understanding of the fire retardancy mechanism for polymer/clay nanocomposites. Polystyrene in two different molecular weight grades were compounded with alkylammonium treated montmorillonite, imidazolium, and crown ether treated montmorillonite for comparison. The study demonstrated that the importance of degradation mechanism for organically modified montmorillonite during melt processing and examined the role of processing conditions, such as shear and design. Efforts on the development of organic treatments for montmorillonite and other nano-additives with improving processing stability were carried out. Delocalized imidazolium cation showed better thermal stability than the alkyl ammonium cation.

2.9.4 STUDIES ON SOLUTION METHOD OF PROCESSING OF NANOCOMPOSITES

Kojima et al., [2] synthesized Nylon-6-clay hybrid by montmorillonite intercalated with ε-caprolactam. Properties were characterized by the XRD, TEM and mechanical testings.

Yano et al., [3] reported the synthesis and properties of a polyimide/clay hybrid from a dimethyl acetamide (DMAC) solution of poly(amic acid) and a DMCA dispersion of MMT intercalated with an ammonium salt of dodecylamide. Material showed an excellent gas barrier properties and low thermal expansion coefficient.

Kojima et al., [4] examined the sorption of water in the injection-molded Nylon-6/clay hybrids to estimate the resistance to water permeation.

Messersmith and Giannelis, [5] reported the synthesis and barrier properties of Poly(ε-caprolactone) / layered silicated nanocomposites.

Usuki et al., [60] synthesized Nylon-6 / clay hybrid materials using four types of clay minerals; montmorillonite, saponite, hectrite and synthetic mica. The aim of this study was to clarify the origin of the difference in the mechanical properties among four Nylon hybrid materials.

Lee and Jang, [61] prepared a nanocomposite material by a simple technique of emulsion polymerization using MMA monomer and Na^+- MMT and characterized it by FT-IR, XRD, TGA, DSC and tensile testing.

Lee and Jang, [62] described the structure , synthesis, and thermal property of a hybrid-epoxy-clay nanocomposite prepared by a step type of polymerization in an aqueous emulsion media.

Zerda and Lesser, [63] prepared intercalated nanocomposites of modified MMT clay in a glassy epoxy by crosslinking with diamine curing agents. The goal of this study was to characterize the mechanical behaviour and thoughening mechanisms.

Chang and Park, [64] prepared poly(ethylene terepthalate-co-ethylene naphthalate) (PETN) hybrid films with four different organo-clays (C_{16}-MMT, DTA-MMT, Cloisite-25A and 30A) by solution intercalation method and compared them in terms of their thermal stabilities, mechanical properties, and morphology.

2.9.5 STUDIES ON IN-SITU POLYMERIZATION TECHNIQUE

2.9.5.1 Thermoplastics

Krishnamoorti and Giannelis, [65] studied the rheological properties of end-tethered polymer layered silicate nanocomposites. The series of delaminated hybrids based on poly(ε-caprolactone) (PCL) and Nylon-6 were examined.

Krishnamoorti et al., [66] studied the viscoelastic behaviour of in-situ derived polycaprolactone nanocomposites containing a high level of silicate concentration.

Liang et al., [67] worked on the nano-effect in in-situ Nylon-6 nanocomposites. 12-Aminododecanoic acid modified MMT was incorparated in Nylon-6 by in-situ polymerization. Mechanical and barrier prooperties were examined.

2.9.5.2 Thermosets

Arrighi et al., [68] investigated the dynamic properties of poly(dimethyl siloxane) (PDMS) filled with silica particles by quasielastic-neutron scattering.

Weimer et al., [69] reported the direct synthesis of dispersed nanocomposites by in-situ living free radical polymerization using a silicate-anchored initiator. PS was selected as a polymer.

2.9.6 STUDIES ON SOL-GEL TEMPLATING OF NANOCOMPOSITES

Carrado and Xu, [70] studied the in-situ synthesis of polymer-clay nanocomposites from silica gels. The polymers examined were poly(vinylpyrolidone) (PVP), hydroxypropyl methylcellulose (HPMC), polyacrilonitrile (PACN), polydimethyldialkylammonium (PDDA), and polyaniline (PANI). Polymer loadings were increased up to as high as 86 wt%,and were more useful for nanocomposite applications.

CHAPTER III

EXPERIMENTAL

3.1 MATERIALS

3.1.1 Organoclays

Experiments were carried out with three different types of montmorillonites, namely Cloisite 30B, 15A, and 25A, produced by Southern Clay Products. The thermo gravimetric behavior of samples, TGA diagrams, can be seen in Appendix F. These organoclay structures show differences in selection according to what degree of polarity they have. There is an increase in relative product hydrophobicity and a decrease in product polarity in the order of 30B, 25A, and 15A. Thus, the hydrophobicity resulted from different natures of organic modifiers affects the chemical compatibility between the polymer and the filler. Following sections describe the product properties of these clay types.

3.1.1.1 Cloisite Na^+

Cloisite Na^+ is a natural montmorillonite, showing the following characteristics.

Table 3.1 Properties of Cloisite Na^+

Treatment/Properties	Cloisite Na^+
Organic Modifier	None
Cation Exchange Capacity (CEC)	92.6meq/100g clay
% Moisture	< 2%
% Weight Loss on Ignition	7%
Density, g/cc	2.86

Typical Dry Particle Sizes: (microns, by volume)

10% less than: 2µ; 50% less than: 6µ; 90% less than: 13µ

X Ray Results: d_{001} =11.7Å

3.1.1.2 Cloisite 30B

Cloisite 30B is a montmorillonite modified with a ternary ammonium salt.

Table 3.2 Properties of Cloisite 30B

Treatment/Properties	Cloisite 30B
Organic Modifier *	MT2EtOH
Cation Exchange Capacity (CEC)	90 meq/100g clay
% Moisture	< 2%
% Weight Loss on Ignition	30%
Density, g/cc	1.98

The following figure shows the structure of organic modifier MT2EtOH.

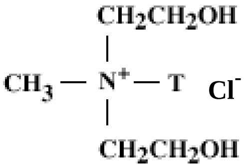

$$CH_3 - \overset{CH_2CH_2OH}{\underset{CH_2CH_2OH}{N^+}} - T \quad Cl^-$$

Figure 3.1 Chemical structure of Cloisite 30B organic modifier

Where T is Tallow (~65% C18; ~30% C16; ~5% C14)
Anion: Chloride

* MT2EtOH: methyl, tallow, bis-2-hydroxyethyl, quaternary ammonium

Typical Dry Particle Sizes: (microns, by volume)

10% less than: 2µ; 50% less than: 6µ; 90% less than: 13µ

X Ray Results: d_{001} =18.5Å

3.1.1.3 Cloisite 15A

Cloisite 15A is a montmorillonite modified with a quaternary ammonium salt.

Table 3.3 Properties of Cloisite 15A

Treatment/Properties	Cloisite 15A
Organic Modifier *	2M2HT
Cation Exchange Capacity (CEC)	125 meq/100g clay
% Moisture	< 2%
% Weight Loss on Ignition	43%
Density, g/cc	1.66

Following figure shows the structure of Cloisite 15A,

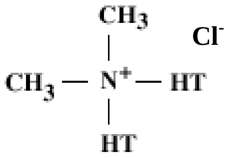

Figure 3.2 Chemical structure of Cloisite 15A organic modifier

Where HT is Hydrogenated Tallow (~65% C18; ~30% C16; ~5% C14)
Anion: Chloride

* 2M2HT: dimethyl, dihydrogenatedtallow, quaternary ammonium

Typical Dry Particle Sizes: (microns, by volume)

10% less than: 2µ; 50% less than: 6µ; 90% less than: 13µ

X Ray Results: d_{001} =31.5Å

3.1.1.4 Cloisite 25A

Cloisite 25A is a montmorillonite modified with a quaternary ammonium salt.

Table 3.4 Properties of Cloisite 25A

Treatment/Properties	Cloisite 15A
Organic Modifier *	2MHTL8
Cation Exchange Capacity (CEC)	95 meq/100g clay
% Moisture	< 2%
% Weight Loss on Ignition	34%
Density, g/cc	1.87

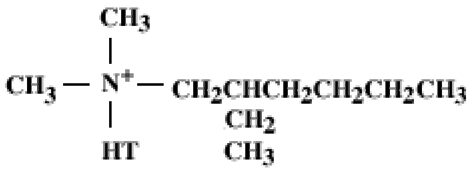

Figure 3.3 Chemical structure of Cloisite 25A organic modifier

Where HT is Hydrogenated Tallow (~65% C18; ~30% C16; ~5% C14)
Anion: methyl sulfate

* 2MHTL8: dimethyl, hydrogenatedtallow, 2-ethylhexyl quaternary ammonium

Typical Dry Particle Sizes: (microns, by volume)

10% less than: 2µ; 50% less than: 6µ; 90% less than: 13µ

X Ray Results: d_{001} = 18.6Å

3.1.2 PET Resin

PET soft drink bottle regrind was obtained from SASA Company in the form of flakes. General physical properties of the used PET are as follows, as specified by SASA.

Table 3.5 Properties of PET Resin

Contaminants	Value (ppm)
PVC	60
Polyethylene	5
Metal pieces	0
Adhesive	10
Paper pieces	3

Table 3.5 Properties of PET Resin (continued)

Lighting Characteristics	Value
Value L, Shining	66.1
Value B, Yellowness	2.6
Value A, Redness	-2.0

Table 3.5 Properties of PET Resin (continued)

Material Properties	Value
Intrinsic Viscosity, [η]	0.750 g/cm.s
Glass Transition Temperature, T_g	60 ºC
Melting Temperature, T_m	255 ºC – 260 ºC

3.2 PREPARATION OF NANOCOMPOSITE SPECIMENS

In the preparation of nanocomposite materials, the following steps shown in Figure 3.4 were carried out.

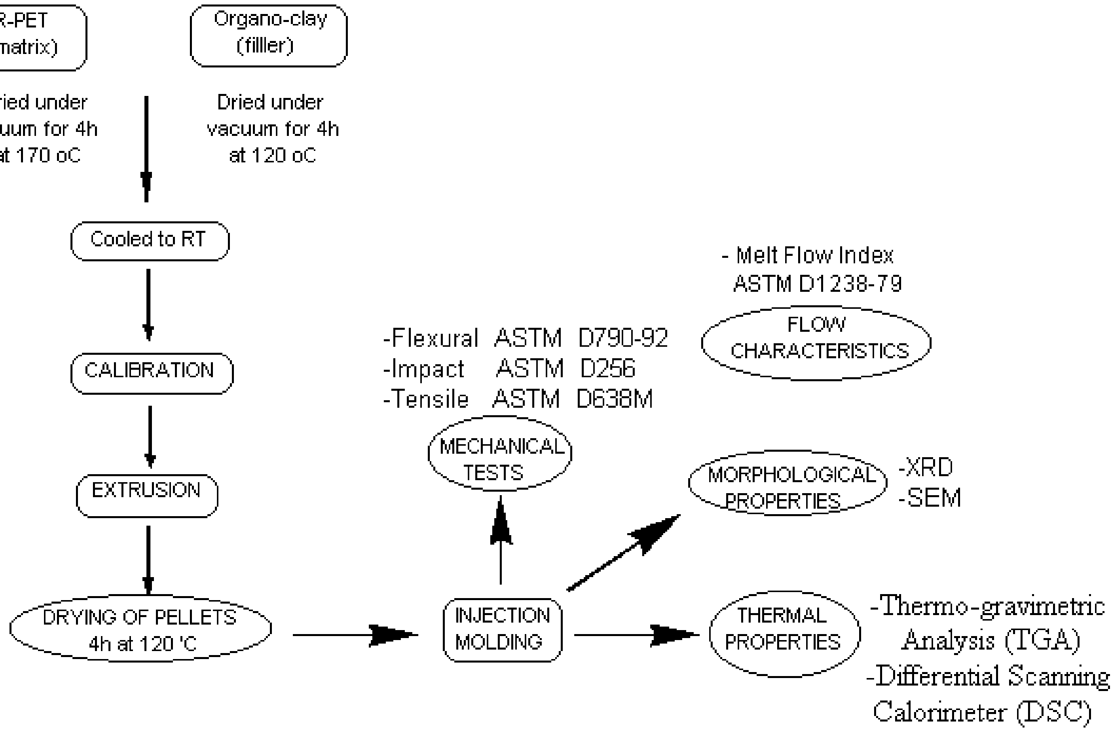

Figure 3.4 Flowchart of nanocomposite specimen preparation, and types of characterization methods used

Briefly the explanations are as follows:

Drying

Because of the sensivity of PET towards degradation by moisture, the resin was dried for 4 hours in a vacuum oven at 170 ^oC. The organo-clay capable of absorbing moisture was dried 4 hours at 120 ^oC. Before each injection molding process, the products needed to be dried in a vacuum for 4 hours at 120 ^oC.

Calibration of the Feeders

Calibration of the feeders mainly depends on the screw speed of each feeder on the extruder. The feeder rpm values were calibrated to get the proper feed rates of the materials. Before each extrusion step, the amounts of the resin and the filler must be balanced according to the percentage desired in the mixture.

During calibration, the feed rate of one of the materials was fixed constant, then the other one was balanced by taking this constant amount as the reference.

Extrusion

The ingredients were fed into the extruder barrel at previously determined speed of the feeders. The screw speed of the extruder was adjusted to three different rpm values, namely 150 rpm, 350 rpm, and 500 rpm, while other parameters were kept constant. Four temperature zones were adjusted and controlled for each extrusion process, optimum operating was obtained when the zone temperatures were kept at 275, 275,275, 250 ^oC in melting, mixing, metering, and feeding sections, respectively. The die temperature was kept at 280 ^oC in each extrusion process. The extrudates were cooled by water at the exit of the die, and then air-cooled, chopped, and stored until the molding process. Materials were vacuum dried for 4 hours at 120 ^oC before each molding process to avoid the effects of moisture. If these samples were stored in a desiccator over 24 hours, redrying in a vacuum oven for 4 hours at 120 ^oC was needed before the injection molding process.

Injection Molding

Keeping the temperature of the injection nozzle constant at 275 ^oC, previously extruded and chopped samples of R-PET/organoclay blends were injection molded.

Adjustments in mold fill time (3-8 sec), molding cycle time (3-5 min), and holding pressure (6-8.5 bars) were made in order to obtain the best-molded part appearance for each composition. Optimum values were 3 sec for fill time, 3 min for cycle time and 8.0 bars for holding pressure.

The samples obtained at the end of these production steps were analyzed and tested according to ASTM Standards, shedding light on three different aspects in material properties: namely mechanical, thermal, and morphological properties.

3.3 CHARACTERIZATION EXPERIMENTS

According to ASTM Standards, following tests were performed.

3.3.1 Morphological Analysis

3.3.1.1 Scanning Electron Microscopy (SEM) Analysis

Scanning electron microscopy (SEM) was performed on small pieces taken from the injection molded samples using a low voltage SEM (JEOL JSM-6400). The fracture surfaces of impact samples were coated with a thin layer of gold before SEM. The SEM photographs were taken at x250 and x3500 magnifications.

3.3.2 Mechanical Tests

Mechanical tests of all compositions were performed at room temperature. The average results and the standard deviations were calculated and reported.

3.3.2.1 Impact Tests

Charpy impact test was performed by using a Pendulum Impact Tester of Coesfeld Material Test; according to the test Method-I Procedure A in ASTM D256-91a (Standard Test Method for Impact Resistance of Plastics). Unnotched samples had dimensions of 50x7.50x2.00 mm, respectively.

3.3.2.2 Tensile Tests

Tensile tests were performed according to ASTM 638-M 91a (Standard Test Method for Tensile Properties of Plastics) by using a Lloyd 30K Universal Testing Machine.

The shape and dimensions conformed to Type M-I. The shape and dimensions of the specimens are given in Figure 3.5 and Table 3.6. The properties, namely tensile strength, Young's modulus, and strain at break values, were recorded at an extension rate of 8.00 mm/min giving a strain rate of 0.1 min^{-1}.

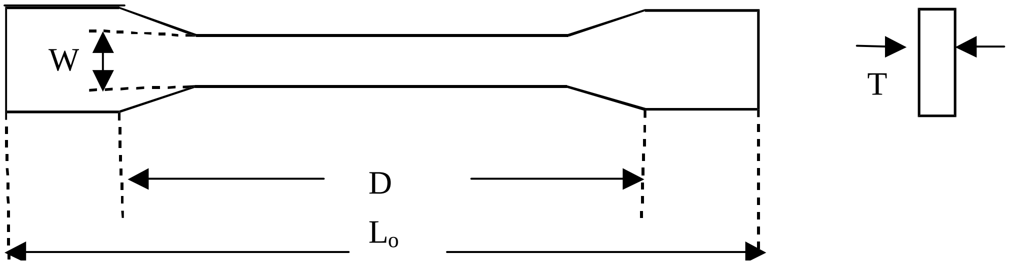

Figure 3.5 Tension Test Specimen (Type M-I)

Table 3.6 Tensile test specimen dimensions

Symbol, Term	**Dimensions (mm)**
D- Distance between Grips	80
L_o - Length Overall	112
W- Width of Narrow Section	7.50
T- Thickness	2.00

3.3.2.3 Flexural Tests

Samples were tested according to the Test Method-I Procedure A in the standard ASTM D790M-92 (Standard Test Method for Flexural Properties of Unreinforced and Reinforced Plastics and Electrical Insulating Materials). Dimensions were 80x7.50x2.00 mm as shown in Figure 2.15. Three point bending was conducted. The support span and the rate of crosshead motion were 50 mm, and 2.08 mm/min, respectively. This corresponds to a strain rate of 0.01 min^{-1}. Strength, strain at break, and modulus properties were studied.

3.3.3 Differential Scanning Calorimeter (DSC) Analysis

Differential scanning calorimeter (DSC) analyses were performed on the fractured pieces of the samples using a General V4.1.C DuPont 2000. Measurements were carried out in the temperature range of 20-280 °C with 20 °C/min heating rate under nitrogen atmosphere. The samples were cooled from 280 °C to 20 °C and reheated back to 280 °C. Thus, values obtained are referred to as Run1 and Run2. Changes in T_g and T_m values were observed according to the changes of clay type and content.

3.3.4 Melt Flow Index (MFI) Test

Melt flow index (MFI) test was performed according to ASTM Standards, ASTM D 1238-79, Condition type T, [71], with the pellets of the samples using a Haake Coesfeld Material Test machine. Measurements were carried out with the load of 2.16 kg at 275 °C, for both the barrel and the die. The method was based on determining the weight, in grams, of the sample that passes through a die in 10 min. Changes in viscosity values were evaluated for each composition and screw speed.

CHAPTER IV

RESULTS AND DISCUSSION

4.1 Morphological Analysis

In order to examine the structural properties, Scanning Electron Microscopy (SEM) was performed.

4.1.1 Scanning Electron Microscopy (SEM)

In order to examine the relationship between the morphological structure and the mechanical behavior of the samples, fracture surfaces of impact specimens were analyzed by Scanning Electron Microscopy (SEM).

Figure 4.1 shows the fracture surfaces of the pellets of amorphous unprocessed PET (APETp), amorphous extruded PET (APETe), and pure recycled-PET (R-PET) resins at magnifications of x250 and x3500. The surface of unprocessed amorphous PET is very smooth and the crack propagation lines can easily be seen on the photograph (a). In photograph (b), we can see the effect of prior extrusion on surface characteristics. Propagation lines are shorter and have dispersed outlook. This would lead to better impact resistance. In photograph (c), we see the fracture surface of recycled-PET (neat resin). There are long, distant, and wider crack propagation lines, due to the heterogeneous nature of the structure, including contaminants such as PVC, metal pieces, polyethylene etc. Except for polyolefin contaminants, they act as stress concentrators on the sample surface.

Figure 4.2 shows the fracture surfaces of samples containing 1, 2, and 5 weight % of Cloisite 30B at the speed of 150 rpm. In these photos, the main difference is the dispersion of the clay platelets. Due to the nature of high clay loading, 5-weight % sample exhibits a structure having large clay aggregates, which act as stress concentrators. This causes localized stresses on the surface of the clay leading to worse impact strength. In sample with 1 weight % clay, long crack propagation lines and clay aggregates, small white objects on the photo, can be observed. In comparison with the sample with 2-weight % clay loading, the surface looks smoother implying easier crack propagation. 2 weight % one has more tortuous structure preventing easy crack propagation.

Figure 4.3 shows the samples containing 2 weight % of 15A clay type processed at different screw speeds, 150, 350, and 500 rpm, respectively. Better clay dispersion is achieved at the speed of 350 rpm in general, as observed from the tortuous nature of the structure.

In the Figure of 4.4, we can observe the processing effect on structures having 2 weight % of 30B type montmorillonite. Three different screw speeds were studied, namely 150, 350, and 500 rpm. The main observation in this case is that the dispersion characteristics of clay changes with the processing speed. The one performed at the speed of 500 rpm exhibits much more smooth surface than the others. Clay particles were not dispersed well and large aggregates on this surface results in easy crack propagation. Crack propagation lines can clearly be seen in this structure at x3500 magnification. Among the other two, the one processed at 350 rpm shows more tortuous path and homogeneous dispersion of clay than the one processed at 150 rpm, leading to higher impact strength.

Figure 4.5 shows the samples containing 2 weight % of 25A clay type processed at three different screw speeds, 150, 350, and 500 rpm. In general, the product processed at 350 rpm exhibits the highest impact resistance, owing to better dispersion of clay. Distances between the crack propagation lines are much smaller than the other two samples.

If we compare the samples containing 2 weight %of 15A, 25A, and 30B clay types at the speed of 150 rpm, (a) photos of Figures 4.3, 4.4, and 4.5, we observe smaller distances between crack propagation lines and more disperse and tortuous characteristic in the composition containing 30B clay type. But, this structure gives lower impact energy than the one containing 25A clay type. The reason could be that, in the samples of 30B adhesion strength between the matrix and the filler may not be as good as the samples containing 25A montmorillonite at this screw speed, thus cracks in samples with 30B may need lower energy to propagate in spite of better dispersion. 15A samples give the lowest impact energy.

The same behavior can be seen at the speed of 350 rpm between the samples, (b) photos of Figures 4.3, 4.4, and 4.5. At the speed of 500 rpm, (c) photos of Figures 4.3, 4.4, and 4.5, in general 25A samples exhibit more tortuous pathway for propagations leading to higher stress absorbance. In the case of 15A and 30B samples, 30B clay type composition has smoother surface and larger clay aggregates acting as stress concentrators, thus easy propagation takes place.

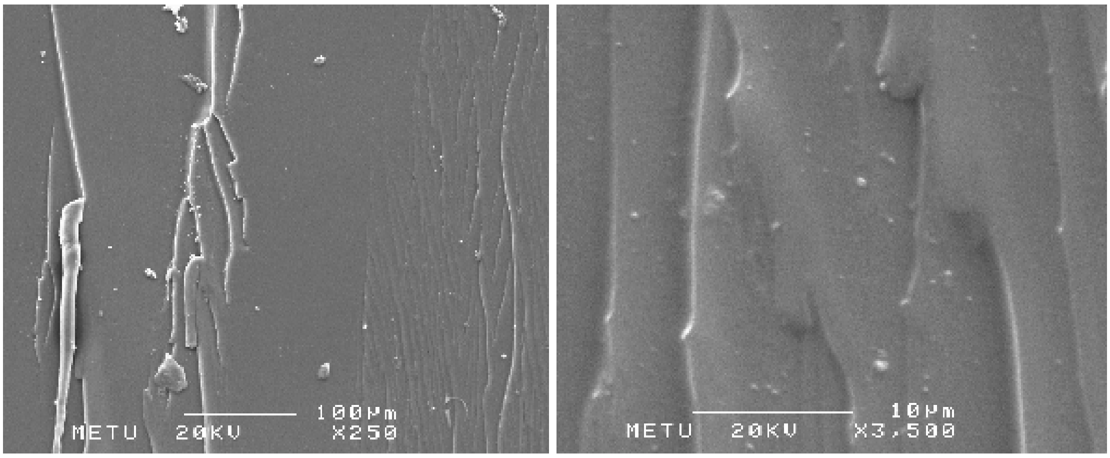

APETp-250 APETp-3500 (a)

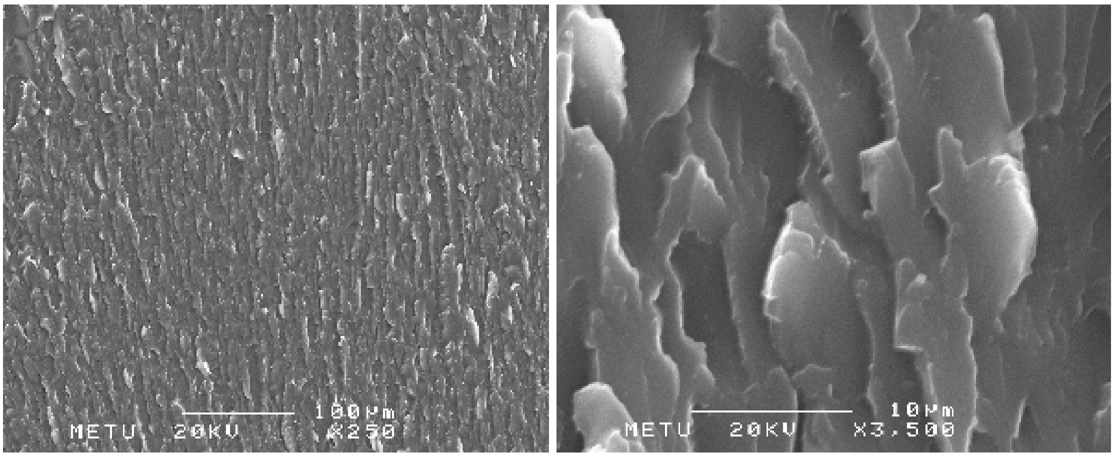

APETe-250 APETe-3500 (b)

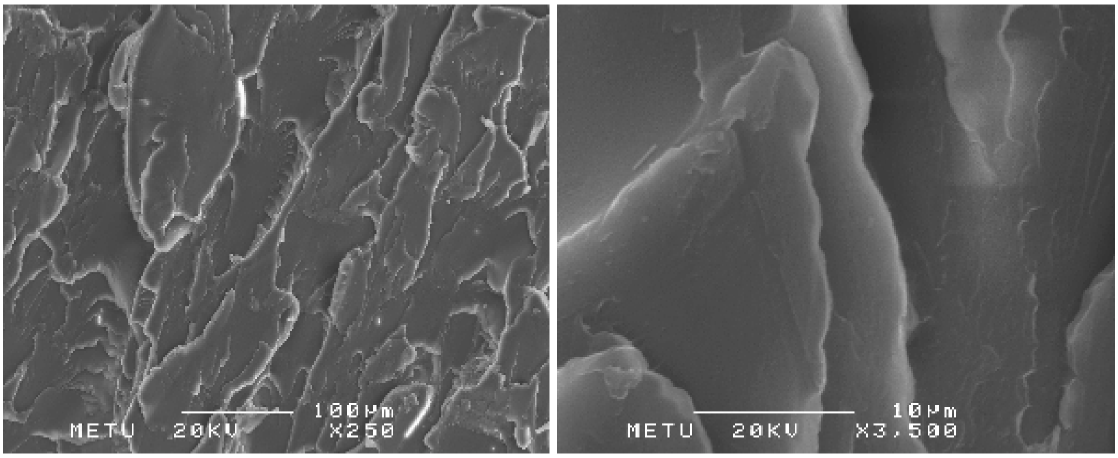

0%RPET150-250 0%RPET150-3500 (c)

Figure 4.1 Fracture surfaces of amorphous-PET in the form of unprocessed pellets and extruded samples (a, b), respectively, and unfilled recycled-PET (neat resin), (c), at 150rpm

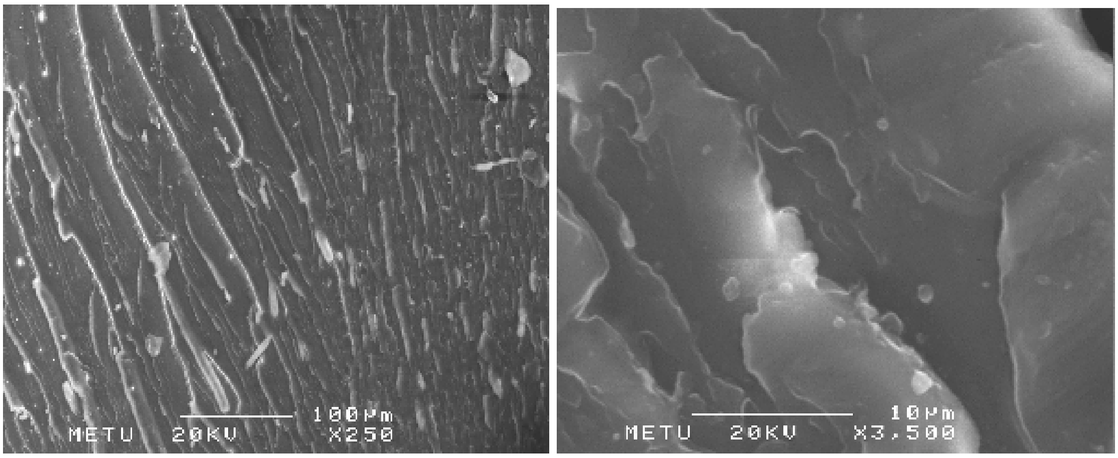

1%3OB150-250 1%3OB150-3500 (a)

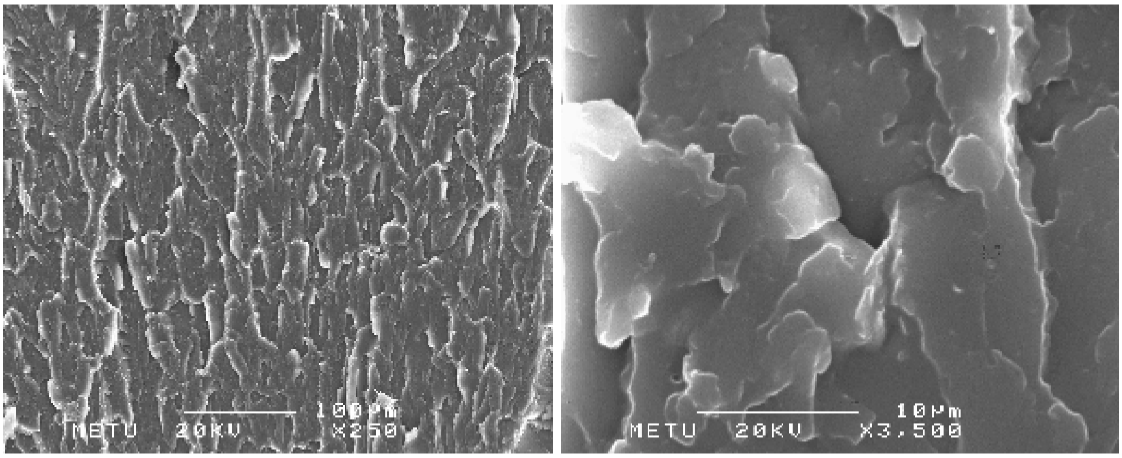

2%30B150-250 2%30B150-3500 (b)

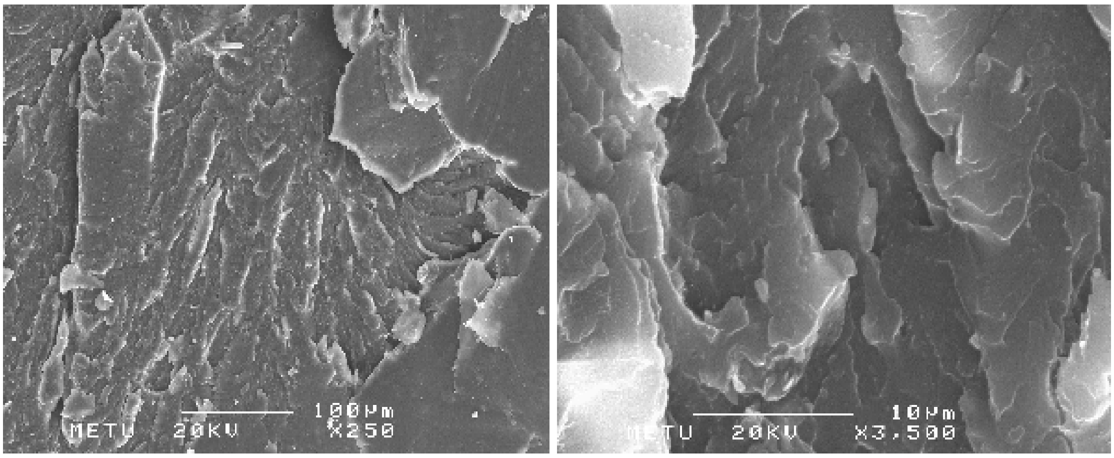

5%30B-250 5%30B-3500 (c)

Figure 4.2 Fracture surfaces of r-PET containing 1, 2, and 5 weight percents of Cloisite 30B, a, b, and c, respectively, at 150 rpm

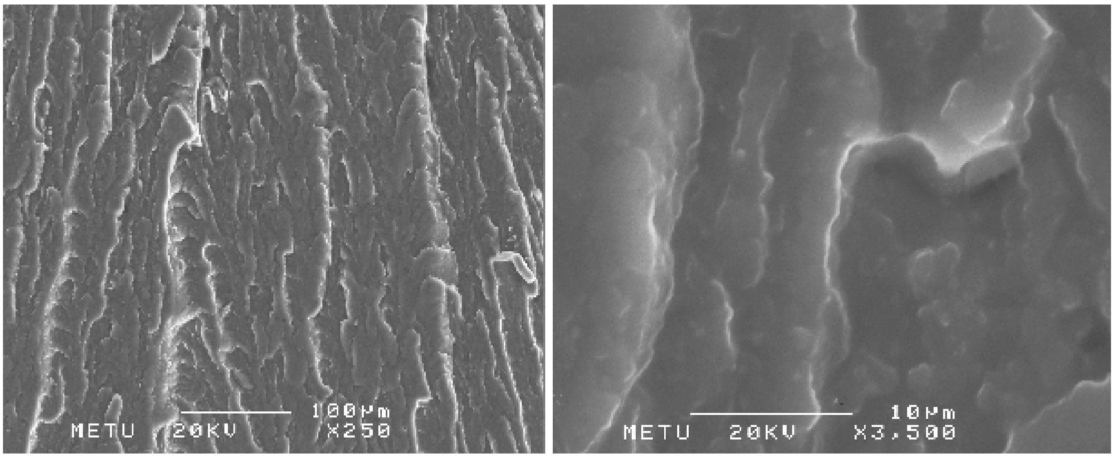

2%15A150-250 2%15A150-3500 (a)

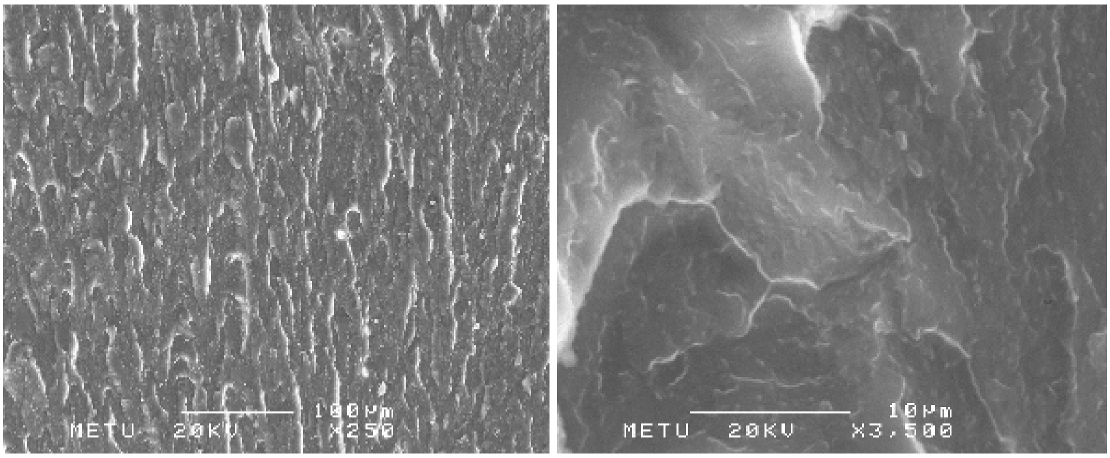

2%15A350-250 2%15A350-3500 (b)

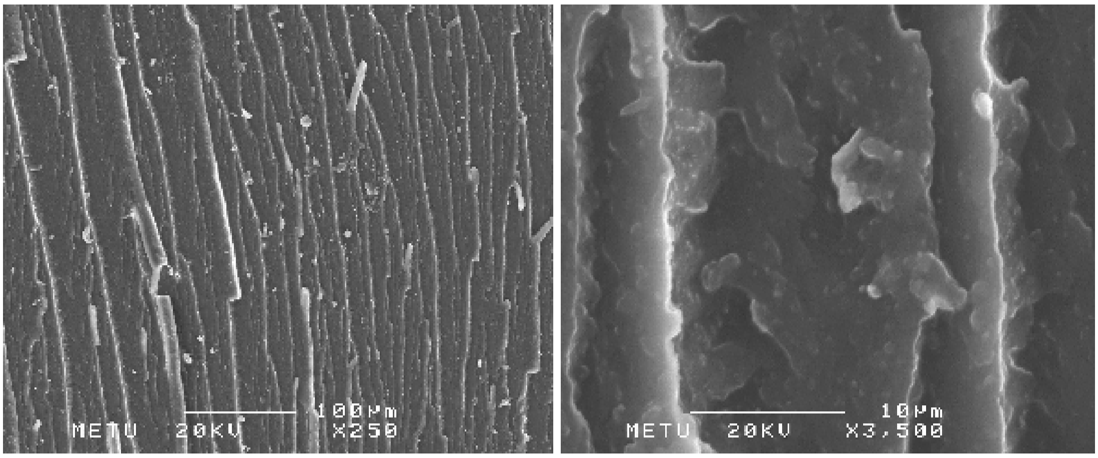

2%15A500-250 2%15A500-3500 (c)

Figure 4.3 Fracture surfaces of r-PET containing 2-weight % of Cloisite 15A at three different screw speeds, 150, 350, and 500 rpm, respectively

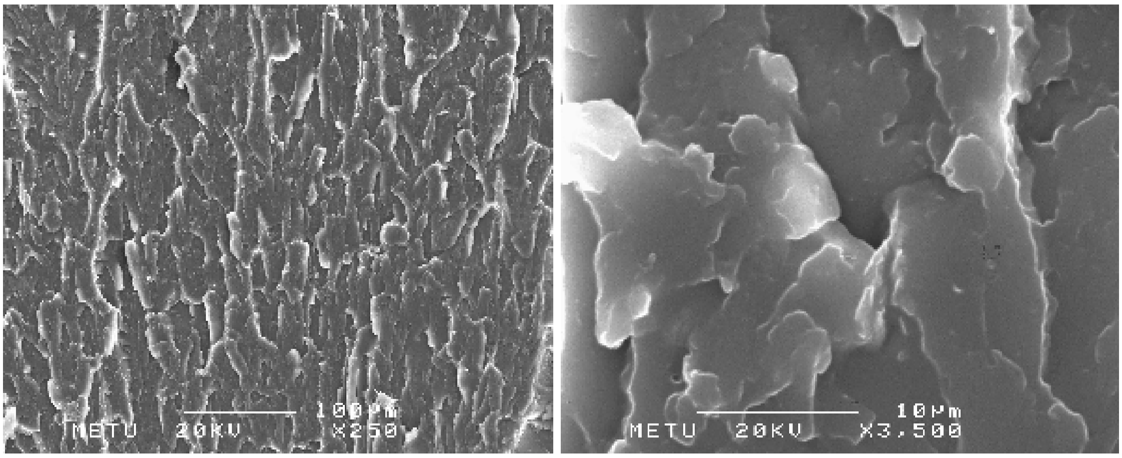

2%30B150-250 2%30B150-3500 (a)

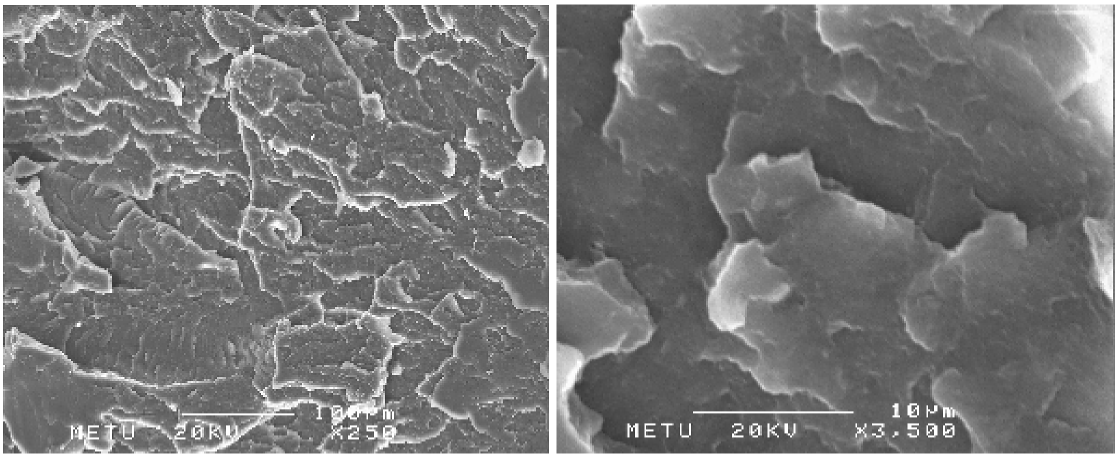

2%30B350-250 2%30B350-3500 (b)

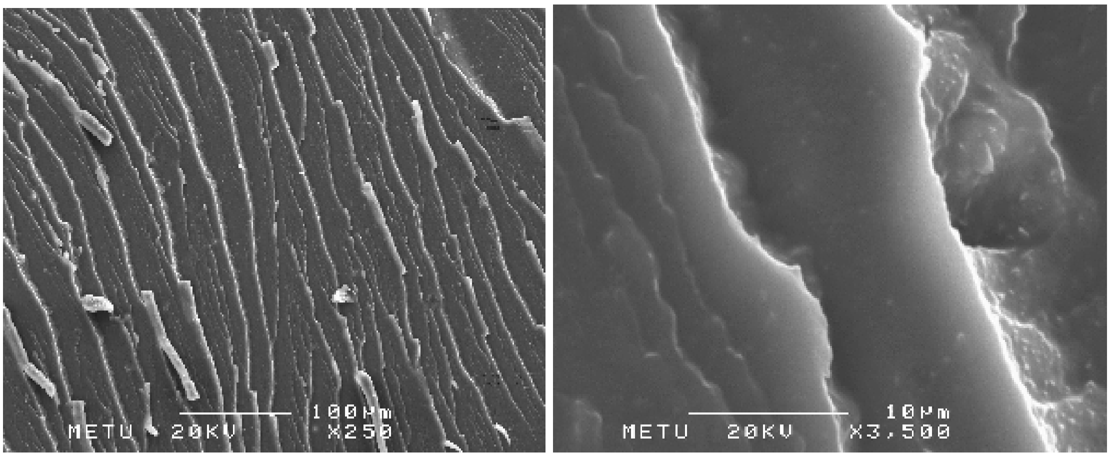

2%30B500-250 2%30B500-3500 (c)

Figure 4.4 Fracture surfaces of r-PET containing 2-weight % of Cloisite 30B at three different screw speeds, 150, 350, and 500 rpm, respectively

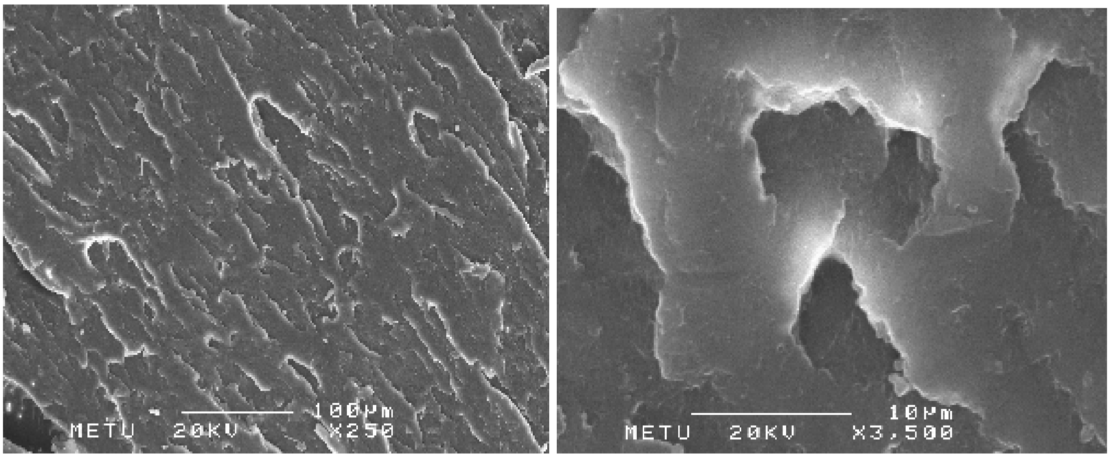

2%25A150-250 2%25A150-3500 (a)

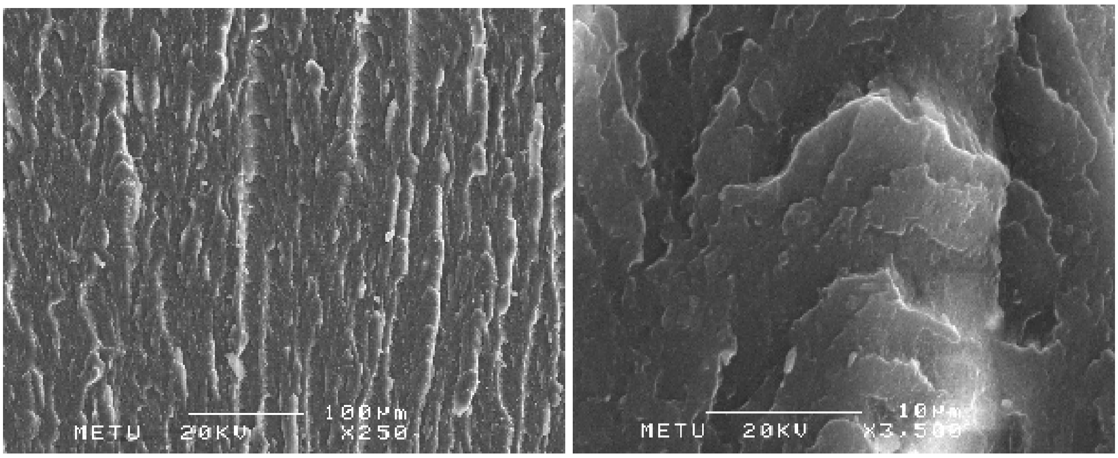

2%25A350-250 2%25A350-3500 (b)

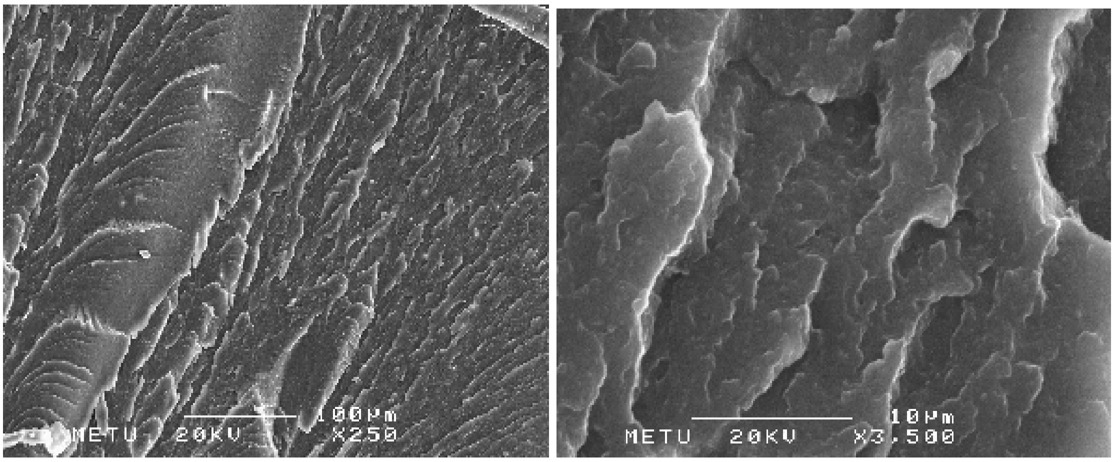

2%25A500-250 2%25A500-3500 (c)

Figure 4.5 Fracture surfaces of r-PET containing 2-weight % of Cloisite 25A at three different screw speeds, 150, 350, and 500 rpm, respectively

4.2 Mechanical Analysis

4.2.1 Impact Strength

This trend is primarily reflected from the fracture energies of materials. [20] The results in impact strength values change according to the structures of the filler and the matrix. Since the particle sizes are in nanometer scale, these structures act as crack stoppers and form tortuous pathways for crack propagation. This increases the ability of the material to absorb energy. In Figure 4.6, beyond a certain amount of clay content, impact strength values decrease due to aggregates of clay acting as stress concentrators. In other words, very high concentrations of stress can occur at the tips of cracks, further, leading to crack development, and decrease an impact resistance of the material. In Figure 4.6, 2 weight % of clay content leads the highest level of strength value when compared to its pure resin (r-PET) and other clay contents.

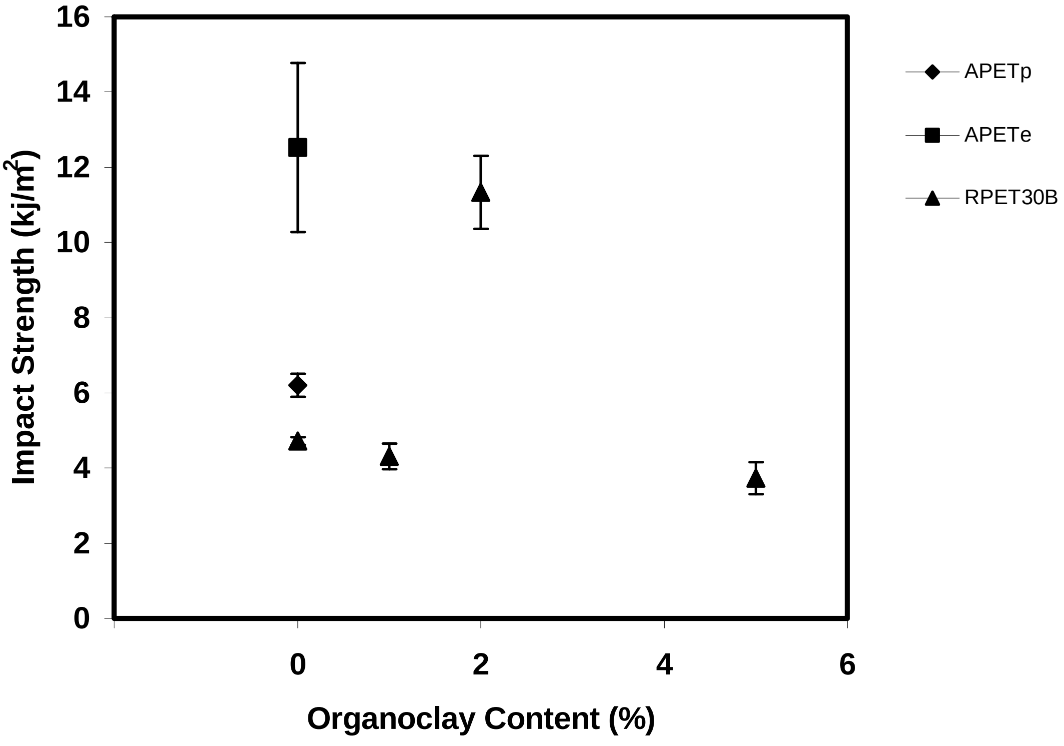

Figure 4.6 Effect of organoclay content on impact strength

In the case of 0 weight clay percentages, namely APETp, APETe, and RPET, the extruded pellets of amorphous PET (APETe) give an impact strength value nearly two times greater than pellets not extruded. The MFI results discussed later indicate that APETe has greater MFI than that of APETp. Thus, the molecular weight of APETe is smaller than the molecular weight of APETp. This makes APETe more impact resistant. RPET gives the lowest value due to contaminants in its content acting as stress concentrators.

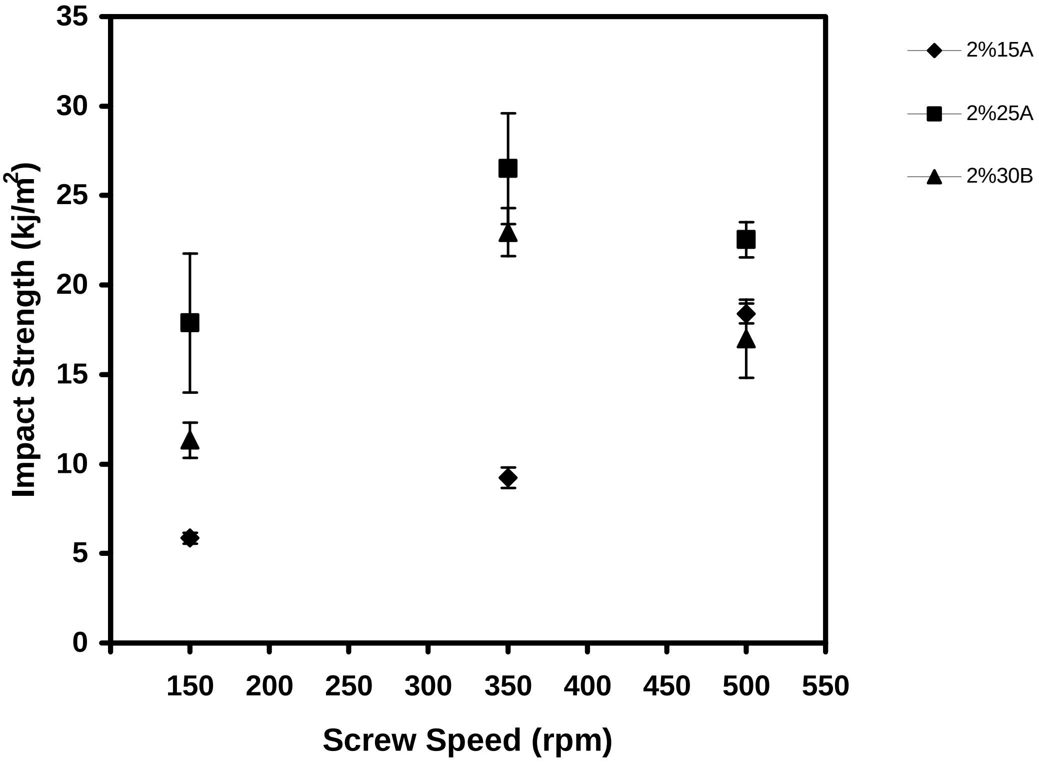

Figure 4.7 Effects of clay type and screw speed on the impact strength

Figure 4.7 shows the effect of processing speed on impact resistance of materials. Screw speed actually has a huge effect on the dispersion mechanism as well as the residence time and distribution, and shear intensity inside the extruder barrel. Higher rpm implies higher shear intensity, but lower residence time in the barrel. As seen in Figure 4.7, the highest values are obtained at the speed of 350 rpm in the clay types of 25A and 30B, but there is a continuous increase in the impact strength of sample containing the clay type of 15A. Increasing the speed to 500 rpm in clay types of 25A and 30B gives worse results. This is due to the shorter residence time observed at this speed. Silicate platelets was not completely delaminated in this short residence time, thus forming clusters of clay resulting in lower mechanical properties. In 15A clay type, which is partially compatible, high screw speeds are needed for high levels of exfoliation, thus high rpm yields positive effect on impact resistance.

4.2.2 Tensile Properties

This feature is illustrated in Figures between 4.8 through 4.17 showing the effects of clay content, clay type, and screw speed on tensile properties.

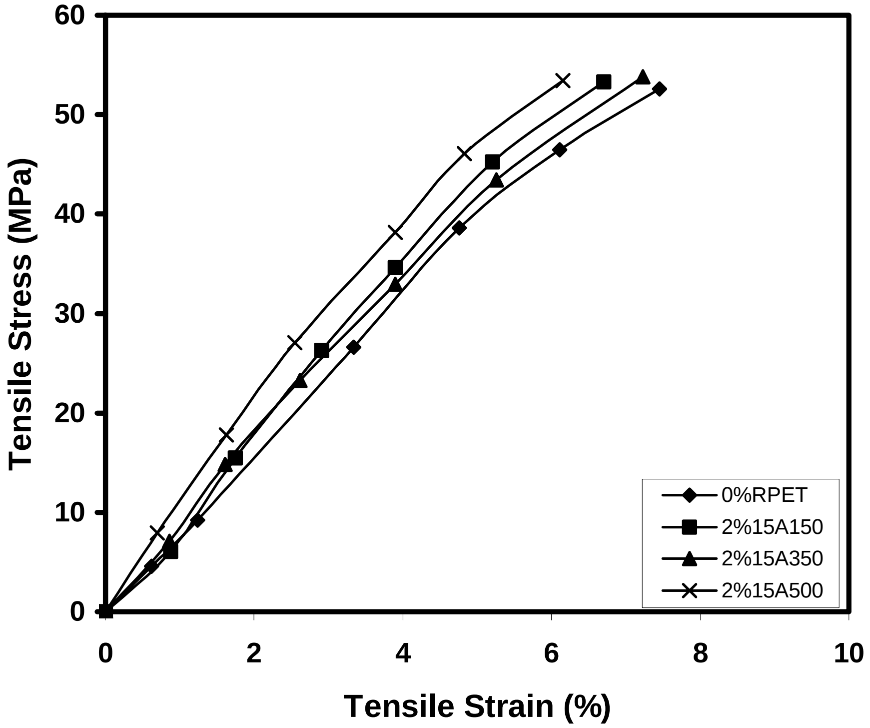

Figure 4.8 Stress-strain behavior of pure resin and nanocomposites containing 2-weight % of 15A clay type at indicated screw speeds

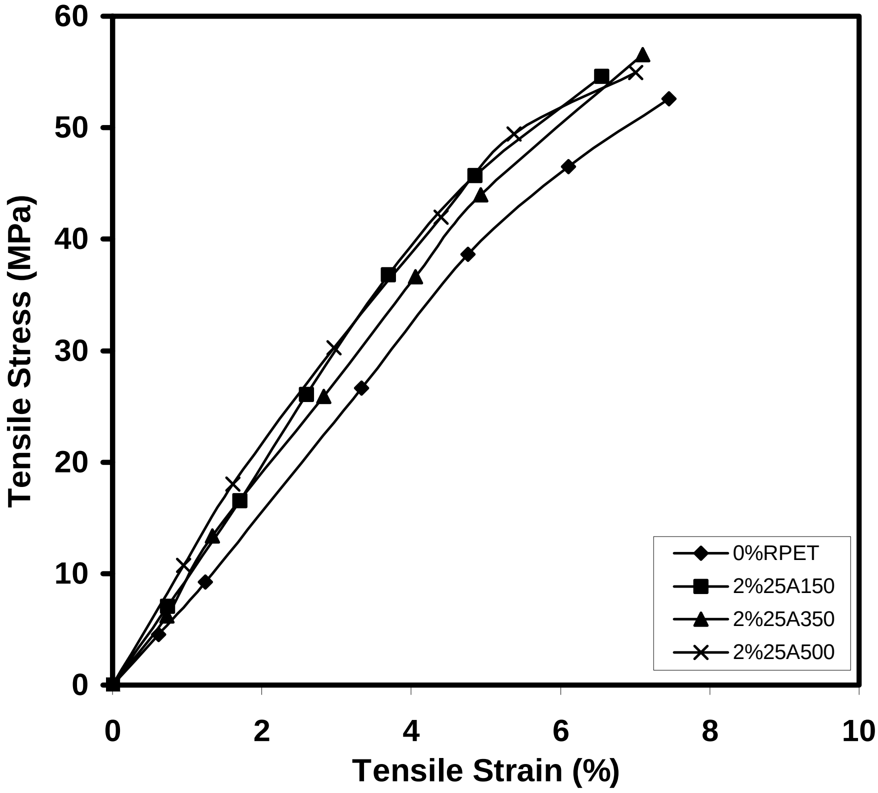

Figure 4.9 Stress-strain behavior of pure resin and nanocomposites containing 2-weight % of 25A clay type at indicated screw speeds

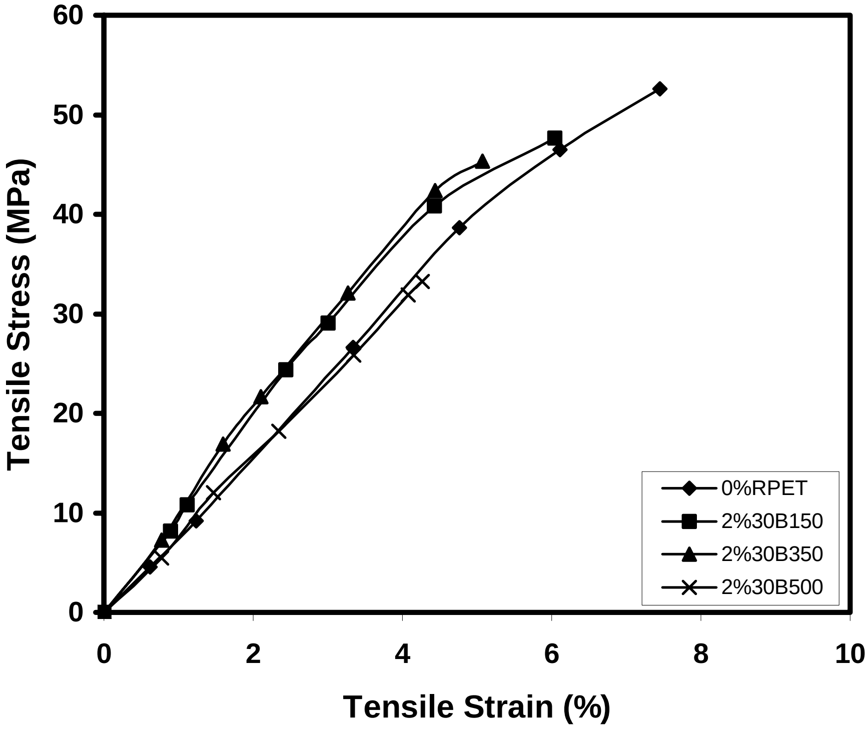

Figure 4.10 Stress-strain behavior of pure resin and nanocomposites containing 2-weight % of 30B clay type at indicated screw speeds

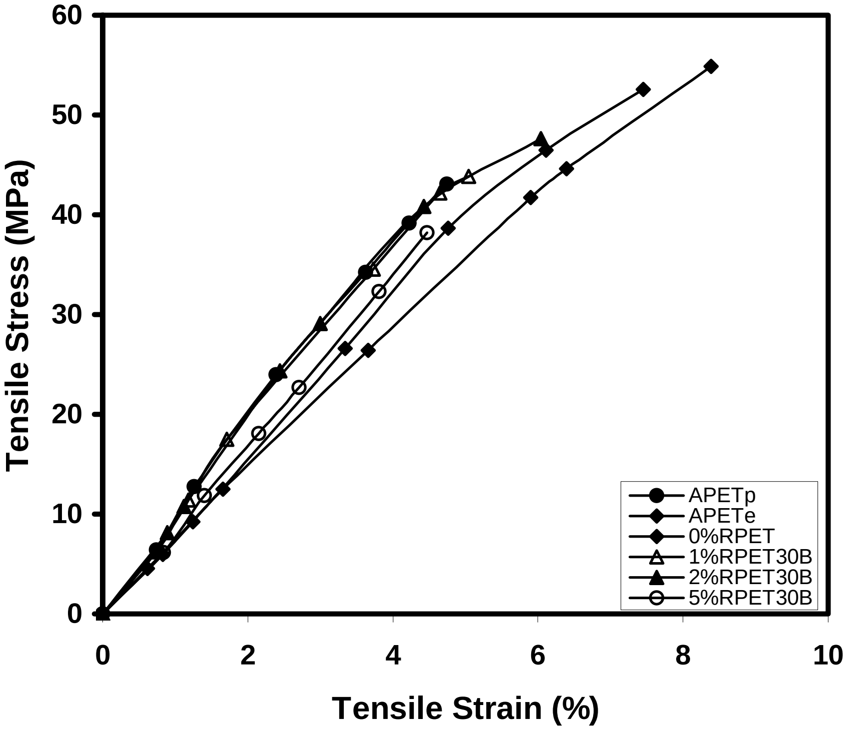

Figure 4.11 Stress-strain behavior of pure resin, amorphous PET's, and nanocomposites containing 1, 2, and 5-weight % of 30B clay type

4.2.2.1 Tensile Strength

Tensile strength shown in Figure 4.12 first increases then decreases with increasing amount of montmorillonite. Small amounts of well dispersed and exfoliated clay at first increases the tensile strength since it reinforces the matrix and deviates the crack propagation path. At high clay content the decrease in the tensile strength can be attributed to weak regions in matrix-filler system. Regions where loops in several chains are in close proximity, but do not entangle with one another, [72]. These aggregates of chain ends cause also microcracks at the interface and lower the available matrix-clay interaction surface. Also at high clay contents, clay agglomerates are present leading to low filler-matrix interactions. All of these possibilities lead to lower strength values as the clay content increases, shown in Figure 4.12.

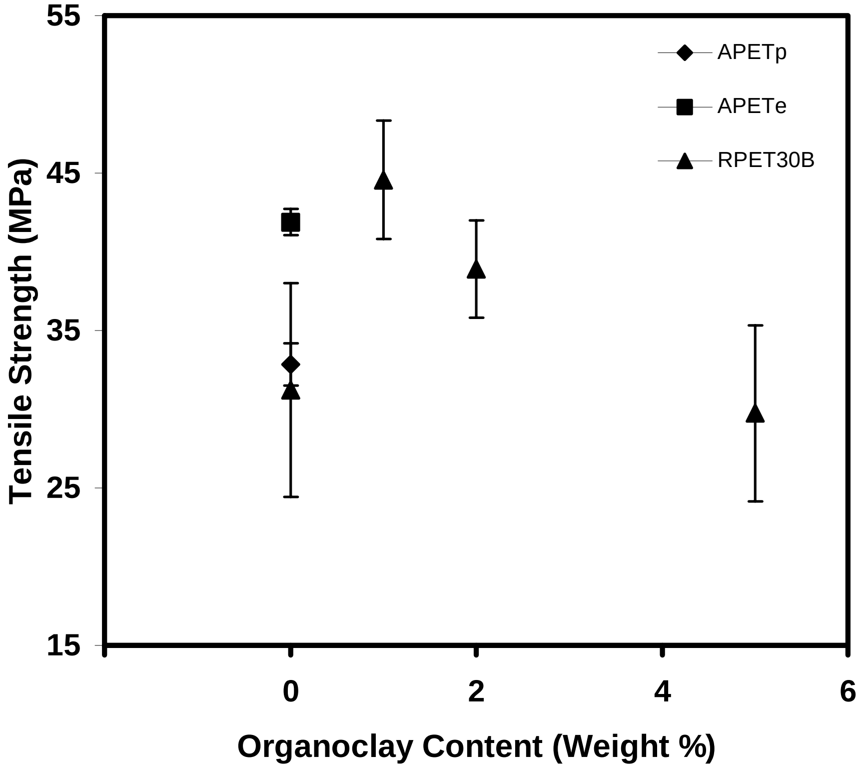

Figure 4.12 Effect of organoclay content on tensile strength

As seen in Figure 4.13, in each clay type the samples exhibit the highest strength value at 350 rpm. This property shows a maximum at 350 rpm. Since individual clay sheets with high aspect ratios are formed at intermediate rpm, dispersion gives enhancement in interfacial interactions and adhesion strength. High speed of processing, i.e. 500 rpm in the experiments, may give rise to some defects in the structure due to the shortness of the residence time.

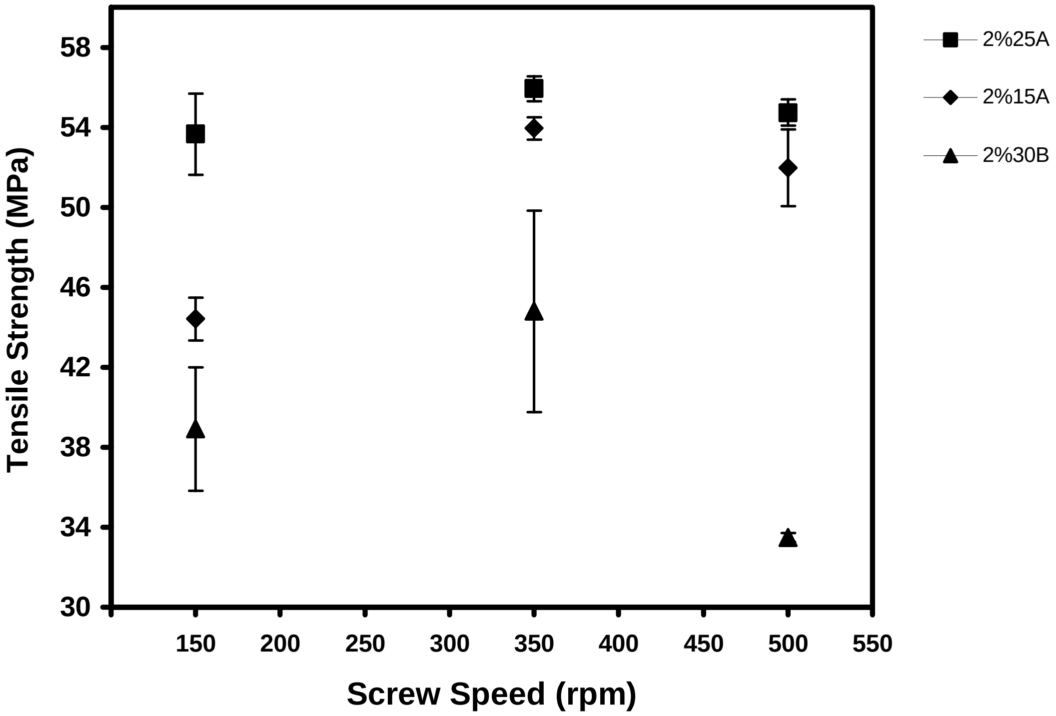

Figure 4.13 Effects of clay type and screw speed on tensile strength

4.2.2.2 Tensile (Young's) Modulus

Tensile modulus increases with increasing amount of clay content as shown in Figure 4.14. The modulus of a composite material depends on the ratio of filler modulus to that of the matrix. Since clay has higher modulus, more rigid structure, the modulus increases with the clay content. APETp and APETe have higher modulus than RPET since they would have higher molecular weight than the recycled PET. Also, it is seen that in extrusion APETe has higher modulus than APETp which implies that in extrusion the molecular weight may have increased owing to polycondensation reaction that may take place at high temperature. At high clay loadings, modulus does not increaseas much due to the tendency of clay particles to agglomerate in the structure. This effect can be seen in Figure 4.14 at 5-weight % of clay loading.

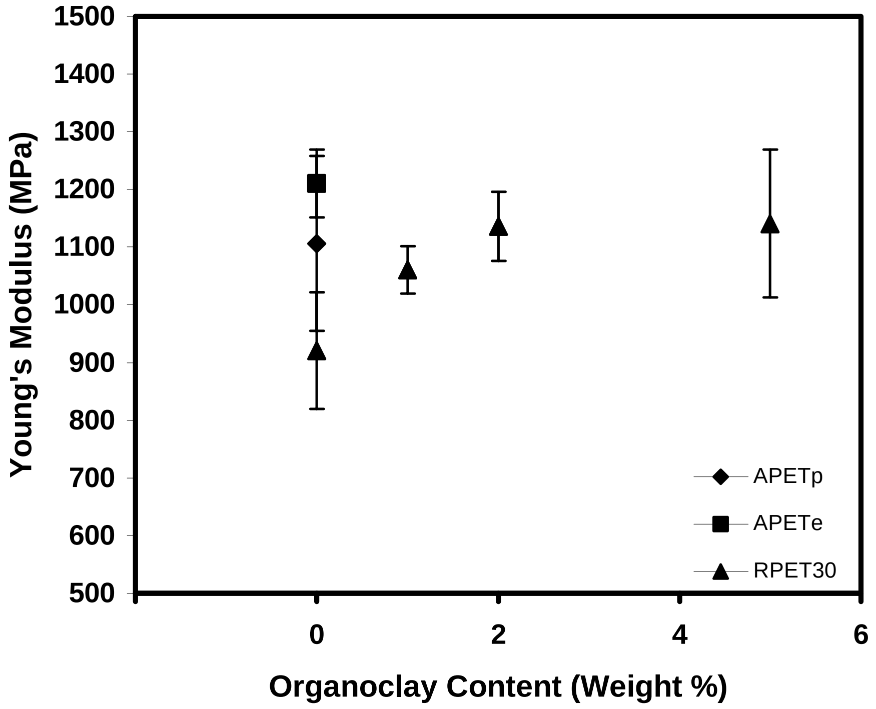

Figure 4.14 Effect of organoclay content on Young's modulus

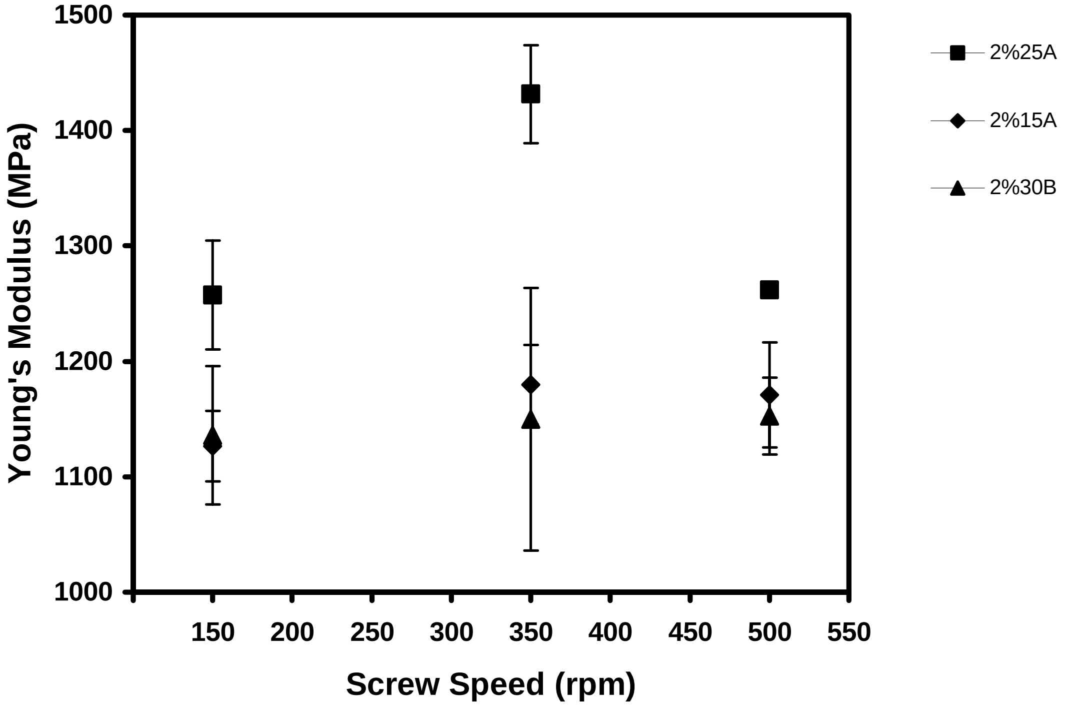

Figure 4.15 Effects of clay type and screw speed of samples on Young's modulus

Figure 4.15 represents the effect of screw speed on moduli of the samples containing three types of clay, 15A, 30B, and 25A, at 2-weight %. 25A clay type samples give the highest modulus. In general, compositions processed at the speed of 350 rpm show maximum in modulus values. Such a maximum may be the result of increasing the available surface area for interactions of the filler and the matrix structures by increasing the area of interface formed. At high rpm, the degree of dispersion and exfoliation are lower due to low residence time.

4.2.2.3 Tensile Strain at Break

As shown in Figure 4.16, increase in clay content results in a maximum in strain at break values. The initial increase in the strain at break is due to the tortuous crack path formed at low clay contents. However, at high clay contents the clay particles agglomerate giving rise to stress concentration. Since the clay particles have rigid structures, the actual elongation of the pure resin decreases as more clay is loaded to the matrix. This trend is observed in Figure 4.16. APETp and APETe have higher tensile strain at break than RPET owing to their higher molecular weight.

Figure 4.17 shows the effect of processing speed on strain at break values of the samples containing three types of clay, 15A, 20B, and 25A, at 2-weight % clay content. At 350 rpm, there is a general tendency to have a minimum or constant value. This is due to the formation of large interface at this condition, preventing the mobility of polymer chains.

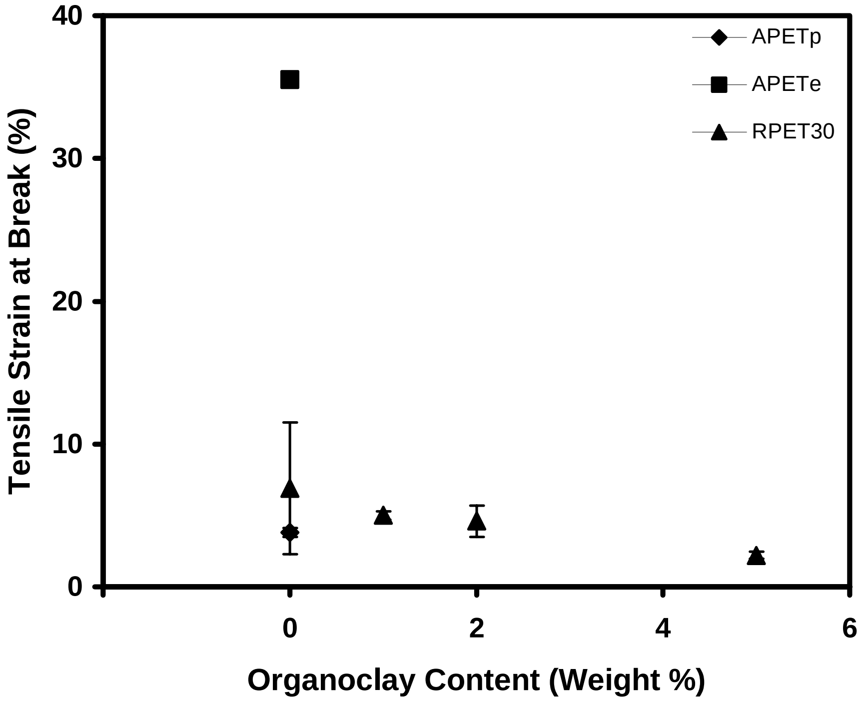

Figure 4.16 Effect of organoclay content on tensile strain at break

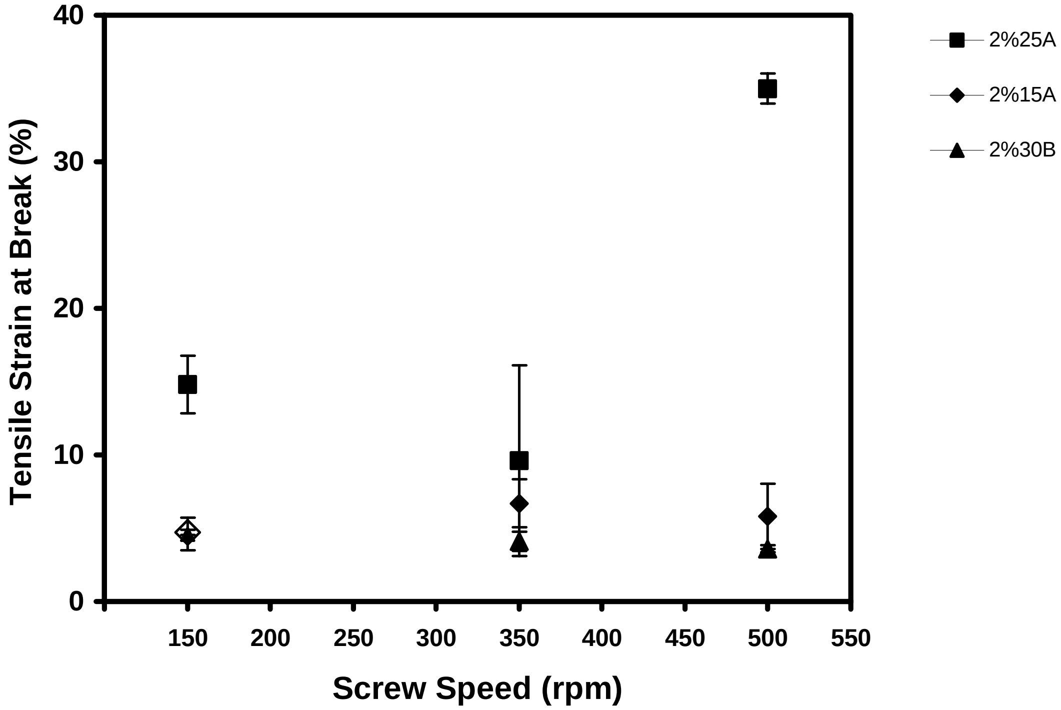

Figure 4.17 Effects of clay type and screw speed on tensile strain at break

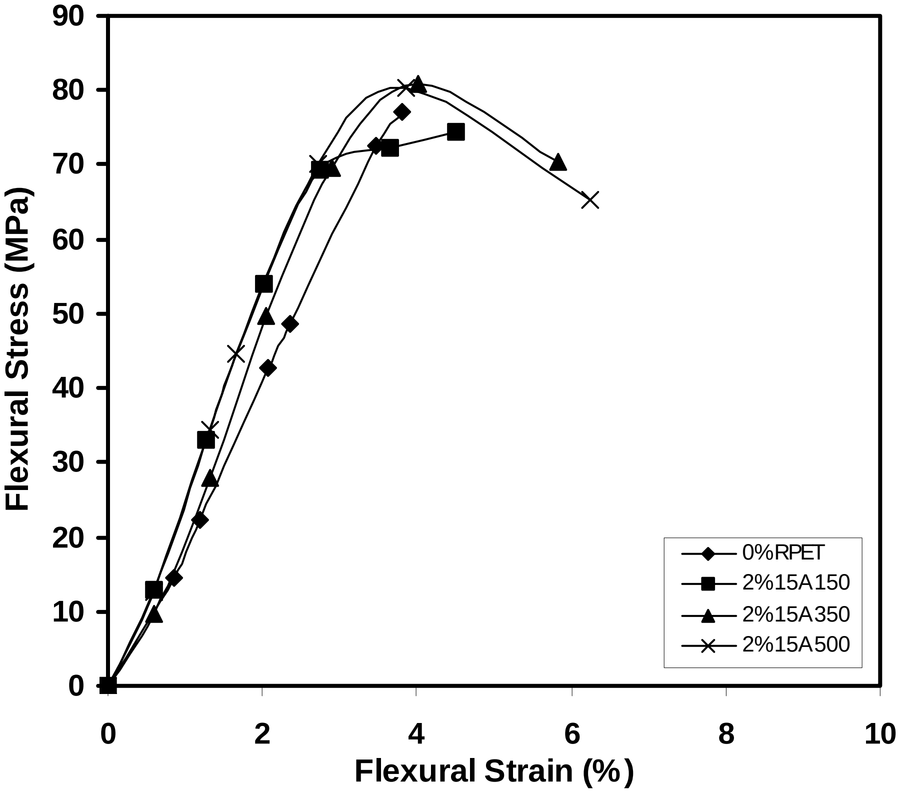

Flexural Stress (MPa)
Flexural Strain (%)
0
10
20
30
40
50
60
70
80
90
0
2
4
6
8
10
0%RPET
2%15A150
2%15A350
2%15A500

(a)

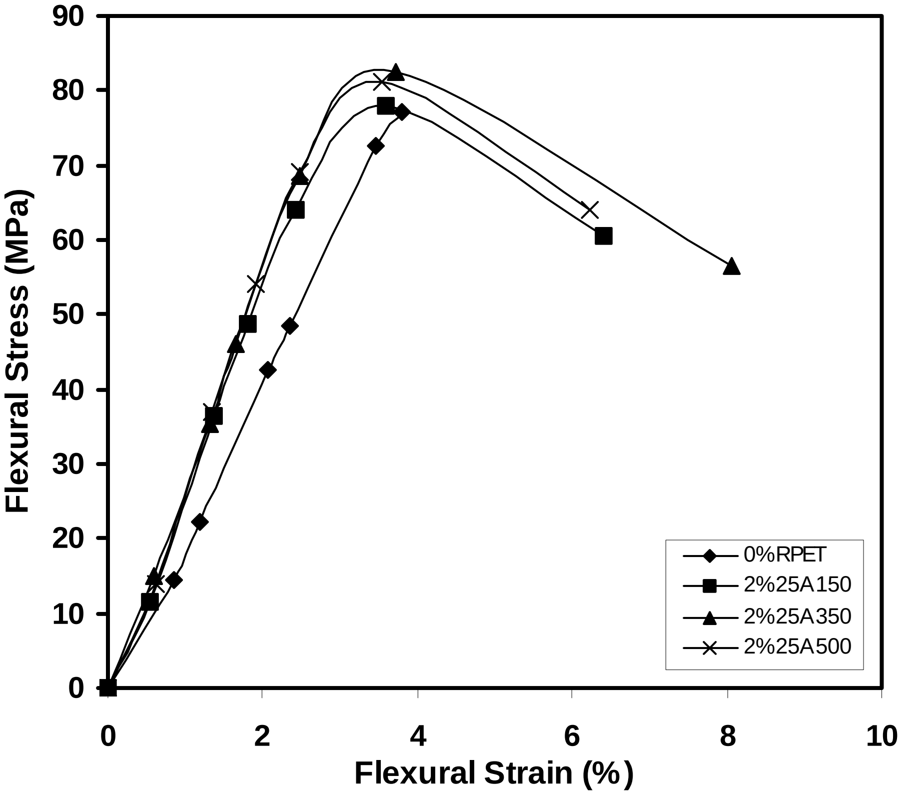

Flexural Stress (MPa)
Flexural Strain (%)
0
10
20
30
40
50
60
70
80
90
0
2
4
6
8
10
0%RPET
2%25A150
2%25A350
2%25A500

(b)

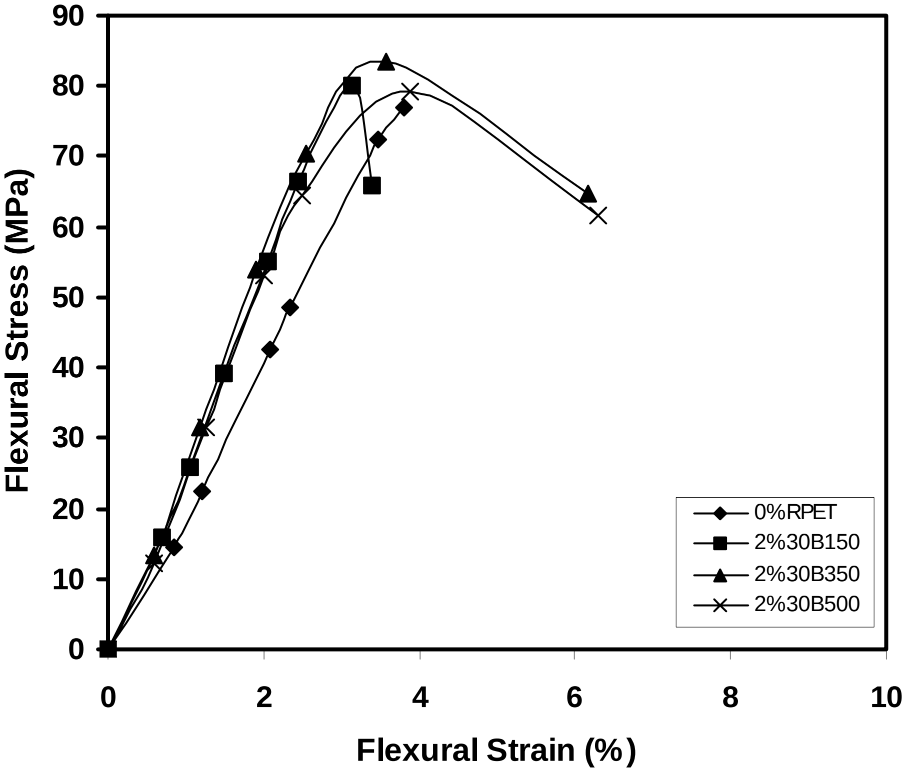

(c)

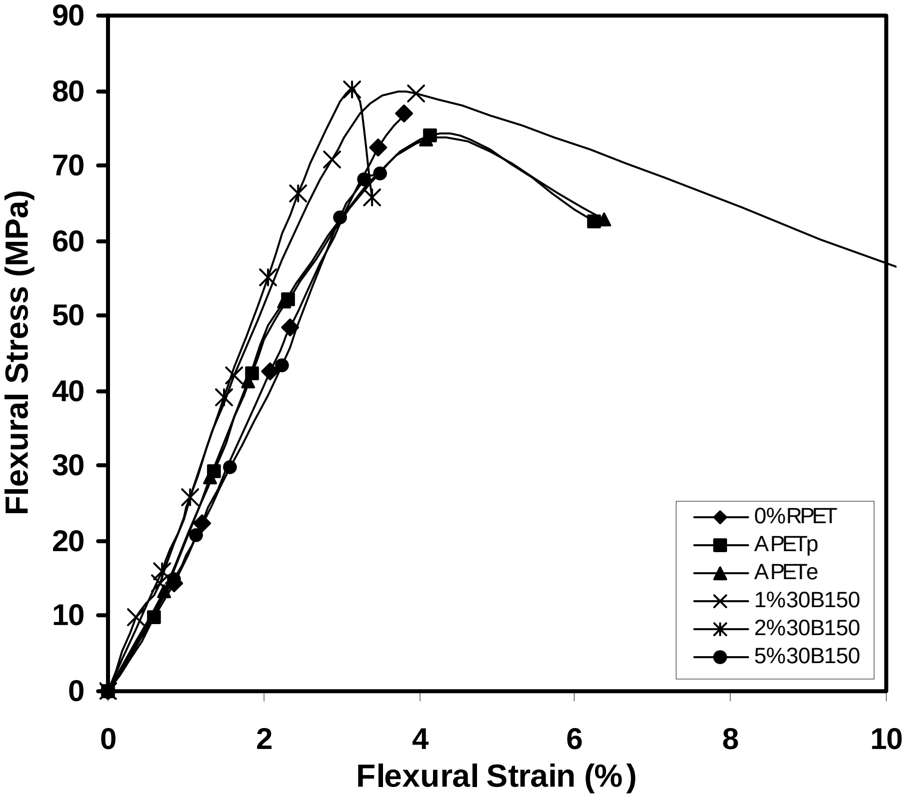

(d)

Figure 4.18 Flexural stress-strain behavior of samples, figures a, b, c, and d

4.2.3 Flexural Properties

The flexural stress-strain curves are given in Figure 4.18 a, b, c, and d. Samples namely 0%RPET, 2%30B150, and 5%30B150 were broken in this test.

4.2.3.1 Flexural Strength

Flexural strength shows similar trend to tensile strength values, as explained before in Figures 4.12 and 4.13. Owing to the nature of the flexural test, strength values are greater than those of tensile samples. In flexural testing the upper half of specimens is in compression while the lower half is in tension. Thus, cracks can not easily propagate towards the compression side. The compressive stresses tend to close the cracks rather than opening them leading to ductile behavior and higher strength. Here, 2 weight % sample gives the best strength value. Figure 4.20 shows the effect of processing speed on the strength values of samples. Having more mixing characteristics, generally the samples processed at 350 rpm exhibit higher strength values and in general the clay type of 25A gives the highest values, except at 150 rpm.

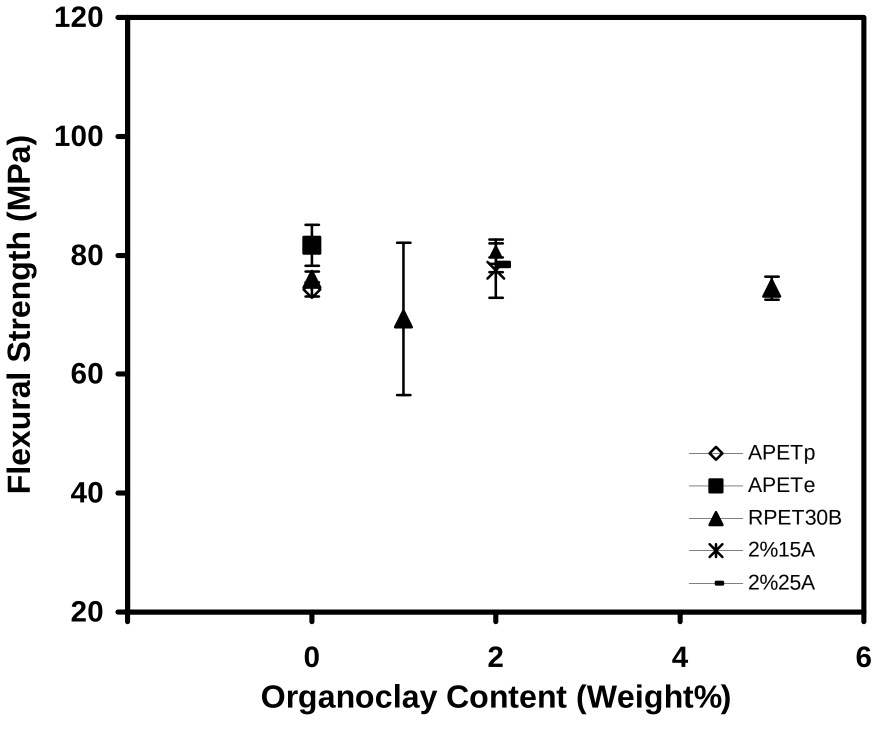

Figure 4.19 Effect of organoclay content on flexural strength

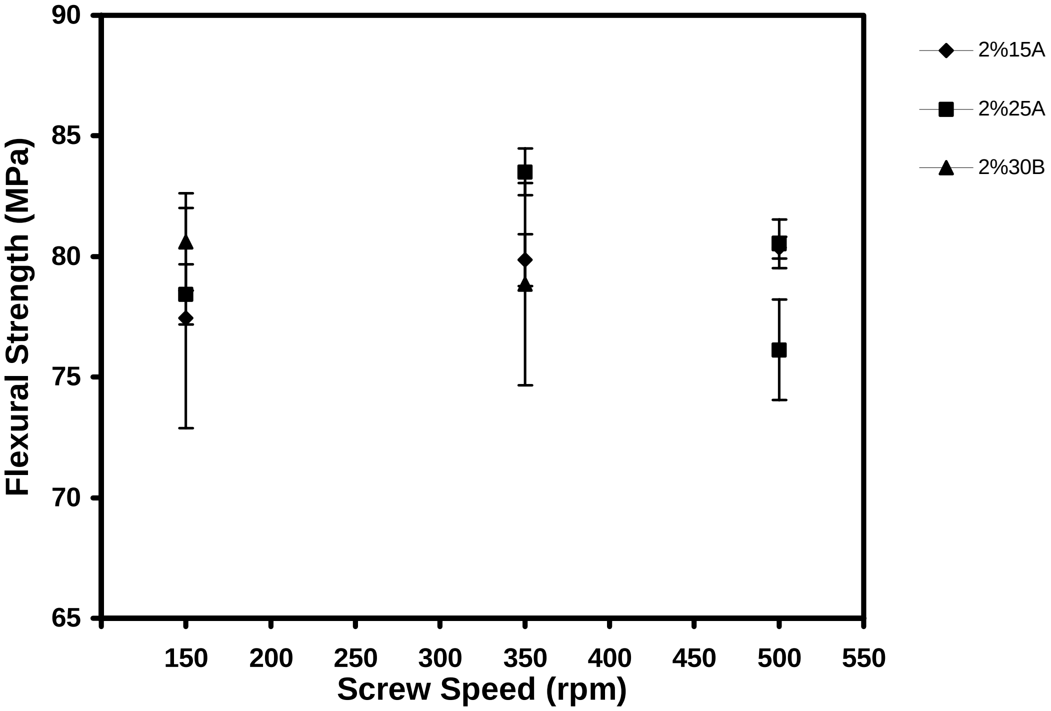

Figure 4.20 Effects of clay type and screw speed on flexural strength

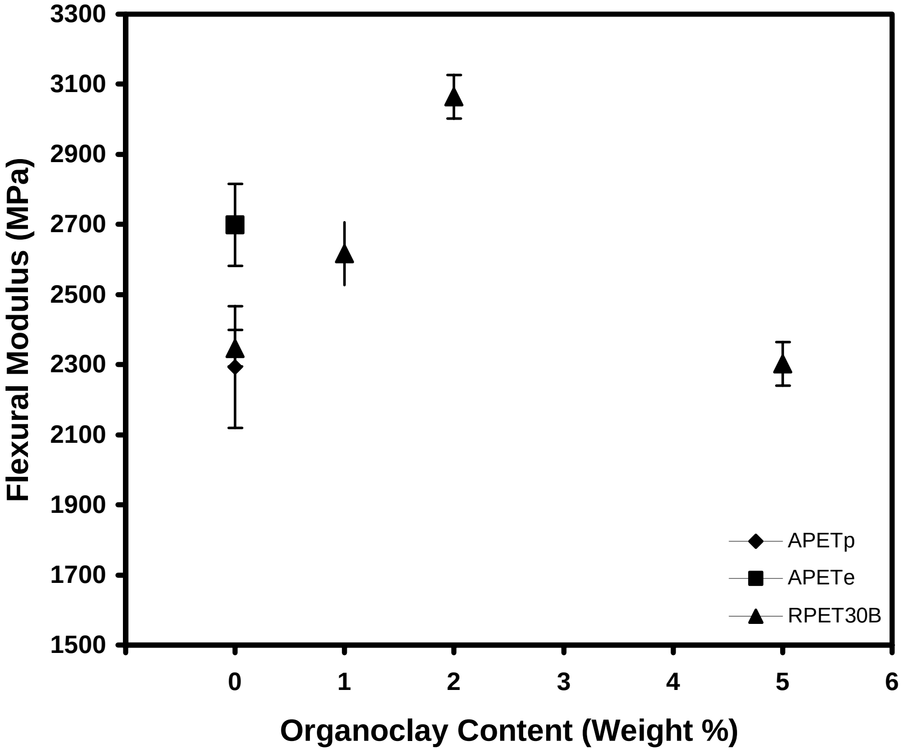

Figure 4.21 Effect of organoclay content on flexural modulus

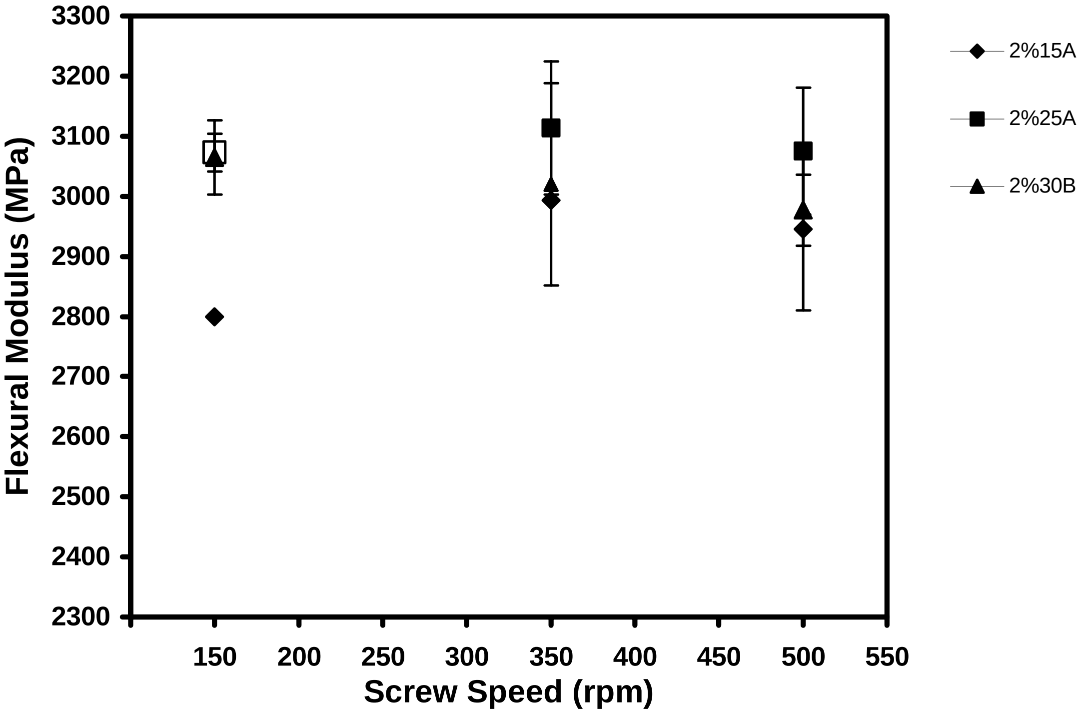

Figure 4.22 Effects of clay type and screw speed on flexural modulus

4.2.3.2 Flexural Modulus

As illustrated in Figure 4.21, flexural modulus increases as the clay content increases, and shows a maxima at 2 weight % clay loading. The decrease in the sample containing 5 weight % of clay is mostly due to imperfections resulted from aggregates (non-uniform structures) in the composition.

Figure 4.22 shows the effects of processing speeds, 150, 350, and 500 rpm, on nanocomposites having three different clay types, 15A, 25A, and 30B, at 2 weight %. Increasing the intensity of mixing leads to better filler distribution at intermediate rpm. However, at high rpm the clay does not exfoliate as much due to low residence time resulting in lower modulus.

4.2.3.3 Flexural Strain at Break

Figure 4.23 shows the effect of organoclay content on the flexural strain at break values of the neat resin and the samples containing 2 and 5 % 30B montmorillonite type by weight. It is similar to tensile strain at break behavior in Figure 4.16. The value shown at 1 % 30B refers to the strain at maximum stress.

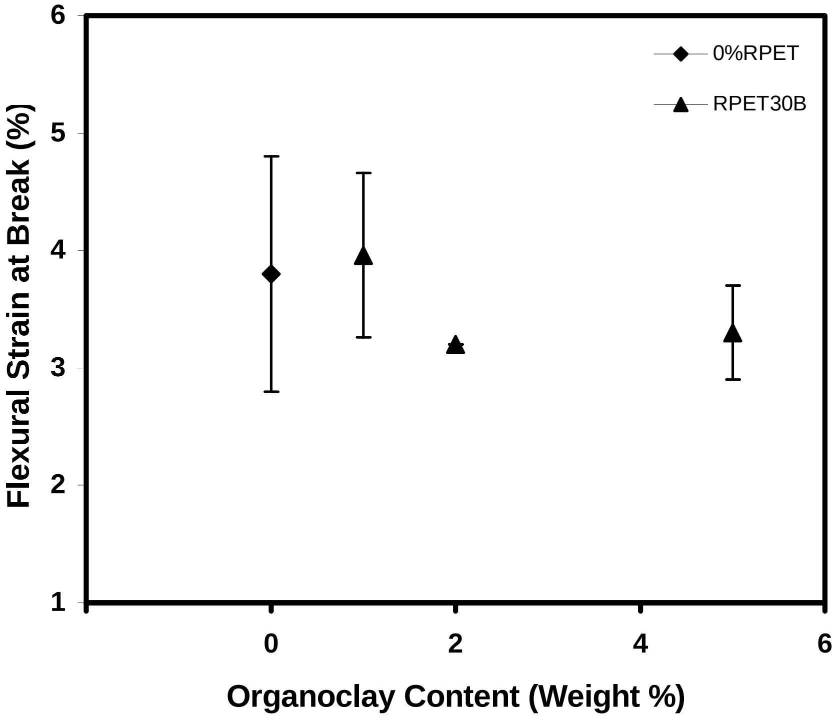

Figure 4.23 Effect of organoclay content on flexural strain at break, at 150 rpm

4.3 Melt Flow Index Test

Melt flow indices were measured to get an information about the viscous properties of the samples. As seen in Table of 4.1, melt flow index values generally decrease at the speed of 350 rpm with respect to that of the neat resin, recycled PET. This indicates an increase in the viscosity. The MFI value of the pure R-PET resin is 252 g/10min at the speed of 350 rpm. MFI value decreases to 111 g/10min, the highest decrease, in the sample of containing 2 weight % of 25A clay type. In neat resins, there are three types of variables affecting the viscosity values; matrix molecular weight, branching structure of the sample, and molecular defects in structure. Viscosity greatly depends on the branching structure of the specimen leading more prevented flow. The viscosity decrease in the sample of amorphous PET extruded is probably due to the physical deterioration during processing by decreasing the matrix molecular weight. In suspensions, the viscosity increases while MFI values decreases with the filler content. However, more important than that, the viscosity increases (MFI decreases) with the filler dispersion level. For example, in general, at 350 rpm the dispersion is highest, thus the viscosity is the highest and the MFI is lowest.

Table 4.1 Melt Flow Index values for pure resins and nanocomposite systems

Sample	0%	1%	2%	5%
APETp	232			
APETe	411			
RPET30B-150rpm	252	239	250	256
RPET30B-350rpm			188	
RPET30B-500rpm			331	
RPET15A-150rpm			200	
RPET15A-350rpm			181	
RPET15A-500rpm			246	
RPET25A-150rpm			277	
RPET25A-350rpm			111	
RPET25A-500rpm			242	

In general, the samples extruded at the speed of 150 and 500 rpm contain large percent of non-exfoliated silicate particles and exhibit lower viscosity and higher MFI in comparison to samples extruded at 350 rpm.

4.4 Differential Scanning Calorimeter (DSC) Analysis

Differential scanning calorimeter analysis was performed in order to evaluate the changes in Tg with increasing clay content. Table 4.2 shows the effects of clay type, clay content, and processing speed on thermal transitions.

Glass transition temperature is largely related to the molecular mobility of polymer chains. The T_g shows a maximum at 350 rpm and T_g values are increased from 81.1 ^oC, for unfilled recycled resin, up to 88.8 ^oC, for 2 weight % of 25A clay type including sample processed at 350 rpm. Also, 81.4 ^oC for 2% RPET25A sample at 500 rpm; and 84.0 ^oC for 2%RPET30B composition at 350 rpm. These increases in glass transition values can be attributed to higher interaction between polymer chains and the layered silicate surfaces. Nanometer sizes of silicate layers and good dispersion of these platelets restrict the segmental motions of polymer chains at the interface leading to increase in T_g values.

In the comparison of the last three compositions, we easily see the effect of processing on structures. Optimum delamination of the silicate layers and the exfoliation of these structures was achieved at the speed of 350 rpm. However in the sample containing 2 weight % of 15A, the T_g decreased to 79.5 ^oC from 81.1 ^oC at 350 rpm. Here the determining factor is mostly chemistry dependent. Since 15A clay type has worse chemical compatibility. It is not exfoliated as much as 25A or even 30B. The crystallization and melting temperatures do not change as much with the clay type, clay content and the screw speed, indicating that the rearrangement capability of the chains into crystals are not much affected.

Table 4.2 Thermal transition temperatures of the chosen samples

Sample Specifications	Glass Transition temp., T_g, (^oC)	Crystallization Temp., T_c, (^oC)	Melting Temperature, T_m, (^oC)
APETe150	80.2	146.8	251.7
0%RPET150	81.1	136.7	250.6
2%RPET30B150	79.4	133.4	251.0
2%RPET30B350	84.0	134.0	251.1
2%RPET30B500	79.0	132.1	250.7
2%RPET15A350	79.5	133.9	251.2
2%RPET25A150	78.7		248.2
2%RPET25A350	88.8	141.9	250.9
2%RPET25A500	81.4	135.1	251.0

CHAPTER V

CONCLUSIONS

Nanocomposites with three different types of montmorillonite organoclay, Cloisite 15A, 25A, and 30B, based on the matrix of recycled PET were prepared at three different screw speeds, 150, 350, and 500 rpm, using a co-rotating twin scrrew extruder. In our studies, we observed the effects of clay type, clay content and the processing speed on structures and properties. Optimum clay content was selected as 2 weight %. Using this clay content, variables including the clay type and the screw speed were studied.

Based on SEM, the main differences between the structures due to the dispersion of clay particles, and the compatibility of montmorillonite types with the recycled PET base resin. We observed the most tortuous path was observed at 2 weight % clay loading implying the highest degree of dispersion and exfoliation. This was later confirmed by the mechanical properties and SEM. At lower clay content (1%), the amount of clay was not enough to improve the properties. At higher clay content (5%), the clay remained mostly as aggregates giving rise to poor properties. Among the clay types, generally the 25A type of montmorillonite produced the highest tortuous structure in SEM micrographs. The screw speed of 350 rpm gave much better dispersion characteristics and more uniform structures. The tortuous surface, small and the heterogeneous crack propagation pathways on micrographs are the evidence of exfoliation of silicate layers in the matrix implying enhancements both in physical and thermal properties.

Mechanical properties showed marked improvements in the clay content of 2 weight % 25A clay type exhibiting the highest mechanical test values in general. Generally the speed of 350 rpm exhibited the more desirable property enhancements and exfoliation.

The composition containing 2 weight % organoclay yielded higher impact strength values than 1, and 5 weight % organoclay samples. At the processing speed of 350 rpm, the sample containing 2 weight % of 25A clay type showed 461% of impact improvement with respect to that of the base resin, recycled PET. Whereas the addition of 2 weight % 15A and 30B clay types yielded 386% and 97% of impact improvements, respectively.

Young's modulus values increased in all compositions yielding maximum at the speed of 350 rpm in general. Addition of 2 weight % of 25A clay type yielded 55.4% modulus improvement, while the 15A clay type gave 28.1%, and the 30B clay type gave 24.8% Young's modulus improvement at 350 rpm with respect to recycled PET.

Flexural modulus of nanocomposites showed the highest values at the speed of 350 rpm. In the case of addition 2 weight % of clay, 15A clay type gave 27.5 % modulus improvement; 25A and 30B clay types gave 32.6 % and 28.7 % modulus improvements with respect to recycled PET.

Tensile strength values of the organoclay samples, except for 5 weight %, increased with respect to pure resin in all processing speeds and clay types. Best increases occurred at the speed of 350 rpm. Addition of 2 weight % of 25A clay type yielded 79.1% tensile strength improvement, while the 15A clay type gave 72.7%, and the 30B clay type gave 43.5% strength improvement. Flexural and tensile strain at break values decreased with increasing clay loading.

DSC analysis showed that the incorporation of clay particles into the base polymer caused changes in T_g values. The maximum increase in T_g values was observed in the sample containing 2 weight % of 25A clay type processed at 350 rpm. The T_g increased from 81.1 ^oC (value of r-PET) to 88.8 ^oC. It should be noted that in this composition, clay type, and process speed give the highest exfoliation and best mechanical properties.

The MFI values also showed a minimum, implying maximum exfoliation for 2 weight % of 25A processed at 350 rpm.

REFERENCES

1. Dennis H.R., Hunter D.L., Chang D., Kim S., White J.L., Cho J.W. and Paul D.R. Polymer, 42, 9513-9522 (2001)
2. Kojima Y., Usuki A., Kawasumi M., Okada A., Kurauchi T., and Kamigaito O., J. of Appl. Polym. Sci., 31, 983-986 (1993)
3. Yano K., Usuki A., Okada A., Kurauchi T., and Kamigaito O., Journal of Polymer Science: Part A: Polymer Chemistry, 31, 2493-2498 (1993)
4. Kojima Y., Usuki A., Kawasumi M., Okada A., Kurauchi T., and Kamigaito O., J. of Appl. Polym. Sci., 49, 1259-1264 (1993)
5. Messersmith P.B., and Giannelis E.P., Journal of Polymer Science: Part A: Polymer Chemistry, 33, 1047-1057 (1995)
6. Guozhen Z., Shichi T. and Takagi K., Materials Letters, 4077, 1858-1862 (2002)
7. Schwartz M., ‘Composite Materials’, Prentice Hall PTR, Upper Saddle River, N.J., USA, Vol.1, (1997)
8. Lubin G., ‘Handbook of Composites’, Van Nostrand Reinhold, New York, (1982)
9. Strong A B., ‘High Performance and Engineering Thermoplastic Composites’, Technomic Pub. Co., Lancaster, Pennsylvannia, (1993)
10. Matthews F.L., R.D. Rawlings, ‘Composite Materials; Engineering and Science’, Chapman&Hall, London, NewYork, (1994)
11. Announcement of Media Briefing, ‘Nanotechnology, the next industrial revolution? Nanotechnology in the EU and US’, Tolouse Conference (FR), 19.Oct.2000
12. A web page of the Southern Clay Products, www.southernclayproducts.com
13. Bower C.A., Iowa Agricultural Experiment Station Research Bulletin, 362, 39 (1949)
14. Blumstein A., Bull. Chim. Soc., 889 (1961)

15. Giannelis E.P., ‘Polymer/Layered-silicate Nanocomposites (PLSNs), An internet paper, www.ccmr.cornell.edu/˜giannelis/research/silicate.html
16. Zanetti M., Lomakin S., Camino G., Macromol. Eng., Vol.279, 1-9 (2000)
17. Lanie R.M., Choi J., and Lee I., Advanced Materials, Vol.13, No. 11, 800-803, (2001)
18. Brechet Y., Cavaille J.Y., Chabert E., Chazeau L., Dendievel R., Flandin L, and Gauthier C., Advanced Engineering Materials, Vol.3, No. 8, 571-577 (2001)
19. Manias E., ‘Origins of the Materials Properties Enhancements in Polymer/Clay Nanocomposites’, http://zeus.plmsc.psu.edu/nano.html
20. Fornes T.D., Yoon P.J., Keskkula H.,and Paul D.R., Polymer, 42, 9929-9940 (2001)
21. Wypych J.G., ‘Fillers’, Chem. Tech. Publishing, Toronto, (1993)
22. Velde B., ‘Origin and Minerology of Clays: Clays and the Environment’, Springer, NewYork, (1995)
23. Haydn H.M., ‘Clays: Survey’, Kirk-Othmer Encyclopedia of Chemical Technology, John Wiley&Sons, Inc. NewYork (2002)
24. Grim R.E., ‘Clay Minerology’, 2nd Edition, McGraw-Hill Inc., NewYork, USA (1968)
25. Billmeyer F.W., ‘Textbook of Polymer Science’, 3rd Edition, John Wiley&Sons, NewYork, (1984)
26. Martinez J.M., Eguiazabal J.I., and Nazabal J., J. Macromol. Sci.-Phys., B34 (1&2), 171-176 (1995)
27. Raunwendaal C., ‘Polymer Mixing: A Self-Study Guide’, Hanser Publishers, NewYork, (1992)
28. Raunwendaal C., ‘Polymer Extrusion’, 3rd Edition, Hanser/Gardner Publishers, NewYork, (1994)
29. Vaia R.A. and Giannelis E.P. Macromolecules, 30, 8000-8009 (1997)
30. Davis C.H., Mathias L.J, Gilman J.W., Schiraldi D.A., Shelds J.R., Trulove P., Sutto T..E., and Delong H.C., J. Polym. Sci. Part B: Polymer Phys., 40, 2661-2666 (2002)
31. Burillo G., Clough R.L., Czvikovszky T.,Guven O., Le Moel A., Liu W., Singh A., Yang J., and Zaharescu T., Radiation Physics and Chemistry, 64, 41-51 (2002)

32. Subramanian P.M., Resources, Conservation and Recycling, 28, 253-263 (2000)
33. Ehrig R.J., ‘Plastics Recycling’, Hanser Publishers, Munich, (1992)
34. Curlee T.R., ‘Plastic Wastes: Management, Control, Recycling and Disposal’, U.S. Environmental Protection Agency, USA, (1991)
35. Paci M., La Mantia F.P., Polymer Degradation and Stability, 61, 417-420 (1998)
36. Paci M., La Mantia F.P., Polymer Degradation and Stability, 63, 11-14 (1999)
37. Shah V., ‘Handbook of Plastic Testing Technology’, 2nd Edition, Wiley-Interscience Publication, (1998)
38. ‘Annual Book of ASTM Standards’, Vol.08.01, American Society for Testing and Materials ASTM D638-91a, Philadelphia, USA (1993)
39. ‘Annual Book of ASTM Standards’, Vol.08.01, American Society for Testing and Materials ASTM D790M, Philadelphia, USA (1993)
40. ‘Annual Book of ASTM Standards’, Vol.08.01, American Society for Testing and Materials ASTM D256, Philadelphia, USA (1993)
41. Callister W., ‘ Materials Science and Engineering’, 4th Edition, John Wiley&Sons, NewYork, USA (1997)
42. Gilman J.W., Jackson C.L., Morgan A.B.,Haris R., Manias E., Giannelis E.P.,Wuthenow M., Hilton D., and Phillips S.H., Chem. Mater., 12, 1866-1873 (2000)
43. Seymour R.B., and Carraher C.E., ‘Structure-Property Relationships in Polymers’, Plenum Press, New York (1984)
44. Li J.X., Wu J. and Chan C.M., Polymer, 41, 6935-6937 (2000)
45. Gloaguen J.M. and Lefebvre J.M., Polymer, 42, 5841-5847 (2000)
46. Sun L, Xiao M, Xiao P, Song J, Wang W, Zhang Y. and Gong K., Mat. Res. Soc. Proc., 661, KK5.14.1 (2001)
47. Zhu A. and Sternstein S., Mat. Res. Soc. Proc., 661, KK4.3.1 (2001)
48. Ke Y., Long C. and Qi Z., J.of Appl. Polym. Sci., 71, 1139-1146 (1999)
49. Tornes N., Robin J.J. and Boutevin B., European Polymer Journal, 36, 2075-2080 (2000)
50. Abu-Isa I.A., Jaynes C.B., and O’gara J.F., J. of Appl. Polym. Sci., 59, 1957-1971 (1996)

51. Incarnato L., Scarfato P., Di Maio L., and Acierno D., Polymer, 41, 6825-6831 (2000)
52. Vaia R.A., Jandt K.D., Kramer E.J., and Giannelis E.P., Chem. Mater., 8, 2628-2635 (1996)
53. Kawasumi M., Hasegawa N., Kato M., Usuki A., and Okada A., Macromolecules, 30, 6333-6338 (1997)
54. Liu L., Qi Z., and Zhu X., J. of Appl. Polym. Sci., 71, 1133-1138 (1999)
55. Huang J., Zhu Z.,Yin J., Qian X., and Sun Y., Polymer, 42, 873-877 (2001)
56. Cho J.W., and Paul D.R., Polymer, 42, 1083-1094 (2001)
57. Lepoittevin B., Devalckenaeve M., Pantoustier N., Alexandre M., Kubies D., Calberg C., Jerome R., and Dubois P., Polymer, 43, 4017-4023 (2001)
58. Shen Z., Simon G.P., and Cheng Y., Polymer, 43, 4251-4260 (2002)
59. Gilman J.W., Kashiwagi T., Morgan A.B., Harris R.H., Brassell L., Awad W.H., Davis R.D., Chyall L., Sutto T., Trulove P.C., and DeLong H., ‘Recent Advances in Flame Retardant Polymer Nanocomposites’, Fire and Materials 2001. 7th International Conference and Exhibition, Jan. 22-24, San Antonio, TX (2001)
60. Usuki A., Koiwai A., Kojima Y., Kawasumi M., Okada A., Kurauchi T., and Kamigaito O., J. of Appl. Polym. Sci., 55, 119-123 (1995)
61. Lee D.C., and Jang L.W., J. of Appl. Polym. Sci., 61, 1117-1122 (1996)
62. Lee D.C., and Jang L.W., J. of Appl. Polym. Sci., 68, 1997-2005 (1998)
63. Zerda A.S. and Lesser A.J., Mat. Res. Soc. Symp. Proc., 661, KK7.2.1 (2001)
64. Chang J., and Park D., Polymer Bulletin, 47, 191-197 (2001)
65. Krishnamoorti R., and Giannelis E.P., Macromolecules, 30, 4097-4102 (1997)
66. Krishnamoorti R, Vaia R.A., and Giannelis E.P., Chem. Mater., 8 1728-1734 (1996)
67. Liang Y., Omachinski S., Longsdon J., Cho J.W., and Lan T., An internet page, Nanocor Inc., www.nanocor.com
68. Arrighi V, Gagliardi S., and Higgins J.S. Mat. Res. Soc. Symp. Proc., 661, KK4.4.1 (2001)
69. Weimer M.W., Chen H., Giannelis E.P., and Sogah D.Y., Journal Am. Chem. Soc., 121, 1615-1616 (1999)
70. Carrado K.A., and Xu L., Chem. Mater., 10, 1440-1445 (1998)

71. ‘Annual Book of ASTM Standards’, Vol.08.01, Standard Test Method for Flow Rates of Thermoplastics by Extrusion Plastometer, ASTM D1238-79, Philadelphia, USA (1993)
72. Lawrence E. N., Robert F. L., ‘Mechanical Properties of Polymers and Composites’, 2nd Edition, Marcel Dekker, Inc., USA (1994)

APPENDIX A

STRESS-STRAIN CURVES

Table A1. The data of tensile stress-strain curves of nanocomposites containing Cloisite 15A

0%		**2%15A150**	
Stress	Strain	Stress	Strain
0	0	0	0
4.56	0.62	6.06	0.875
9.22	1.24	15.47	1.75
26.63	3.34	26.28	2.91
38.63	4.76	34.6	3.9
46.48	6.11	45.26	5.21
52.59	7.45	53.28	6.7

2%15A350		**2%15A500**	
Stress	Strain	Stress	Strain
0	0	0	0
7.09	0.86	7.92	0.7
14.83	1.61	17.79	1.63
23.24	2.62	27.06	2.55
32.92	3.9	38.16	3.9
43.46	5.26	46.05	4.83
53.84	7.23	53.44	6.15

Table A2. The data of tensile stress-strain curves of nanocomposites containing Cloisite 25A

0%		**2%25A150**	
Stress	Strain	Stress	Strain
0	0	0	0
4.56	0.62	7.05	0.74
9.22	1.24	16.56	1.71
26.63	3.34	26.04	2.6
38.63	4.76	36.79	3.7
46.48	6.11	45.68	4.85
52.59	7.45	54.63	6.55

2%25A350		**2%25A500**	
Stress	Strain	Stress	Strain
0	0	0	0
6.19	0.73	10.76	0.95
13.38	1.34	18.01	1.61
25.88	2.83	30.25	2.97
36.63	4.06	41.95	4.4
43.97	4.93	49.44	5.38
56.54	7.1	54.93	7.01

Table A3. The data of tensile stress-strain curves of nanocomposites containing Cloisite 30B

0%		**2%30B150**	
Stress	Strain	Stress	Strain
0	0	0	0
4.56	0.62	8.14	0.89
9.22	1.24	10.78	1.12
26.63	3.34	24.39	2.44
38.63	4.76	29.09	3
46.48	6.11	40.85	4.43
52.59	7.45	47.65	6.04

2%30B350		**2%30B500**	
Stress	Strain	Stress	Strain
0	0	0	0
7.24	0.77	5.47	0.77
16.89	1.6	12.04	1.47
21.65	2.1	18.18	2.34
32.07	3.27	25.87	3.35
42.38	4.44	31.87	4.08
45.36	5.07	33.27	4.27

Table A4. The data of tensile stress-strain curves of pure resin, and nanocomposites containing 1, 2, and 5 weight % of Cloisite 30B

0%		**1%**	
Stress	Strain	Stress	Strain
0	0	0	0
4.56	0.62	6.19	0.74
9.22	1.24	11.43	1.18
26.63	3.34	17.51	1.71
38.63	4.76	34.54	3.73
46.48	6.11	42.21	4.65
52.59	7.45	43.84	5.047

2%		**5%**	
Stress	Strain	Stress	Strain
0	0	0	0
8.14	0.89	6.15	0.84
10.78	1.12	11.85	1.4
24.39	2.44	18.08	2.15
29.09	3	22.72	2.71
40.85	4.43	32.32	3.81
47.65	6.04	38.2	4.47

Table A5. The data for flexural stress-strain curves of all samples

APETp

Stress	Strain (%)
0	0
9.93	0.59
29.38	1.35
42.35	1.86
52.25	2.32
74	4.15
62.5	6.24

APETe

Stress	Strain (%)
0	0
13.35	0.72
28.43	1.3
41.4	1.8
51.88	2.25
73.6	4.08
62.95	6.38

0%RPET

Stress	Strain (%)
0	0
14.42	0.860
22.33	1.200
42.63	2.070
48.58	2.350
72.53	3.470
77.05	3.800
38.73	4.110

1%30B150

Stress	Strain (%)
0	0
9.73	0.36
14.3	0.66
41.95	1.62
70.78	2.87
79.73	3.96
52.65	11.07

5%30B150

Stress	Strain (%)
0	0
14.95	0.860
20.8	1.140
29.95	1.580
43.5	2.240
63.07	2.970
68.28	3.300
69	3.500

2%15A150

Stress	Strain (%)
0	0
12.78	0.6
33	1.27
53.98	2.02
69.43	2.74
70	3.66
74.38	4.520

2%25A150

Stress	Strain (%)
0	0
11.63	0.55
36.43	1.38
48.63	1.81
64.08	2.43
77.83	3.6
60.65	6.4

2%30B150

Stress	Strain (%)
0	0
15.96	0.700
25.85	1.050
39.21	1.500
55.08	2.050
66.380	2.450
80.1	3.125
65.8	3.400

2%15A350

Stress	Strain (%)
0	0
9.73	0.6
28.05	1.32
49.6	2.05
69.63	2.9
80.88	4.01
70.3	5.82

2%25A350

Stress	Strain (%)
0	0
15	0.6
35.48	1.31
46.15	1.65
68.68	2.49
82.4	3.72
56.65	8.06

2%30B350

Stress	Strain (%)
0	0
13.35	0.6
31.65	1.17
53.98	1.89
70.38	2.54
83.35	3.58
64.65	6.18

2%15A500

Stress	Strain (%)
0	0
12.6	0.6
34.33	1.32
44.63	1.67
70.2	2.73
80.3	3.87
65.2	6.24

2%25A500

Stress	Strain (%)
0	0
13.93	0.62
37	1.34
54.18	1.9
69.05	2.48
81.03	3.54
64	6.24

2%30B500

Stress	Strain (%)
0	0
12.2	0.59
31.48	1.25
53.03	2
64.48	2.5
79.15	3.87
61.6	6.31

APPENDIX B

TENSILE PROPERTIES

Table B1. The data for tensile strength values of all compositions

Composition	Tensile Strength (MPa)	std.dev.
APETp	32.84	1.33
APETe	41.88	0.83
0%RPET	31.22	6.81
1%30B150	44.57	3.77
5%30B150	29.75	5.59
2%15A150	44.41	1.07
2%15A350	53.94	0.56
2%15A500	51.97	1.92
2%25A150	53.66	2.03
2%25A350	55.93	0.62
2%25A500	54.73	0.65
2%30B150	38.91	3.1
2%30B350	44.8	5.04
2%30B500	33.49	0.22

Table B2. The data for tensile (Young's) modulus values of all compositions

Composition	Young's Modulus (MPa)	std.dev.
APETp	1106.4	151.17
APETe	1210.03	58.59
0%RPET	920.9	101.28
1%30B150	1060.37	40.71
5%30B150	1140.66	128.18
2%15A150	1126.67	30.46
2%15A350	1179.92	34.33
2%15A500	1170.9	45.57
2%25A150	1257.48	47.38
2%25A350	1431.54	42.47
2%25A500	1262.17	0.77
2%30B150	1136.05	60.03
2%30B350	1149.76	113.59
2%30B500	1152.57	33.36

Table B3. The data for tensile strain at break values of all compositions

Composition	Tensile Strain at break (%)	std.dev.
APETp	3.8	0.32
APETe	35.5	44.62
0%RPET	6.9	4.62
1%30B150	5	0.28
5%30B150	2.2	0.25
2%15A150	4.7	0.17
2%15A350	6.7	1.63
2%15A500	5.8	2.250
2%25A150	14.8	1.95
2%25A350	9.6	6.52
2%25A500	3.5	1.02
2%30B150	4.6	1.11
2%30B350	4.1	0.65
2%30B500	3.6	0.25

APPENDIX C

FLEXURAL PROPERTIES

Table C1. The data for flexural strength values of all samples

Composition	Strength (MPa)	std. dev.
APETp	74.23	1.21
APETe	81.67	3.42
0%RPET	76	1.21
1%30B150	69.29	12.78
5%30B150	74.47	1.91
2%15A150	77.44	4.56
2%15A350	79.85	1.07
2%15A500	80.37	0.46
2%25A150	78.43	1.25
2%25A350	83.51	0.98
2%25A500	80.52	1.01
2%30B150	80.6	2.02
2%30B350	78.85	4.19
2%30B500	76.13	2.08

Table C2. The data for flexural modulus values of all compositions

Composition	Modulus (MPa)	std. dev.
APETp	2293.4	173.86
APETe	2699.13	117.48
0%RPET	2346.74	52.1
1%30B150	2617.32	89.48
5%30B150	2301.82	62.24
2%15A150	2800	0
2%15A350	2993.23	0
2%15A500	2945.48	135.67
2%25A150	3072.92	31.27
2%25A350	3113.8	111.08
2%25A500	3075.26	105.64
2%30B150	3064.4	61.64
2%30B350	3020.14	168.06
2%30B500	2976.91	59.24

Table C3. The data for flexural strain at break values of samples

Composition	Srain at break (%)	std. dev.
0%	3.8	1.00
1%30B150 *****	3.96	0.7
2%30B150	3.2	0.00
5%30B150	3.3	0.4

***** No break was observed during the test. The value indicates the strain at maximum stress.

APPENDIX D

IMPACT STRENGTH

Table D1. The data for impact strength values of all compositions

Composition	Impact Strength (kj/m^2)	std. dev.
APETp	6.2	0.31
APETe	12.52	2.25
0%RPET	4.72	0.11
1%30B150	4.31	0.34
5%30B150	3.73	0.42
2%15A150	5.86	0.31
2%15A350	9.22	0.57
2%15A500	18.4	0.56
2%25A150	17.88	3.87
2%25A350	26.51	3.09
2%25A500	22.53	0.98
2%30B150	11.33	0.97
2%30B350	22.95	1.35
2%30B500	17	2.19

APPENDIX E

DIFFERENTIAL SCANNING CALORIMETER (DSC) ANALYSIS

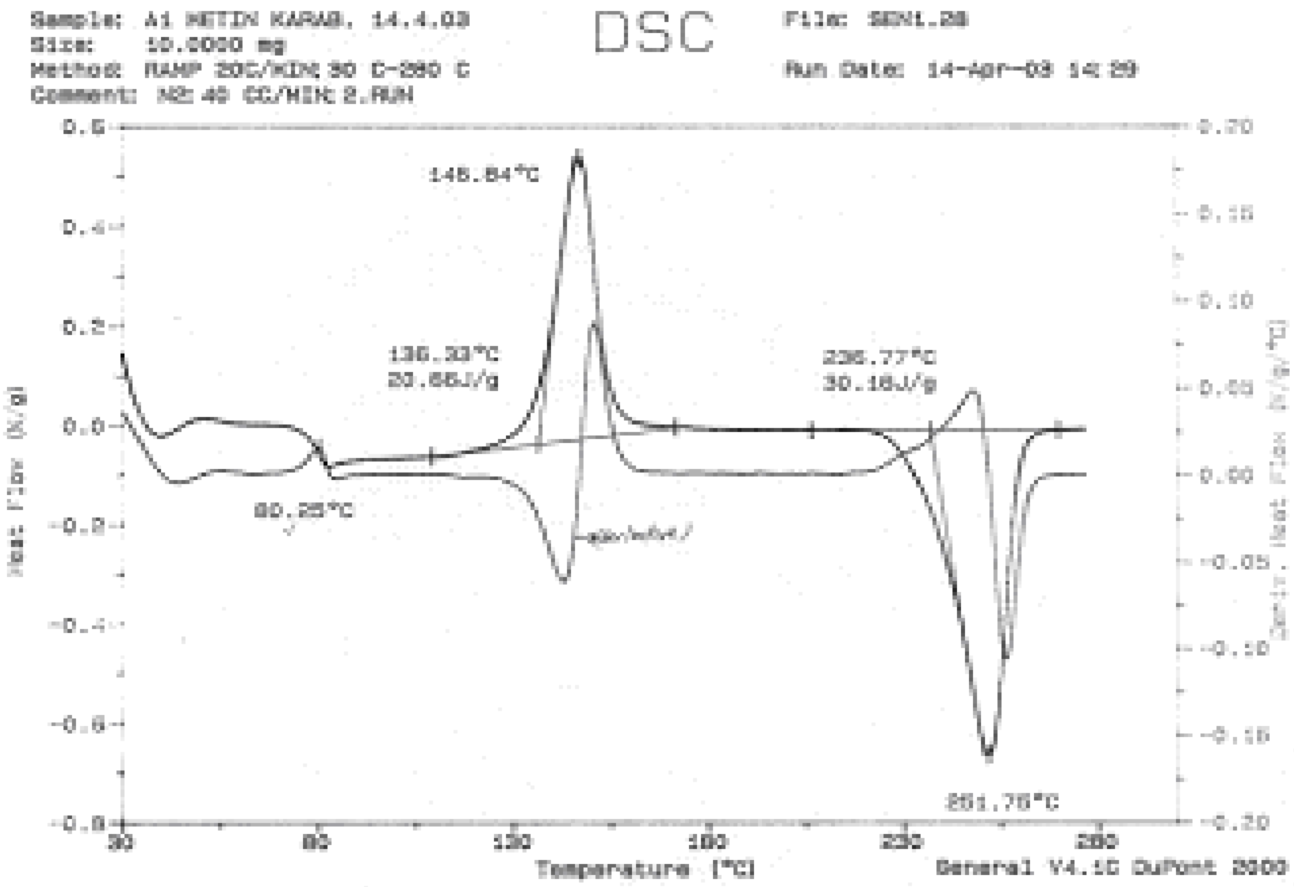

Figure E1. DSC diagram of extruded amorphous PET (AEPTe)

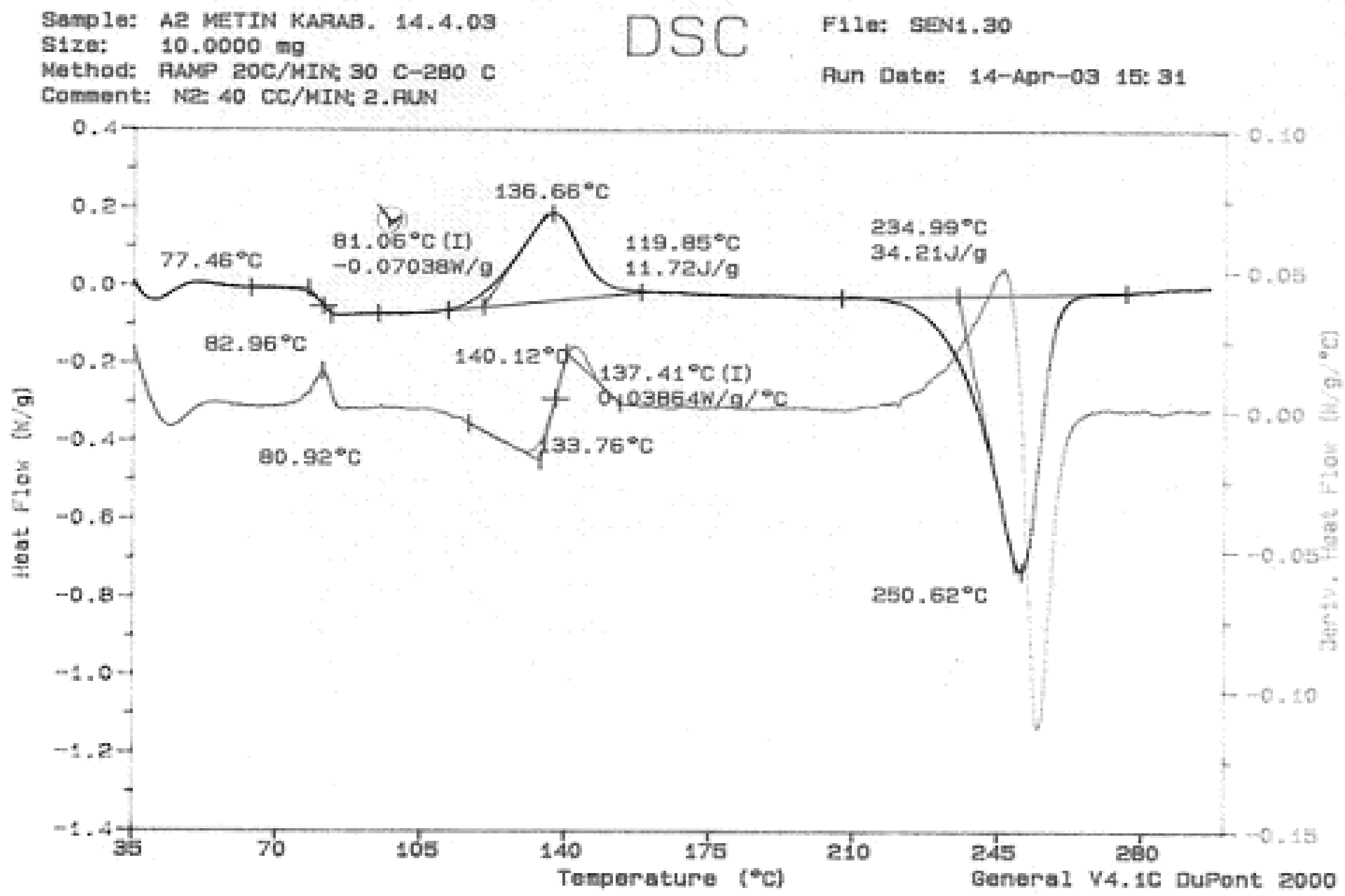

Sample: A2 METIN KARAB. 14.4.03
Size: 10.0000 mg
Method: RAMP 20C/MIN; 30 C-280 C
Comment: N2: 40 CC/MIN; 2.RUN

File: SEN1.30
Run Date: 14-Apr-03 15: 31

Figure E2. DSC diagram of recycled PET , base resin

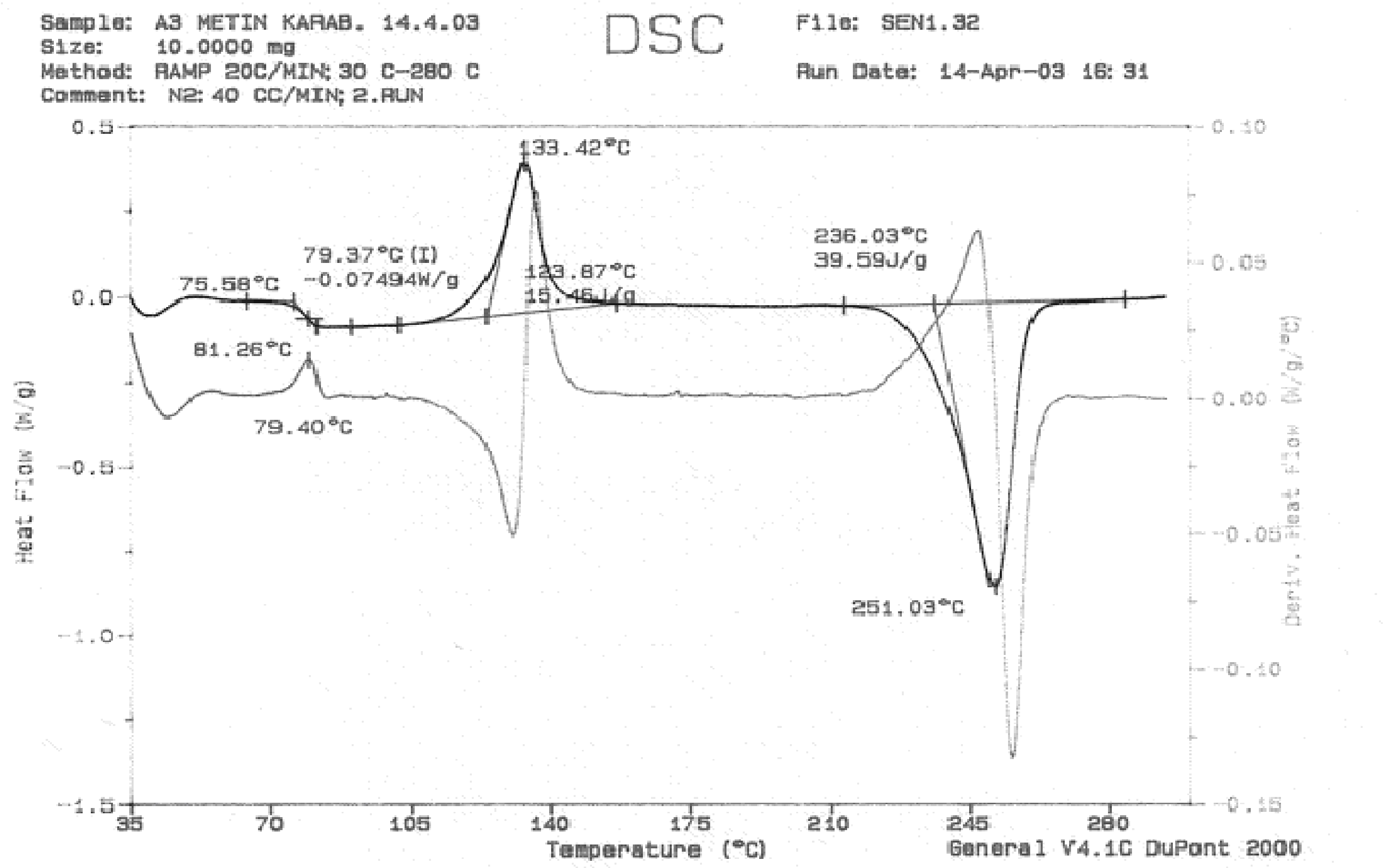

Figure E3. DSC diagram of the sample containing 2 weight % 30B at 150 rpm

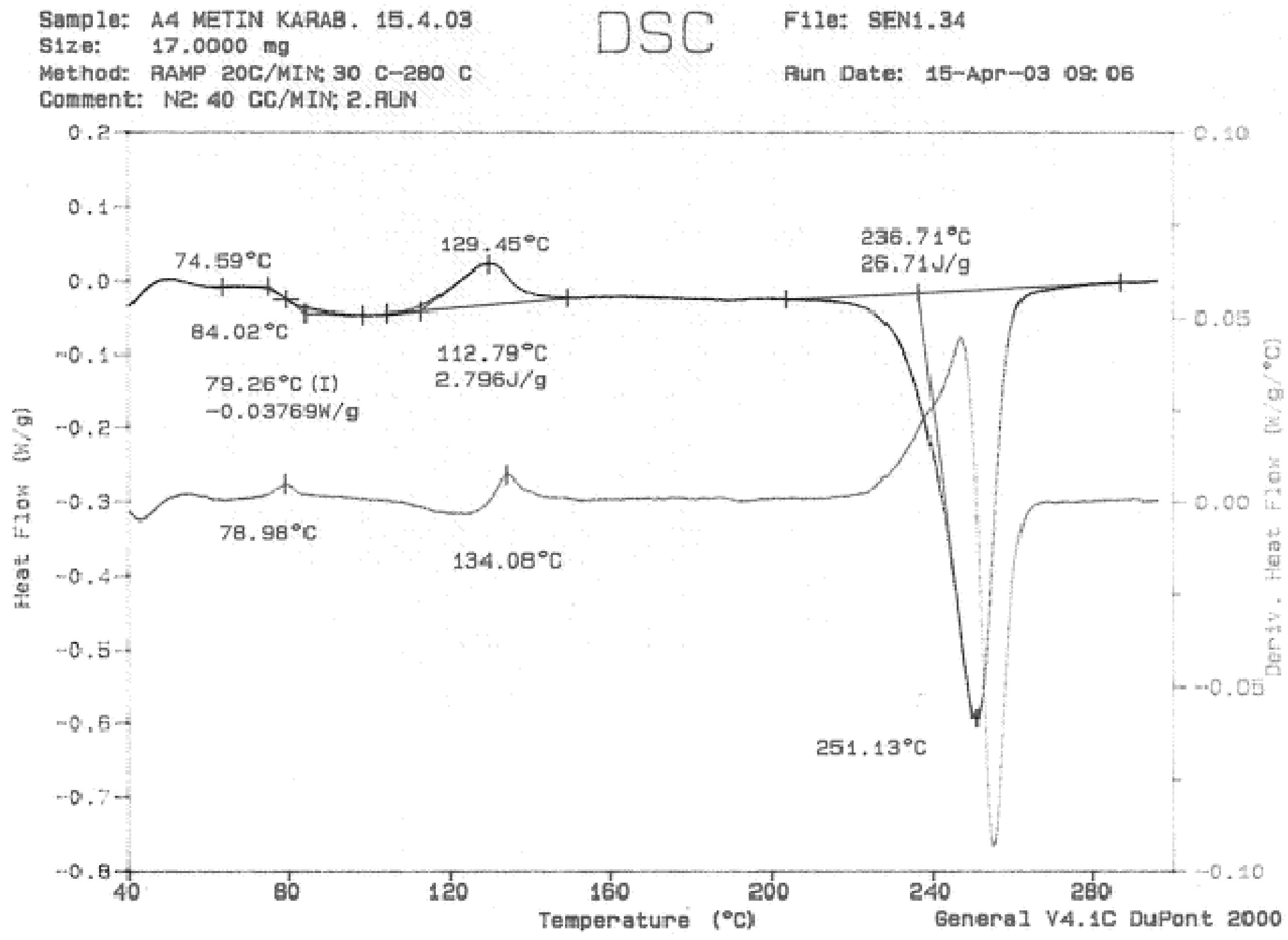

Figure E4. DSC diagram of the sample containing 2 weight % 30B at 350 rpm

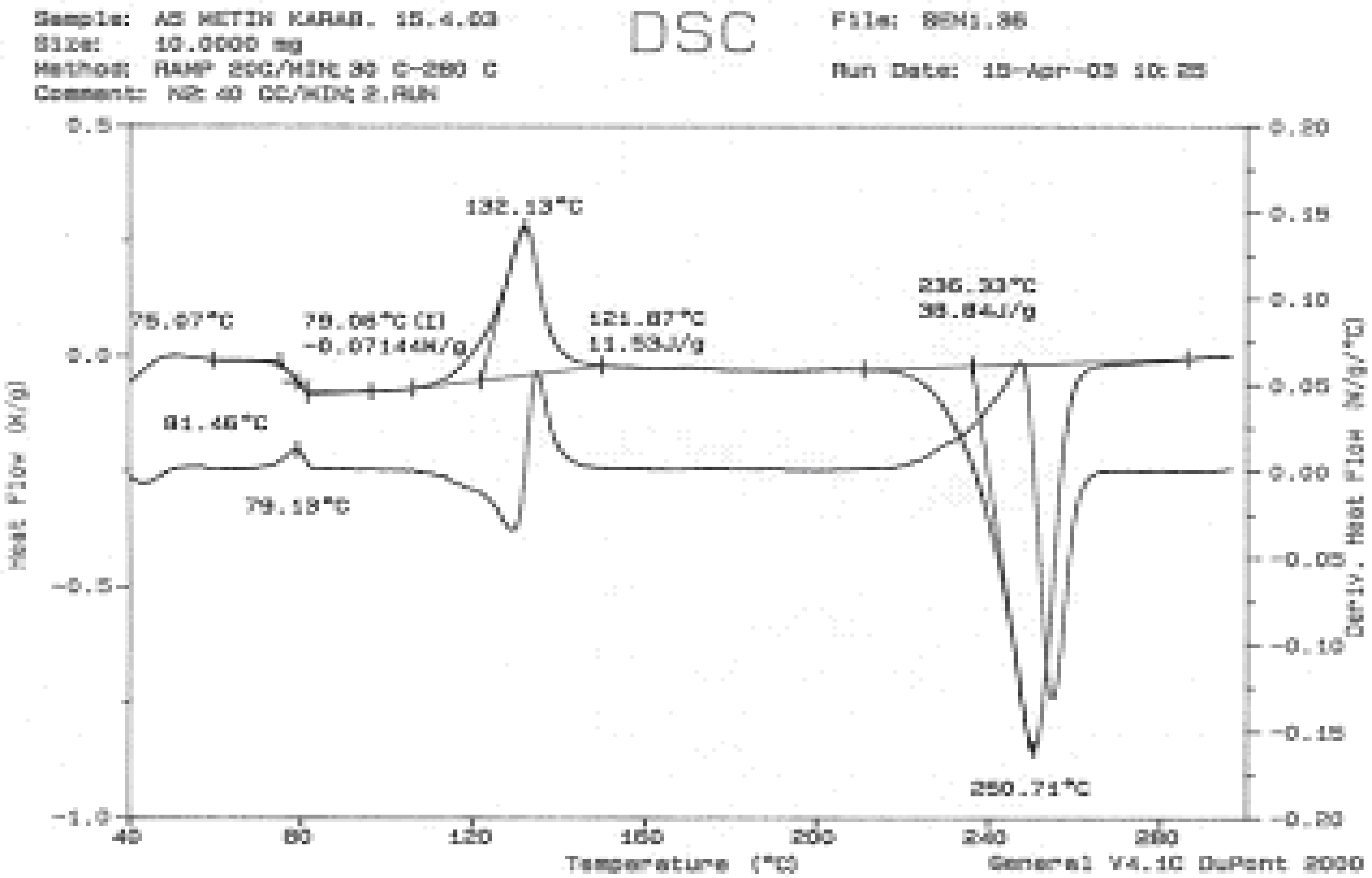

Figure E5. DSC diagram of the sample containing 2 weight % 30B at 500 rpm

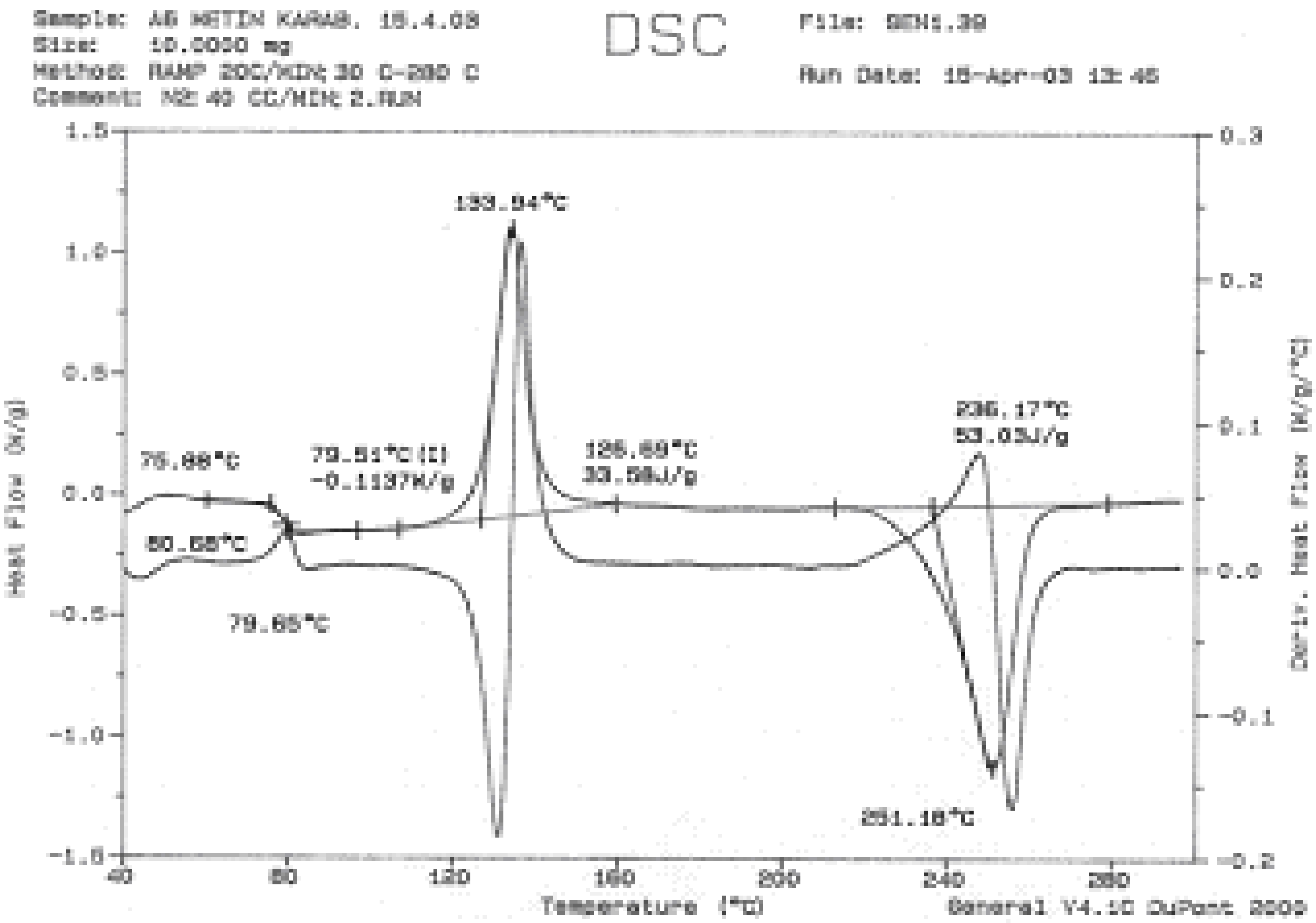

Figure E6. DSC diagram of the sample containing 2 weight % 15A at 350 rpm

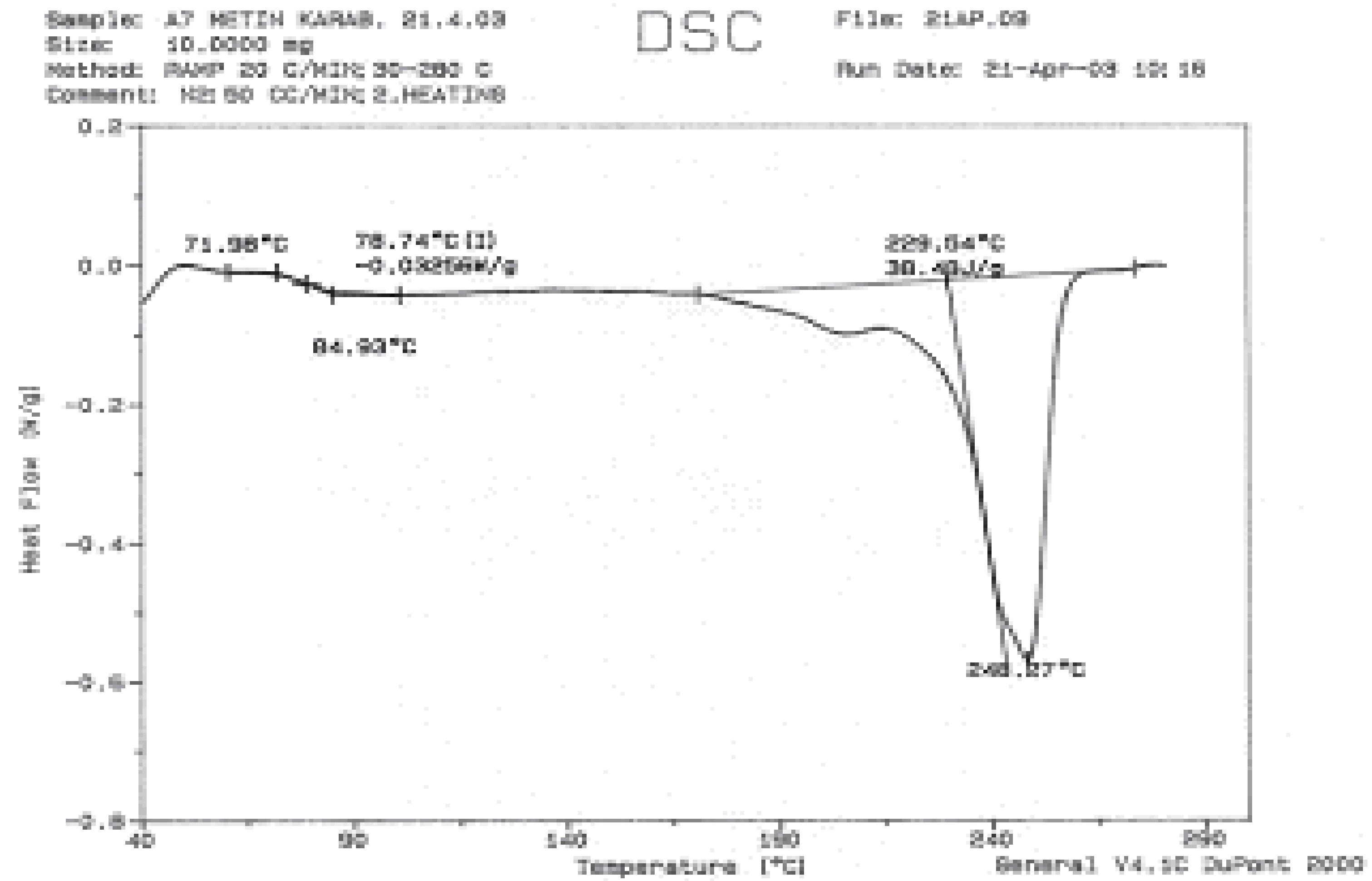

Figure E7. DSC diagram of the sample containing 2 weight % 25A at 150 rpm

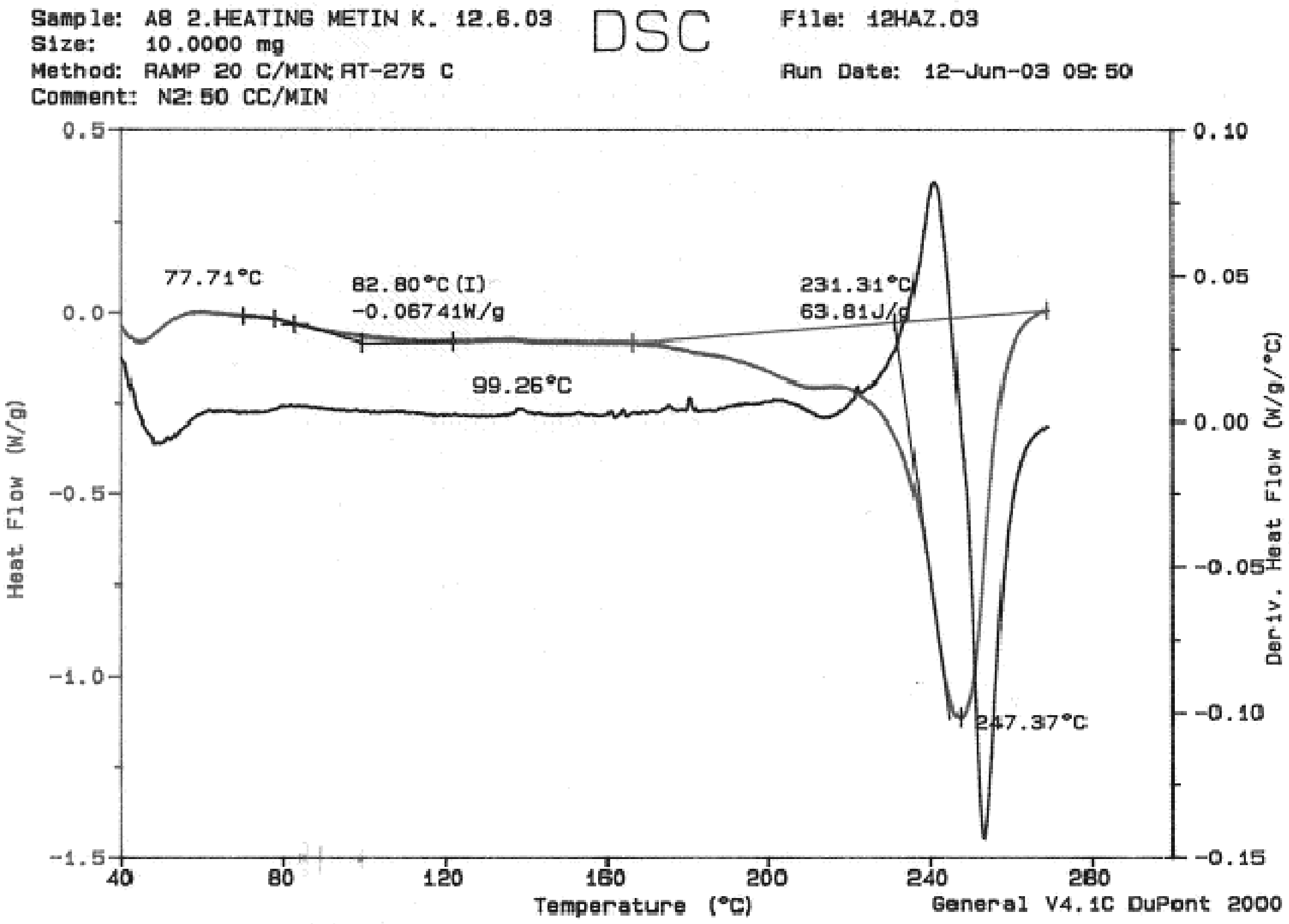

Figure E8. DSC diagram of the sample containing 2 weight % 25A at 350 rpm

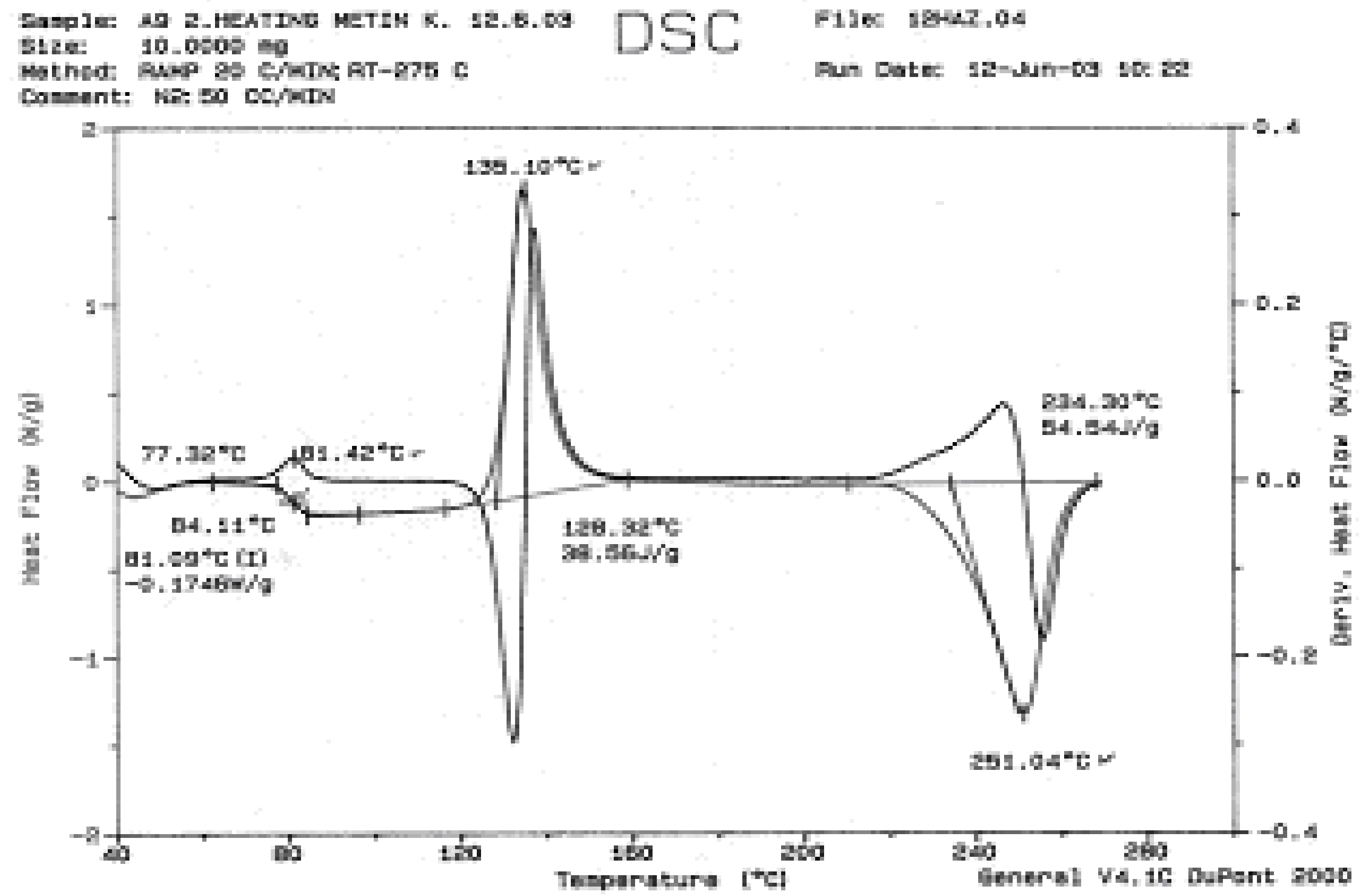

Figure E9. DSC diagram of the sample containing 2 weight % 25A at 500 rpm

APPENDIX F

THERMO GRAVIMETRIC ANALYSIS (TGA)

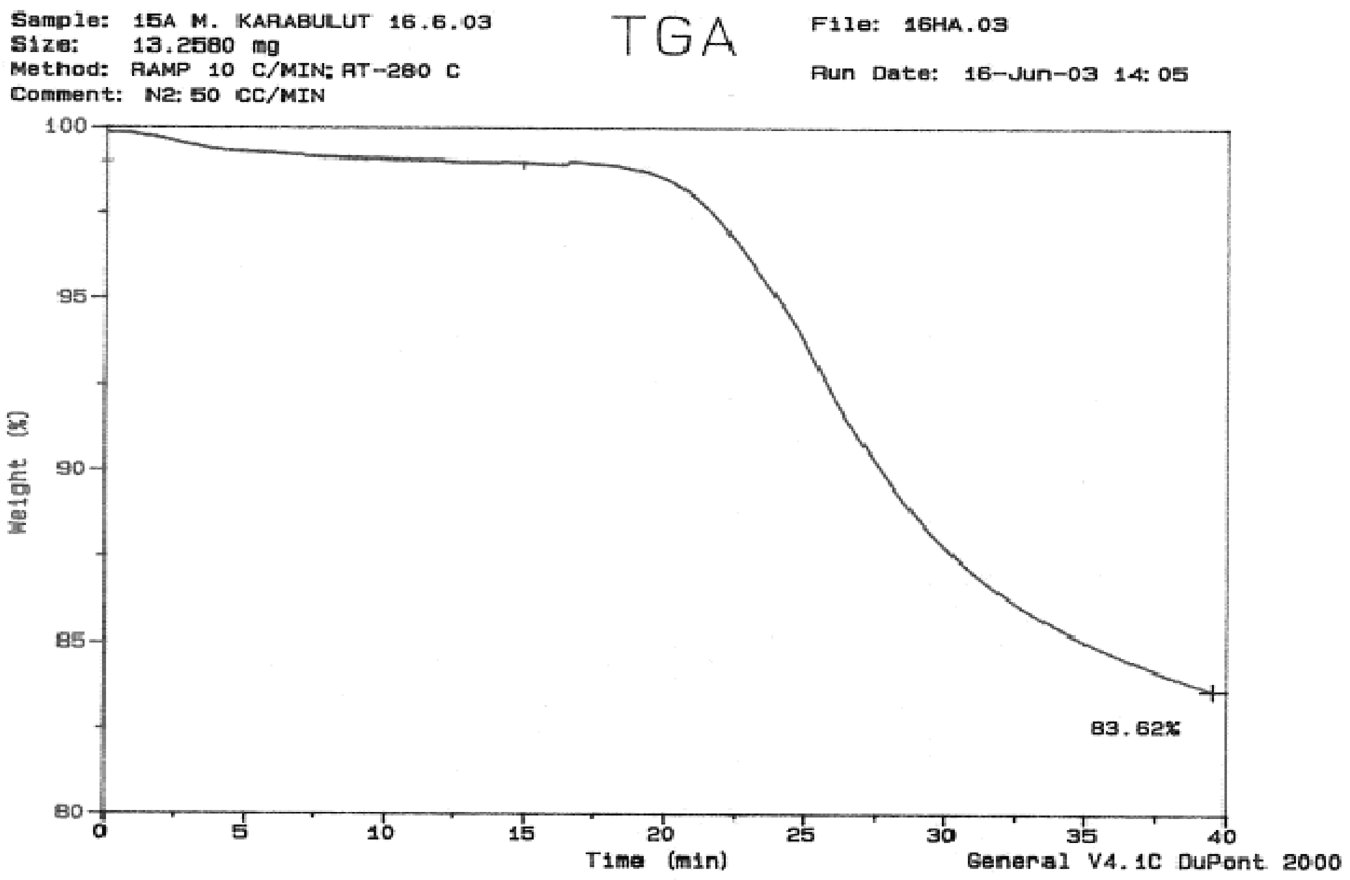

Figure F1. TGA diagram for 15A montmorillonite

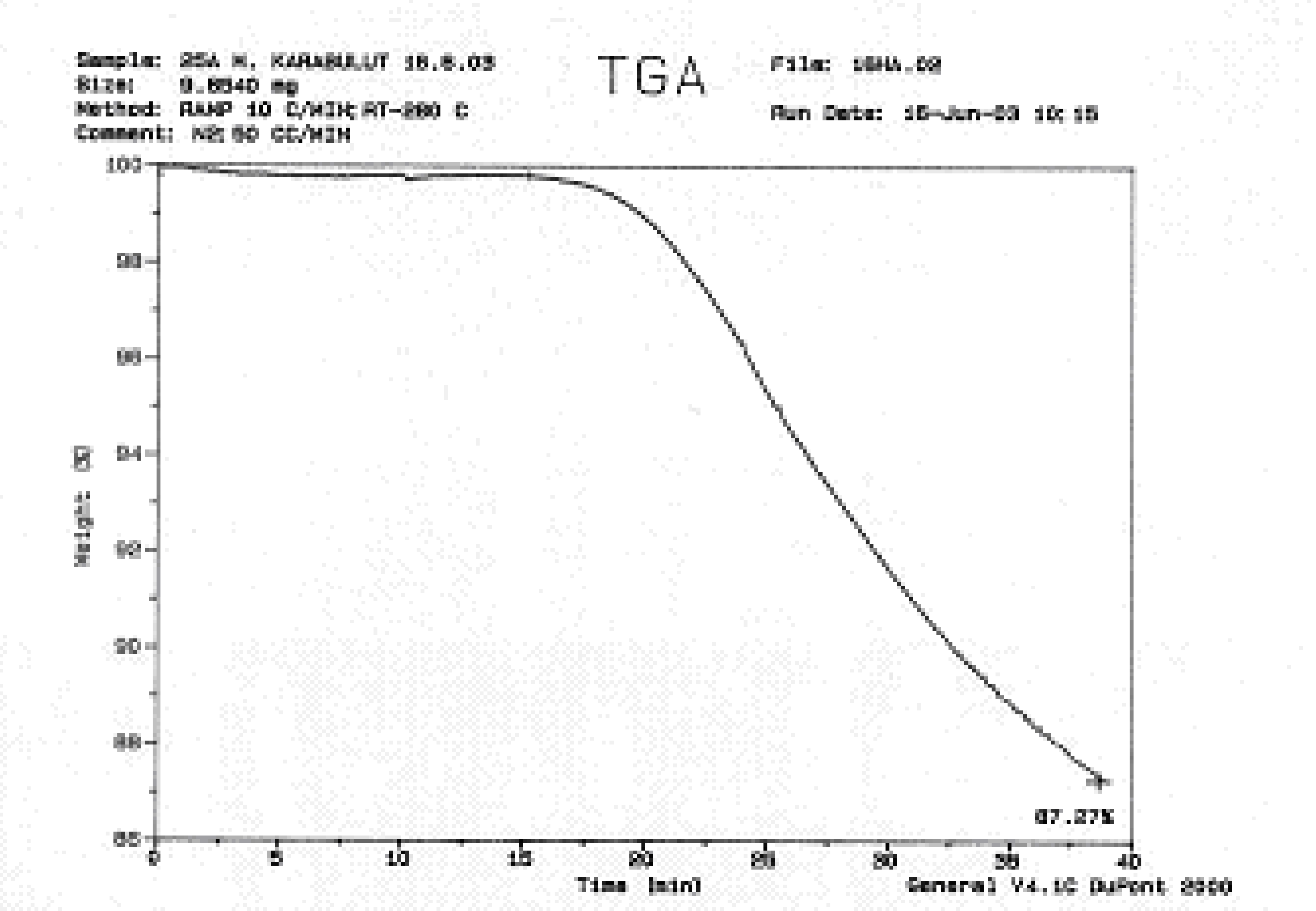

Figure F2. TGA diagram for 25A montmorillonite

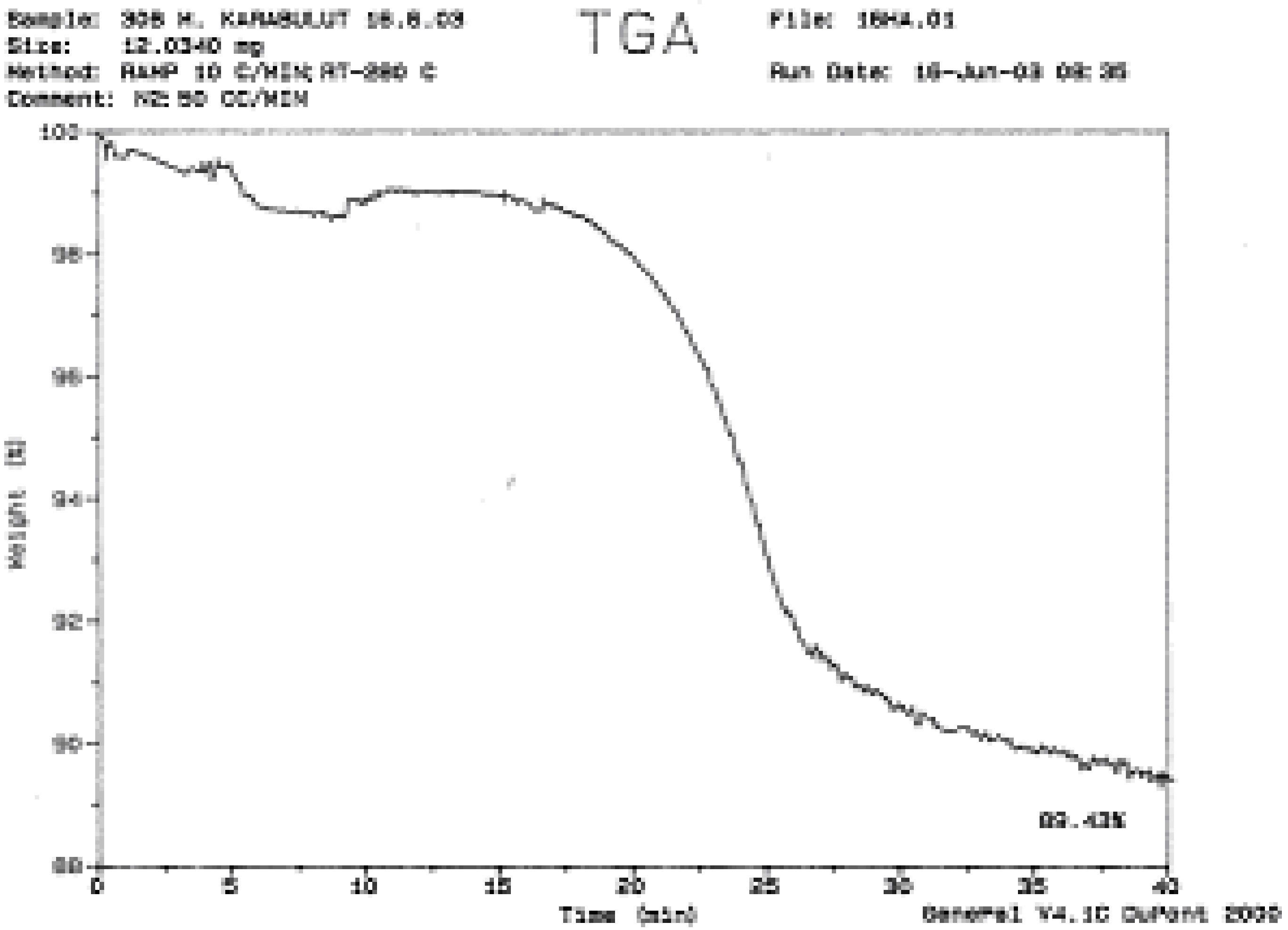

Figure F3. TGA diagram for 30B montmorillonite